

# Essays on the Econometric Analysis of Structural Instabilities and Systemic Risk

Inauguraldissertation  
zur Erlangung des akademischen Grades  
eines Doktors der Wirtschaftswissenschaften  
der Universität Mannheim

vorgelegt von

So Jin Lee

im Frühjahrs-/Sommersemester 2025

Abteilungssprecher:	Prof. Dr. Thomas Tröger
Referent:	Prof. Dr. Carsten Trenkler
Referent:	Prof. Dr. Christoph Rothe
Vorsitzender der Disputation:	Prof. Dr. Matthias Meier

Tag der Disputation:	29.07.2025
----------------------	------------

# ACKNOWLEDGMENTS

It was a long journey supported by many great and kind people. First, I would like to express my deepest gratitude to my supervisor, Carsten Trenkler. I am truly grateful for the opportunity to be guided and supported by his insight, knowledge, and wisdom. Nothing would have been possible without his guidance. I also wish to extend my sincere thanks to Christoph Rothe, whose insightful econometrics course at the beginning of the program sparked my interest in the field. I am especially grateful for his critical support during the final years of my doctoral study.

I am deeply indebted to the staff in our program. I could not have navigated this path without the support and guidance of Julia from the Welcome Center. Our center managers, Golareh, Marion and Caroline, were pillars of support during the most turbulent days. I am especially thankful for the care and assistance of Anja, Regina, Ute, and Yi. I truly appreciate the organizational help and generous guidance of Frau Rosenkranz throughout the dissertation process.

I am grateful to the professors and colleagues from whom I learned so much along the way: Otilia Boldea, Juan J. Dolado, and Christian Brownlees, for their thoughtful and kind advice on my work. I also thank Pavel Čížek, Denis Kojevnikov, Bas Werker, Weihao Chen, and the members of TiSEM; Antonio Cabrales, Juan Carlos Escanciano, Jesús Gonzalo, Nazarii Salish, Carlos Velasco, Andrey Ramos, Alejandro Puerta, and the members of the UC3M Department of Economics; Matteo Barigozzi; Rebekka Buse and the organizers and participants of HKMetrics 2022; Daniele Bianchi, Maria Grith, Daniele Massacci, Rosnel Sessinou, and the organizers and participants of the FinEML 2023 conference; André Santos, Martina Zaharieva, Audrone Virbickaitė, and the seminar participants at the Department of Quantitative Methods, CUNEF; Mathias Dewatripont, Marc Hallin, George Kirchsteiger, Luca Paolo Merlino, Davy Paindaveine, and the members and seminar participants at ECARES, Université Libre de Bruxelles; Tsung-Hsien Li, Geert Mesters, and the organizers and participants of the SETA 2024 conference.

I was fortunate to have the opportunity to share ideas and discussions with Antonio Ciccone, Matthias Meier, and Nicolas Schutz. I thank them for their invaluable and insightful suggestions and advice. I am grateful to Christian Conrad, Kathrine von Graevenitz, Moritz Kuhn, Krzysztof Pytka, and Camille Urvoy for their advice and support during my job market phase. I also extend my heartfelt thanks to Lars and Lea for their invaluable support.

During my years here, I was fortunate to be surrounded by wonderful friends and colleagues — Büşra, Chiara, Kate, Sabine, Sandra, Tania, Yulia, Giovanni, Johannes, Lukas, and Thibault — who stood by me during many difficult moments. I am sincerely grateful for their friendship and wish them all the very best for the future.

# CONTENTS

PREFACE	VI
1 ESTIMATING POINTS OF STRUCTURAL CORRELATION INSTABILITIES WITH LATENT FACTOR MODELS	1
1.1 Introduction	1
1.2 Cross-correlation Instabilities and Latent Factor Models	3
1.2.1 Modeling Covariance Dynamics with Standard Latent Approximate Factor Model	3
1.2.2 Benchmark Model and Assumptions	6
1.2.3 Structural Break as a Factor Space Change	8
1.3 Detection of Structural Breaks	10
1.3.1 Measure of Factor Space Change	10
1.3.2 Estimation of the Distance Measure	11
1.3.3 Information Criterion	13
1.3.3.1 Selection between models with or without a break	13
1.3.3.2 Early Warnings of Structural Breaks	15
1.3.3.3 Breakpoint Detection Algorithm	16
1.4 Simulations	19
1.4.1 Estimation of Single Breakpoint Locations	19
1.4.2 Detection of No Breakpoint	21
1.4.3 Multiple Breakpoints	22
1.4.4 The Main to the Simplified Algorithm	24
1.5 Applications	25
1.5.1 Instabilities in the Stock Market During the Early Stages of the Global Financial Crisis	25
1.5.2 Structural Breaks in Cross-Variable Correlations among Macroeconomic and Financial indicators	26
1.6 Concluding Remarks	27
APPENDIX TO CHAPTER 1	28
A.1 Extended Discussion on Covariance Dynamics and Factor Space Change	28
A.1.1 Section 1.2.1	28

A.1.2	Section 1.2.2 . . . . .	28
A.1.2.1	Benchmark Assumptions . . . . .	28
A.1.2.2	Model Extension . . . . .	31
A.2	Proofs . . . . .	32
2	SYSTEMIC INFLUENCE IN STRUCTURAL BREAKS: GRANULAR TIME SERIES DETECTION . . . . .	37
2.1	Introduction . . . . .	37
2.2	Structural Breaks in a System with Latent Factors . . . . .	39
2.2.1	Covariance Dynamics and Factor Space Changes . . . . .	40
2.2.1.1	Benchmark Model and Assumptions . . . . .	40
2.2.1.2	Identifiable Changes in the Unobservable Factor Loadings . . . . .	42
2.2.2	Interpreting Structural Breaks: Factor space, Network centrality, and Equilibrium . . . . .	44
2.3	Systemic Influence in Structural Breaks . . . . .	45
2.3.1	Bridging the Idiosyncratic Dimension and the Structural Break . . . . .	46
2.3.2	A Measure of Systemic Influence . . . . .	47
2.3.2.1	The Concentration Matrix Revisited . . . . .	48
2.3.3	Criteria for Detecting Granular Units . . . . .	50
2.3.3.1	Detection Criteria . . . . .	51
2.4	Estimation . . . . .	52
2.4.1	Estimation with a Known Breakpoint . . . . .	52
2.4.2	Simulation . . . . .	56
2.5	Applications . . . . .	58
2.5.1	Dot-Com Bubble . . . . .	60
2.5.2	2007-2008 Financial Crisis . . . . .	61
2.6	Concluding Remarks . . . . .	63
	APPENDIX TO CHAPTER 2 . . . . .	64
B.1	Proofs . . . . .	64
B.2	A Network-based Interpretation of Latent Factor Models . . . . .	70
B.3	A Note on the First Order Effect . . . . .	74
B.4	A Geometrical Interpretation on the Detection Criteria . . . . .	75
3	GENERAL INSTABILITIES IN NETWORKED SYSTEMS AND EARLY WARNINGS . . . . .	78
3.1	Introduction . . . . .	78
3.2	Unobservable Networks and Latent Factor Models . . . . .	79
3.2.1	Static Latent Network–Factor Model . . . . .	79
3.2.2	Changing Networks and Structural Breaks in Latent Factor Model . . . . .	80

3.3	Latent Network-Factor Model with Instabilities . . . . .	81
3.3.1	Factor Model Representation of Changing Networks . . . . .	82
3.3.2	Instabilities in Factor Structure: Discrete vs. Continuous . . . . .	84
3.4	Early Warnings of Structural Changes in a Networked System . . . . .	85
3.4.1	Small Perturbations in Factor Structure . . . . .	86
3.4.2	Optimal Factor Space and Residual Probability . . . . .	87
3.4.3	Probability of Structural Changes and Early Warnings . . . . .	89
3.5	Concluding Remarks . . . . .	91
APPENDIX TO CHAPTER 3		92
C.1	Further discussions on Network–Factor Model . . . . .	92
C.2	Proof . . . . .	92
BIBLIOGRAPHY		95

# PREFACE

This dissertation consists of three chapters in a study of structural instabilities and systemic risk analysis. A system of interest is assumed to be interconnected, but the underlying structure is unknown or unobservable.

Chapter 1 develops a method to detect and localize the points of structural instabilities in the cross-correlation structure of a panel. Cross-correlation structures contain valuable information about the underlying linkages among variables and the channels of spillovers across cross-sectional units. Instabilities in these structures often signal structural changes within the system. We propose a novel method for detecting instabilities in cross-correlation structures using a latent factor model framework. We introduce a suitable object – the column space of the loading matrix (the *factor space*) – to capture structural correlation changes while being free from the inherent identification issue of the latent model. The resulting detection criterion is based on an intuitive distance measure between two factor spaces, integrating both the detection and localization of breakpoints. In applications, our methods effectively detect instability points consistent with the development of the subprime mortgage crisis, as well as major policy changes such as the repeal of the Glass–Steagall Act and the U.S.–China trade war.

Chapter 2 proposes a novel framework to identify the most influential units behind structural breaks. In a system represented by panel data, a break in the cross-correlation structure can empirically indicate volatility propagation from individual (idiosyncratic) dimensions to the entire system. Individual units contributing the most to this break can act as systemic risk components, potentially driving further instability across the system. We propose a novel method to detect these main contributors — referred to as ‘granular units’ — as an early detection tool for potential systemic risk components. Assuming a standard approximate latent factor structure to model system covariance dynamics agnostically, we introduce a straightforward influence measure to evaluate the contributions of individual (idiosyncratic) second moments to the structural break. Applied to S&P 100 daily return data across major economic crisis periods, the proposed detection scheme effectively identifies likely sources of systemic risk from early crisis stages.

Chapter 3 designs a new sequential early warning framework for structural changes that accommodates a broad range of instabilities in the underlying latent network. Network and

factor models are two important techniques for analyzing interconnected systems, and we demonstrate that an interconnected system can naturally have a dual representation through our network-factor model. This modeling enables the analysis of instabilities in the latent network using various tools from factor analysis. This online warning framework can be of practical importance for application to network-supported data in which the underlying structure is unknown or unobservable.

NOTATIONS. Throughout the chapters, we denote the norms for a matrix  $M$  or a vector  $\mathbf{v}$  as follows: For a matrix  $M$ , we denote the Frobenius norm as  $\|M\|_F \equiv \sqrt{\text{tr}(M'M)}$ , and the max norm as  $\|M\|_{\max} \equiv \max_{ik} |M_{ik}|$ . To simplify notations, we use the expression  $\|\cdot\|$  in either of two ways. For a vector  $\mathbf{v}$ , it denotes the  $\ell_2$  norm  $\|\mathbf{v}\| = \|\mathbf{v}\|_2 \equiv \sqrt{\mathbf{v}'\mathbf{v}}$ . For a matrix  $M$ , it denotes the operator norm  $\|M\| = \|M\|_{op} \equiv \sqrt{\lambda_{\max}(M'M)}$ , the matrix norm induced by the  $\ell_2$  norm.

A superscript  $\perp$  on a vector subspace  $W$  denotes the orthogonal complement in terms of the Euclidean inner product in  $N$ -dimensional space,  $W^\perp \equiv \{\mathbf{v} \in \mathbb{R}^N \mid \mathbf{v}'\mathbf{w} = 0, \forall \mathbf{w} \in W\}$ . For a column augmentation  $P$  of orthonormal basis vectors of  $W$ ,  $P^\perp$  (or  $P_\perp$ ) denotes a column augmentation of basis vectors of the orthogonal complement  $W^\perp$  such that  $P^\perp P'^\perp = I - PP'$ . The projector expressions can be shorthanded by  $\mathcal{P} \equiv PP'$  and  $\mathcal{P}^\perp \equiv I_N - \mathcal{P}$ .

Superscripts in the form of  $N_r \times N_c$  denote the row ( $N_r$ ) and column ( $N_c$ ) dimensions of a matrix. A single subscript implies  $N_r = N_c$ . For a rank  $K$  real matrix  $P^{N \times K}$ , the linear space spanned by the column vectors  $\{\mathbf{p}^k\}$  of  $P$  is denoted by  $\text{span}(P) \equiv \left\{ \sum_{k=1}^K r_k \mathbf{p}^k \mid r_k \in \mathbb{R} \right\}$ .  $\mathcal{N}$  denotes the set of all cross-sectional indices,  $\{1, \dots, N\}$ . The letter  $i$  is reserved for the cross-sectional index, and  $j$  is for the regime index.

$a \wedge b \equiv \min(a, b)$  and  $a \vee b \equiv \max(a, b)$ .  $a \lesssim b$  if  $a \leq cb$  for some constant  $c > 0$ .  $a \asymp b$  if  $a \lesssim b$  and  $b \lesssim a$ .

# 1 ESTIMATING POINTS OF STRUCTURAL CORRELATION INSTABILITIES WITH LATENT FACTOR MODELS

## 1.1 INTRODUCTION

Correlation structures contain rich information about underlying linkages among variables—or channels of spillovers among cross-sectional units. Instabilities in the cross-correlation structure can indicate ongoing structural changes in a given system.

In this paper, we first show that the cross-correlation structure can be naturally modeled and analyzed through a latent-factor model, and then propose a novel method to detect points of instability. The task of analyzing structural instabilities in cross-correlations is closely related to identifying large breaks in latent factor loadings.

As factor models have long been a crucial workhorse in economic analysis, a break or instability in these models has become an important subject of study in the related literature. In studies on factor-loading instabilities, substantial breaks in the loading matrix have been interpreted as structural changes in the system—that is, as changes in the transmission mechanism of common macro or systematic factors to the entire system. Dates of the breakpoints have been shown to correspond to important economic events such as the 1979–1980 oil-price shock or the Great Moderation (e.g., [Stock and M. Watson, 2009](#), [Chen et al., 2014](#), [Ma and Su, 2018](#), [Baltagi et al., 2021](#)). [Banerjee et al., 2008](#) and [Yamamoto, 2016](#) provide evidence that accounting for such breaks is important for forecasting.

Latent-factor models offer a minimalistic framework and well-established tools to analyze cross-correlation structures and their instabilities. However, because the factors are unobserved, there is an inherent identification issue: do the instabilities stem from the latent loading matrix or from the latent factor signals? We show that the column space of the loading matrix (the *factor space*) is a suitable object for capturing structural correlation changes and is free from this identification problem. The resulting detection scheme relies on an intuitive distance measure between two factor spaces.

The contribution of our approach is its simplicity. Modeling cross-correlation structures and their instabilities is agnostic and non-parametric within a latent factor model framework.

Compared with studies of structural breaks in the loading matrix, we offer a technical innovation that avoids the identification issue noted above. The proposed detection scheme is also straightforward, integrating two kinds of model selection—whether a breakpoint exists and where it is located—into a single criterion.

In the empirical exercise, we apply our breakpoint-detection method to a daily stock-return panel and to a collection of monthly macro-financial variables. In the stock-return application, our method detects early instability points ahead of the global financial crisis, consistent with the development of the subprime-mortgage crisis. In the macro-financial exercise, it identifies two dates corresponding to the repeal of the Glass–Steagall Act in 1998–1999 and the U.S.-China trade war in 2018–2019.

**RELATED LITERATURE** Numerous methods have been developed to detect large breaks in the factor-loading matrix under a standard approximate unobservable factor model. One branch of studies exploits the observational equivalence between a loading break and a factor signal covariance break in the conventional factor specification, providing tests for breaks (e.g., [Chen et al., 2014](#), [Han and Inoue, 2015](#)) or estimates of multiple breakpoints (e.g., [Baltagi et al., 2021](#)). A second branch focuses on estimating breakpoints (e.g., [Chen, 2015](#), [Cheng et al., 2016](#), [Ma and Su, 2018](#)), employing a residual-least-squares objective function.

All these approaches require factor signal covariance to remain fixed under the null of no loading change; otherwise, a factor signal covariance change would be observationally equivalent to a loading change. When one investigates a change in one part (the loading matrix) of the two latent objects (loadings and factor signals), the other part (the factor signal covariance) must be fixed under the null. Note that, with the number of factors held constant, a change in the loading matrix that can be translated into a factor signal covariance change does not alter the column space of the loading matrix—the factor space. [Düker and Pipiras, 2024](#) and [Koo et al., 2024](#) provide additional criteria to determine whether a loading change alters the factor space.

A major difference in our approach is that we do not require any assumption of factor signal covariance stability, provided a strong factor structure exists. The factor space representation we employ automatically absorbs mere factor signal covariance changes, is invariant to redundant internal rotations, and separates out factor signal strengths. By working directly with the factor space representation, our method sidesteps the need for additional arguments to ensure that a change in the transmission rule is not simply an artifact of unobservability. In this sense, focusing on the factor space is the simplest way to disentangle structural changes in the transmission rule (the loading matrix) from changes in the latent signals (factors) it carries.

This paper proceeds as follows. Section 1.2 explains how changes in the factor space capture substantial breaks in the major cross-correlation structure. Section 1.3 introduces a distance measure between factor spaces and proposes a detection criterion and algorithm based on this

measure. Simulation results follow in Section 1.4. Section 1.5 presents applications to a daily S&P 500 return panel and to [McCracken and Ng, 2016](#)'s collection of macro-financial variables. Section 1.6 concludes.

## 1.2 CROSS-CORRELATION INSTABILITIES AND LATENT FACTOR MODELS

We consider a panel with a large cross-sectional dimension ( $N$ ) for a single variable, such as a panel of stock returns. The cross-correlation structure and its instabilities contain rich information for portfolio choice and risk analysis, considering the spillover or transmission of risk factors across units through a hidden network topology.

Latent factor models can provide an agnostic description of the cross-correlation structure and its instabilities. In the first section, we review the characteristics of the standard approximate factor model – one of the most popular workhorse models in econometrics – as the modeling of the cross-sectional covariance. It will discuss the pros and cons of employing latent factor models to describe structural correlation instabilities. We detail the object of our strategic interest to contain the information of the structural break. The second section will formally introduce the benchmark model.

### 1.2.1 MODELING COVARIANCE DYNAMICS WITH STANDARD LATENT APPROXIMATE FACTOR MODEL

Let  $N$ -dimensional process  $\mathbf{y}_t = [y_{1t}, \dots, y_{Nt}]'$  follow a standard approximate factor model during a certain period of time,

$$\mathbf{y}_t^{N \times 1} = \boldsymbol{\chi}_t + \mathbf{u}_t, \quad \text{for all } t \in \mathcal{I}_0. \quad (1.1)$$

That is,  $\mathbf{y}_t$  can be decomposed into two parts: the common component  $\boldsymbol{\chi}_t$ , which contains systematically important information, and the idiosyncratic component  $\mathbf{u}_t$ , the remaining part. We assume all processes to be mean-zero.

In the most conventional form, the common component is specified to have a multiplicative structure,

$$\boldsymbol{\chi}_t = B\mathbf{f}_t, \quad \text{for all } t \in \mathcal{I}_0, \quad (1.2)$$

which consists of a small number of (say,  $K$ ) common factor signals  $\mathbf{f}_t = (f_t^k)_{k=1, \dots, K}$  and their loadings  $B^{N \times K}$ . Those are considered systemically important because the cross-sectional units are correlated mainly through the loadings of the common factors. The transmission rule – how all cross-sectional units are affected by the latent factor signals – contained in the loading matrix  $B$  is crucial to explain the major cross-correlation structure.

A benefit of the latent factor models in describing the cross-correlation structure is that they stay agnostic and robust to the true identity of the systematically important information. The factors and loadings are unknown or unobservable, but we can still distinguish the systematically important part from the data. How do we do that? It is done by conditioning the system covariance structure so that it can have the additive decomposition into two symmetric matrices:

$$\Sigma_y = \Sigma_\chi + \Sigma_u, \quad t \in \mathbb{I}_0. \quad (1.3)$$

One part  $\Sigma_\chi$  is of low rank but dense and dominating in size, and the other part  $\Sigma_u$  is of full rank but sparse and relatively negligible in size. The existence of the two uncorrelated sub-processes  $\chi_t$  and  $\mathbf{u}_t$  are guaranteed such that  $\Sigma_\chi = E[\chi_t \chi_t']$ , and  $\Sigma_u = E[\mathbf{u}_t \mathbf{u}_t']$ . The major correlation structure of the system covariance is captured by the dense, low-rank part  $\Sigma_\chi$ , or by the sub-process  $\chi_t$ , or, under the conventional specification (1.2), by the loadings of the factor signals. A point to make is that the latent factor model is essentially a model at the level of the system covariance. We say a system has a factor structure if it has this decomposability.

In related literature, substantial breaks in the factor loading matrix have been naturally interpreted as structural changes in the system, reflecting changes in how common macroeconomic (systematic) factors transmit to the entire system. For instance, breakpoints correspond to important economic events such as the 1979-1980 oil price shock or the Great Moderation, e.g., in [Stock and M. Watson, 2009](#), [Chen et al., 2014](#), [Ma and Su, 2018](#), and [Baltagi et al., 2021](#).<sup>1</sup> Employing the factor models in modeling cross-correlation structure opens a ground of natural economic interpretation connecting the system correlation instabilities and structural breaks in macroeconomic shock transmission mechanisms.

We focus on structural cross-correlation instabilities that correspond to structural breaks in the transmission mechanism. In general, the likely unknown true transmission mechanism can be complex in nature, which renders direct modeling and analysis convoluted. The agnostic approach based on a latent factor model is robust to specifications of the true transmission mechanism. Robustness of this approach, however, does not come free. As both the factor signals and the loading matrix are unobservable, one can not always distinguish the instabilities of the loading matrix  $B$  from those of the factor signals. More precisely, the variance of each common factor  $f_t^k$ , or the correlations between  $f_t^k$  and  $f_t^{k'}$  can vary, and neither can be distinguished from a change of the loading matrix  $B$ .

The loading matrix is an object containing the transmission rule, but not a good representation to work with. Our solution for this issue is to use a different object to represent the transmission rule. We introduce the object  $\mathcal{P} = PP'$ , which is the projector representation of the column space of the loading matrix  $B$ . The object  $\mathcal{P}$  can be constructed from the normalized

---

<sup>1</sup>[Banerjee et al., 2008](#) and [Yamamoto, 2016](#) have provided evidence that consideration of such breaks is important in forecasting.

loading matrix  $\tilde{P} \equiv B(B'B)^{-1/2}$ , such that  $\mathcal{P} = \tilde{P}\tilde{P}' = B(B'B)^{-1}B'$ . The information  $\mathcal{P}$  carries is essentially the ratio of the loadings across the units, how each unit receives the impact of the latent common factors relative to each other. This distributive characteristic of the factor loading matrix underpins the central characteristic of the transmission rule.

The object  $\mathcal{P}$  can be equivalently constructed by having the spectral decomposition (or thin SVD)

$$\Sigma_\chi = P\Lambda_\chi P', \quad (1.4)$$

which guarantees  $\mathcal{P} = PP'$ . That is, the conventional specification (1.2) and the generic spectral decomposition of the low rank symmetric matrix (1.4) guarantee that the loading matrix

$$B = \tilde{P}(B'B)^{1/2}, \quad (1.5)$$

where  $\tilde{P} = P\mathcal{O}$  for some orthonormal transformation  $\mathcal{O}$ . The expression (1.5) is the *polar decomposition* of a matrix  $B$ . Intuitively, one can always distinguish the *directional* information of given  $B$  by a semi-orthonormal matrix  $\tilde{P}$  ( $\tilde{P}'\tilde{P} = I_K$ ), from the *size* information of  $B$  captured by the remaining part. The directional information of  $B$  is identical to that of  $P$ , in the sense that the column space of the loading matrix  $B$  is equivalent to the column space of  $P$ , represented as  $\mathcal{P} = PP'$ .

The object  $\mathcal{P} = PP'$  is invariant under changes of the covariance structure of  $\Sigma_f = E[\mathbf{f}_t\mathbf{f}_t']$ , as long as the rank of the common component is fixed, which we discuss in Properties 1 below. If the rank of  $\Sigma_\chi$  or the number of the common factors is changed, it does imply a change in the transmission rule. It is conceptually natural, as an introduction or removal of a factor necessitates an emergence or disappearance of specific pathways of transmission.

**Properties 1.** Assume that the decomposability (1.3) is guaranteed.  $\mathcal{P}$  is invariant under any rank preserving change of  $\Sigma_f = E[\mathbf{f}_t\mathbf{f}_t']$ .

Any changes in the common factor covariance,  $\Sigma_\chi \rightarrow \tilde{\Sigma}_\chi$  can be captured by a combination of the rotation  $\mathbf{f}_t \mapsto Q\mathbf{f}_t$ , and the rescaling  $\mathbf{f}_t \mapsto D\mathbf{f}_t$ . First, the expression  $PP'$  is invariant under a transformation  $P \mapsto PQ$  for any orthonormal  $Q$ , as  $QQ' = Q'Q = I_K$ . Second, at the population level, the eigenvector information  $P$  is not affected by the change of the diagonal scales. Hence,  $\mathcal{P}$  is invariant under the potential instabilities in  $\Sigma_f$ . A more detailed discussion follows in Appendix A.1.1.

Changes of the introduced object  $\mathcal{P}$  capture instabilities in the factor loading that are not observationally equivalent to the factor signal covariance change. This object will be named *factor space* from now on, with its defining characteristics summarized below.

**FACTOR SPACE.** Let the spectral decomposition  $\Sigma_\chi = P\Lambda_\chi P'$ . *Factor space* is the space spanned by the columns of  $P$  in  $N$ -dimensional space (that is,  $\text{col}(P)$ , the column space of  $P$ ), or equivalently, the column space of  $B$ , under the specification (1.2). That is,

$$\text{span}(P) \equiv \text{col}(P) = \left\{ \sum_{k=1}^{K_j} r_k \mathbf{p}_j^k \mid r_k \in \mathbb{R} \right\} = \text{col}(B). \quad (1.6)$$

Note that any space can be identified by a projection operator that projects any vectors onto that space. Hence, we identify the factor space by its projector representation, such that  $\mathcal{P} = PP'$ . The term *factor space* will naturally indicate both the object  $\text{span}(P)$  and its representation  $\mathcal{P} = PP'$ .

## 1.2.2 BENCHMARK MODEL AND ASSUMPTIONS

In this subsection, we properly introduce the benchmark model of system covariance dynamics based on a standard latent factor model. The model considers the evolution of the factor space in discrete steps from one regime (period  $\mathcal{I}_0$ ) to another regime (period  $\mathcal{I}_1$ ), indexed by  $j \in \mathcal{J} = \{0, 1\}$ . Note that it neither restricts the number of regimes to two nor assumes recursiveness. The number of regimes ( $|\mathcal{J}|$ ) can be any integer  $J \in \mathbb{Z}_+$ . In the current discussion, we showcase the case  $J = 2$  solely for expository purposes. The regime is defined by the factor space, and the change of regime is defined by the change of the factor space. A regime can be either non-recursive or recursive. Our framework is not bound to these characteristics. The benchmark model is stated as follows:

For each  $j \in \{0, 1\}$ ,  $\mathbf{y}_{j,t}$  is decomposed into common component  $\boldsymbol{\chi}_{j,t}$  and idiosyncratic component  $\mathbf{u}_t$ , such that

$$\mathbf{y}_{j,t} = \boldsymbol{\chi}_{j,t} + \mathbf{u}_t, \quad \text{for all } t \in \mathcal{I}_j. \quad (1.7)$$

Further,  $\mathbf{y}_{j,t}$ ,  $\boldsymbol{\chi}_{j,t}$  and  $\mathbf{u}_t$  are all conventional mean-zero objects. Although  $\mathbf{u}_t$  is allowed to be regime( $j$ ) specific, the regime index is omitted from this component only to emphasize that the low-dimensional component defines the regime change. We will impose the following assumptions:

**Assumption 1.**  $\Sigma_{y,j} = \Sigma_{\chi,j} + \Sigma_{u,j}$ , where  $\Sigma_{\chi,j} = P_j \Lambda_{\chi,j} P_j'$  in terms of  $K_j \ll N$  non-zero eigenvalues  $\lambda_{\chi,j}^k \asymp N$  for  $\Lambda_{\chi,j} = \text{diag}(\lambda_{\chi,j}^k)_{k=1,\dots,K_j}$  and  $P_j' P_j = I_{K_j}$ .

**Assumption 2.** There exists a constant  $q_j \in [0, 1]$  such that

$$c_{u,j} \equiv \max_{i=1,\dots,N} \sum_{i'=1,\dots,N} |\text{COV}(u_{it}, u_{i't})|^{q_j} = O(1).$$

**Assumption 3.**  $\|P_0 P_0' \Sigma_{u,0} P_0^\perp P_0^{\perp'}\|_F = o(1)$ .

**Assumption 4.**  $\Sigma_{y,1} = \Sigma_{y,0} + Z$ , where  $\|P_0' Z P_0^\perp\|_F \asymp N$ .

$\Sigma_{\chi,j} = P_j \Lambda_{\chi,j} P_j'$  is the (thin) singular value decomposition of the common component covariance matrix. The non-zero eigenvalues  $\lambda_{\chi,j}^k$  are in descending order.

Assumptions 1 and 2 – standard conditions of the approximate factor model – that guarantee the decomposability or the identifiability of the factor structure (1.7), defining what makes the  $\Sigma_{\chi,j}$  distinguishable from the remaining part. The idiosyncratic components can be correlated but in a bounded fashion for any size of the cross-sectional dimension  $N$ , as stated in Assumption 2. On the other hand, the common components prevail no matter how large (measured by  $N$ ) the system is, following Assumption 1. As captured by the unbounded eigenvalues of  $\Sigma_{\chi,j}$ , the size of common component covariance is not dissipating in the large  $N$  limit.<sup>2</sup> The major correlation structure of the system is captured by a small number,  $K_j$ , of important directions  $\{\mathbf{p}_j^k\}_{k=1,\dots,K_j}$  in which the non-dissipating eigenvalues are loaded; or more precisely, it is captured by the factor space  $\text{span}(P_j) \equiv \left\{ \sum_{k=1}^{K_j} r_k \mathbf{p}_j^k \mid r_k \in \mathbb{R} \right\}$  spanned by the important directions.<sup>3</sup> Under these two assumptions with a perturbation bound result (the  $\sin \theta$  theorem) of [Davis and Kahan, 1970](#), the eigenspace of the  $K_j$ –leading eigenvalues of  $\Sigma_{y,j}$  is consistent with the factor space at the population level.

Assumption 4 hypothesizes that the regime 0 covariance experiences a substantial perturbation that is off-diagonal with respect to the previous basis  $[P_0 \ P_0^\perp]$ . Let  $P_j^\perp$  denote a column augmentation of  $N - K_j$  basis vectors of the space  $\text{span}(P_j)^\perp = \{v \in \mathbb{R}^N \mid v'p = 0, \forall p \in \text{span}(P_j)\}$ , the orthogonal complement of the factor space  $\text{span}(P_j)$ . Then, up to an error  $E$  of order  $o(1)$  (note that  $\|E\|_{\max} = \max_{i,i'} |E_{ii'}| = o(1)$  by Assumption 3) for large  $N$ , the regime 0 covariance can be written in terms of  $P_0$  as

$$\Sigma_{y,0} \simeq \begin{bmatrix} P_0 & P_0^\perp \end{bmatrix} \begin{bmatrix} \Lambda_{1,0} & \mathbf{0}_{K_0 \times (N-K_0)} \\ \mathbf{0}_{(N-K_0) \times K_0} & \Lambda_{2,0} \end{bmatrix} \begin{bmatrix} P_0' \\ P_0^{\perp'} \end{bmatrix}. \quad (1.8)$$

Due to the assumed perturbation, a sizable perturbation  $P_0' Z P_0^\perp$  (and  $P_0^{\perp'} Z P_0$ ) will be added to the initially zero off-diagonal blocks in the expression (1.8). After such a perturbation, the previous important directions (or a basis of the regime-0 factor space)  $P_0$  can no longer

<sup>2</sup>Although there is a natural explanation – [Wang and Fan, 2017](#) equation (1.1) – the rate is assumed to be linear in  $N$  mainly to simplify the later discussion. This can be easily generalized.

<sup>3</sup>Such directional information can be interpreted regarding a network centrality. We will discuss this in the latter part of this section.

explain the system's major correlation structure. The new regime will thus admit a new set of important directions represented by  $P_1$  such that

$$\Sigma_{y,1} \simeq \begin{bmatrix} P_1 & P_1^\perp \end{bmatrix} \begin{bmatrix} \Lambda_{1,1} & \mathbf{0}_{K_1 \times (N-K_1)} \\ \mathbf{0}_{(N-K_1) \times K_1} & \Lambda_{2,1} \end{bmatrix} \begin{bmatrix} P_1' \\ P_1^{\perp'} \end{bmatrix}, \quad (1.9)$$

which implies that the factor space has changed from  $\text{span}(P_0)$  to  $\text{span}(P_1)$ . Appendix A.1.2.1 contains a further discussion on covariance dynamics and factor space change, in which we explain that the existence of factor structure in both regimes (Assumptions 1 and 2) also suggests the type of perturbation characterized in Assumption 4.

The expression (1.7) can be further specified for  $\chi_{t,j}$  in a multiplicative form such as (1.2). Note that such a multiplicative specification has an uncountable degree of freedom without further restrictions on the structure of the factor covariance  $E[\mathbf{f}_{j,t}\mathbf{f}_{j,t}']$ . For example, one can assume that the underlying latent factors satisfy  $E[\mathbf{f}_{j,t}\mathbf{f}_{j,t}'] = I_{K_j}$  and loaded increasingly more heavily as the cross-sectional dimension of the system increases; that is,  $\chi_{j,t} = B_j \mathbf{f}_t$  for the loading matrix  $B_j$  whose singular values growing as  $N$  grows. For another example, one can assume that  $\chi_{j,t} = P_j \mathbf{f}_t$  with a fixed sized loading  $P_j$  while the latent factor signals grow more intensive in larger systems, such that  $\lambda^k(E[\mathbf{f}_{j,t}\mathbf{f}_{j,t}']) \asymp N$  for all  $k = 1, \dots, K_j$ . All possible specifications indicate the unique factor structure  $\Sigma_{y,j} = \Sigma_{\chi,j} + \Sigma_{u,j}$  of our benchmark model, sharing the same factor space –  $\text{span}(B_j) = \text{span}(P_j)$ , for the above mentioned two examples. The covariance dynamics of our model are robust to the particularity of such extra modeling of factor-loading structure and can be equivalently described by any of the possible specifications. The benchmark model can be extended to allow certain types of non-stationarity within regimes. We discuss the extended features of the model in Appendix A.1.2.2.

### 1.2.3 STRUCTURAL BREAK AS A FACTOR SPACE CHANGE

We have discussed how structural correlation instabilities can be captured by factor space changes. It connects the existing literature on the structural breaks in the factor loading, or the transmission rule, based on latent factor models. Due to the importance of such structural breaks in economic studies, there are numerous methods to detect large breaks in the factor loading matrix. Most of them imposed the factor signal covariance to be fixed, to avoid the observational equivalence of the change in the loading and the change in the factor signal covariance. Otherwise, as in the recent studies [Düker and Pipiras, 2024](#) and [Koo et al., 2024](#), additional layers should be introduced to distinguish if the observable factor loading changes result in changes to the factor space.

By working with the factor space rather than the loading matrix, we can provide a more straightforward way to disentangle a structural change of the transmission rule (the factor loading) from that of the latent signals (the factors), without restrictive assumptions or extra layers

of analysis. Properties 1 in Section 1.2.1 implies that changes of the factor space can capture any changes in the factor loading that are not observationally equivalent to the factor signal covariance changes. In this subsection, we will fully specify the types of structural breaks of our interest captured by factor space changes. To assist this end, let us recall some important characteristics of factor spaces.

As discussed in Section 1.2.1, it is conceptually natural that changes of the rank of the  $\Sigma_f$  or the number of the common factors imply a change in the transmission rule, as an introduction or removal of a factor should involve an emergence or disappearance of specific pathways of transmission. Recall that the factor space  $\mathcal{P}$  corresponds to the normalized factor loading matrix. The information it carries is essentially the ratio of the loadings across the units; in other words, how each unit receives the impact of the latent common factors relative to each other. The factor space contains the distributive characteristic of the factor loading matrix, which is the essence of the concept of the transmission rule.

The way the factor space captures the distributive characteristic of the factor loading is geometrical, or more precisely, directional. It means that one can grasp the transmission rule by directional information in  $N$ -dimensional space, carried by the factor space.

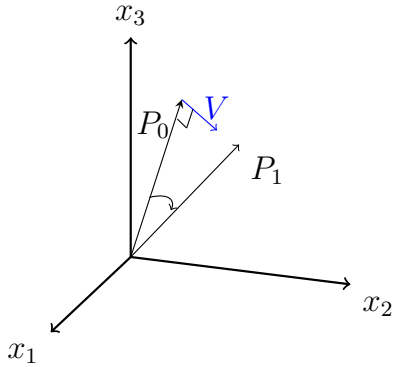


Figure 1.1: A rotating 1-dimensional factor space in  $N = 3$  dimension.  $P_0$  ( $P_1$ ) represents a basis of the regime 0 factor space  $\text{span}(P_0)$  ( $\text{span}(P_1)$ , resp.). (All vectors representing directional information ( $P_0, P_1$ , and  $V$ ) have their lengths normalized to 1.)

For example, let there be 1-dimensional latent factor models governing the process before and after a structural break. To ease the graphical exposition, assume that the cross-sectional dimension is small as  $N = 3$ . (Figure 1.1). In this example, the factor space of regime 0 is the collection of all vectors scaled by any real number,  $\text{span}(P_0) = \{r P_0 \mid \forall r \in \mathbb{R}\}$ , for  $P_0$  a basis vector of unit length. Graphically, it is the line stretched in the direction of the basis vector  $P_0$ . The conventionally chosen unit vector  $P_0$  has sufficient information to convey the directional information. In Figure 1.1, we can read that the units 1 and 2 receive relatively less loading than the unit 3, and the signs of the impact of the latent common factors are equal across all units. This information is given regardless of the absolute strength of the latent factor signal. The same type of interpretation applies to the regime 1 factor space spanned by  $P_1$ . In general, the factor spaces will be subspaces of different dimensions  $K_j$ , conveying the same line of information through multi-dimensional collections of their basis vectors.

We focus on structural breaks that associate new information on the transmission rule compared to the old one. The representation of such a structural break will be directional, as it is a change of the factor space that captures a change in the loading matrix robust to the latent loading-factor specification. Such structural breaks correspond to two types of factor space changes, comparing the true factor space before and after a break. The first type involves directional changes in the basis of the true factor space, preserving the dimension of the factor space. The above-discussed simple example falls into this type, where the existence of the vector  $V$  (Figure 1.1) indicates the occurrence of a directional change keeping the factor space dimension constant, literally and geographically. The second type of change is an increase in the factor space dimension after the break due to the emergence of a new direction to explain the after-break factor space. In general, a factor space change that incurs updated directional information will be a combination of both types of changes. On the contrary, if the factor dimension is reduced without introducing a new direction, we will not consider this a structural break of interest. The major correlation structure of the system can still be explained within the knowledge of the present regime in such cases. We summarize this specification below:

**Assumption 5.** A structural break introduces new directional information to explain the factor space of the new regime. There is no structural break if  $\text{span}(P_1)$  is a subspace of  $\text{span}(P_0)$ .

In Section 1.3, we will introduce a measure of factor space changes designed to capture this type of structural break.

## 1.3 DETECTION OF STRUCTURAL BREAKS

We discussed so far how to capture structural correlation instabilities by changes of the factor space, assuming a latent factor structure. The regime  $j$  factor space, like any linear space, can be identified as the projector operator  $\mathcal{P}_j = P_j P_j'$  projecting any vectors on that space. Such an expression is free from any identification issue of the standard unobservable factor models. In this section, we introduce a measure of factor space changes and construct information criteria to detect the structural breakpoints. Related aspects of estimation will also be discussed.

### 1.3.1 MEASURE OF FACTOR SPACE CHANGE

Assume that there are two time windows  $I_0$  and  $I_1$  indicating two supposed regimes. The level of disparity of the factor spaces  $\mathcal{P}_0$  and  $\mathcal{P}_1$  from two windows can be captured by a distance measure between these two spaces.

**PROJECTION METRIC** The distance between factor spaces can be measured by the following projection metric (Edelman et al., 1998):

$$d_{\text{proj}}(\text{span}(P_0), \text{span}(P_1)) \equiv \sqrt{\text{tr}(\mathcal{P}_0^\perp \mathcal{P}_1)},$$

which is the projected distance between two spaces  $\text{span}(P_0)$  and  $\text{span}(P_1)$  represented by the form of projectors, where  $\mathcal{P}_0^\perp = I_N - \mathcal{P}_0$ . We utilize the square of the projection metric,

$$d(\text{span}(P_0), \text{span}(P_1)) \equiv d_{\text{proj}}^2 = \text{tr}[\mathcal{P}_0^\perp \mathcal{P}_1]. \quad (1.10)$$

The structural breaks of interest stated in Assumption 4 will be captured by the distance measure (1.10) being non-zero, theoretically. Under the specification in Assumption 5, if there is no structural break, the true  $d = 0$ . When the factor space dimensions are not changed across regimes,  $d = 0$  if and only if there is no directional change. When there is no directional change in  $\mathcal{P}_1$  compared to  $\mathcal{P}_0$ , by construction,  $\mathcal{P}_0^\perp \mathcal{P}_1 = \mathbf{0}$ . For the same reason,  $d$  is zero when the factor space dimension is simply reduced without introducing a new basis, as the factor space  $\text{span}(P_1)$  is spanned by a subset of the previously important directions;  $\mathcal{P}_0$  is still orthogonal to  $\mathcal{P}_1$ . On the contrary, if a new direction emerges in  $\mathcal{I}_1$ , then  $d \neq 0$ . For an increased factor space dimension from  $K_0$  to  $K_1$ , there are  $N - K_0$  independent directions consisting  $\mathcal{P}_0^\perp$ . These directions can not be all orthogonal to  $\mathcal{P}_1$ ; if we suppose they are, it implies that there are  $N + K_1 - K_0 > N$  independent bases in an  $N$ -dimensional space, which is a contradiction.

The sample analogue of the distance measure (1.10) will be

$$\hat{d} \equiv \text{tr}[\hat{\mathcal{P}}_0^\perp \hat{\mathcal{P}}_1]. \quad (1.11)$$

We will discuss additional estimation aspects before constructing the information criteria based on the distance measure.

### 1.3.2 ESTIMATION OF THE DISTANCE MEASURE

The benchmark model (Section 1.2.2) is essentially written in terms of the second-moment structure, rather than employing the conventional specification of factor loadings and signals, as in (1.2). In this section, we revisit the connection between our second-moment-level descriptions and the conventional factor model framework, which was partly discussed in Section 1.2.1.

Some more notations are introduced. The symbol  $\mathcal{I}$  denotes the entire time period  $\bigsqcup_{j \in \mathcal{J}} \mathcal{I}_j$ , the disjoint union of the true regime windows  $\mathcal{I}_j$ . The length of each regime is given as

$|I_j| = T_j = \kappa_j T$ , for some constant  $\kappa_j \in (0, 1)$  where  $|I| = T$ . Recall from the models, we have size  $T_j$  data for regime  $j$ , following

$$\mathbf{y}_{j,t} = \boldsymbol{\chi}_{j,t} + \mathbf{u}_t, \quad \text{for all } t \in I_j \quad (2.1)$$

where the corresponding  $\Sigma_{\chi,j} = P_j \Lambda_{\chi,j} P_j'$  has all nonzero  $K_j$  eigenvalues of  $\Lambda_{\chi,j}$  diverging linearly of order  $N$ . Combined with the boundedness of the second moments of the idiosyncratic component (Assumption 2 in Section 1.2.2), this guarantees identifiability of the factor structure at the population level.

The low-rank part  $\boldsymbol{\chi}_{j,t}$  can be specified in a conventional way (Assumption 6). Under such a specification, Assumption 1 in Section 1.2.2 is conditioned on  $B_j$  to absorb the linearly growing eigenvalues of the low-rank component covariance  $\Sigma_{\chi,j}$ , while the second moments of  $\mathbf{f}_t$  are bounded regardless of  $N$ .

**Assumption 6.** For any  $j \in \mathcal{J}$ ,

$$\boldsymbol{\chi}_{j,t} = B_j \mathbf{f}_{j,t}, \quad \text{for all } t \in I_j \quad (1.2)$$

where  $B_j$  denotes the rank  $K_j$  factor loading matrix fixed within regime for a given  $N$ , and  $\mathbf{f}_{j,t}$  denotes  $K_j$  factor signals. The smallest (that is,  $K_j$ -th) eigenvalue of  $B_j' B_j$  is of order  $N$ .

**Assumption 7.**  $(\mathbf{f}_t, \mathbf{u}_t)$  is weakly stationary,  $E[\mathbf{f}_t] = \mathbf{0}^{K_j \times 1}$  and  $E[f_{kt} u_{it}] = 0$  for all  $i \in \mathcal{N}$  and  $k = 1, \dots, K_j$  for  $t \in I_j$  for any  $j \in \mathcal{J}$ .

As the factor signal process  $\mathbf{f}_t$  explicitly enters the model description, the modeling requires more distributional assumptions regarding  $\mathbf{f}_t$  and  $\mathbf{u}_t$ . Mainly,  $\mathbf{f}_t$  and  $\mathbf{u}_t$  present exponential tail bounds (Assumption 8), weak dependence (Assumption 9), and satisfy certain bounded higher moment conditions (Assumption 10). The contents of the following Assumptions 7 to 11 are in line with standard regularity conditions in the related studies, closely resemble Assumptions 1 to 4 of [Fan et al., 2013](#), Section 3, but allowing weak stationarity for  $\mathbf{f}_t$  and  $\mathbf{u}_t$ . Under this set of assumptions, the factor space dimensions and directions are consistent through PCA on the sample covariance matrix, combined with [Bai and Ng, 2002](#). We refer to the original paper ([Fan et al., 2013](#)) for the full discussion.

**Assumption 8.** There exist constants  $r_1, r_2, b_1, b_2 > 0$  such that for any  $s > 0$ , for all  $i \in \mathcal{N}$ , for any  $j \in \mathcal{J}$  and  $k = 1, \dots, K_j$  for  $t \in I_j$ ,

$$\begin{aligned} \sup_{t \in I_j} \Pr(|u_{it}| > s) &\leq \exp\{-s/b_1\}^{r_1}, \\ \sup_{t \in I_j} \Pr(|f_{kt}| > s) &\leq \exp\{-s/b_2\}^{r_2}. \end{aligned}$$

For Assumption 9, denote the  $\sigma$ -fields

$$\mathcal{F}_{L_1}^{L_2} \equiv \sigma(\{(\mathbf{f}_t, \mathbf{u}_t) \mid t \in [L_1, L_2]\})$$

and let the mixing coefficient be

$$\alpha(T) \equiv \sup_{\ell \in \mathbb{Z}} \sup_{A \in \mathcal{F}_{-\infty}^{\ell}, B \in \mathcal{F}_{\ell+T}^{\infty}} |\Pr(A \cap B) - \Pr(A) \Pr(B)|. \quad (1.12)$$

**Assumption 9.** There exist  $C_r > 0$  and  $r_3 > 0$  such that  $3r_1^{-1} + (3/2)r_2^{-1} + r_3^{-1} > 1$ , satisfying  $\alpha(T) < \exp(-C_r T^{r_3})$  for all  $T \in \mathbb{Z}_+$ .

**Assumption 10.** There exists  $C > 0$  such that, for any  $i \in \mathcal{N}$ , for any  $j \in \mathcal{J}$ , and  $s, t \in \mathcal{I}_j$ ,

$$(a) \quad \|\mathbf{b}_{i,j}\|_{max} < C, \text{ for the } i\text{-th row vector } \mathbf{b}_{i,j} \text{ of } B_j.$$

$$(b) \quad \mathbb{E}\left[\left(N^{-1/2}\{\mathbf{u}_{s,j}'\mathbf{u}_{t,j} - \mathbb{E}[\mathbf{u}_{s,j}'\mathbf{u}_{t,j}]\}\right)^4\right] < C,$$

$$(c) \quad \mathbb{E}\left[\|N^{-1/2}B_j'\mathbf{u}_{t,j}\|^4\right] < C.$$

**Assumption 11.**  $\ln(N) = o(T^{\gamma/6})$  for  $\gamma^{-1} \equiv 3r_1^{-1} + (3/2)r_2^{-1} + r_3^{-1} + 1$ , and  $T \asymp N^r$  for some  $r \in (0, 2)$ .

### 1.3.3 INFORMATION CRITERION

We propose an information criterion that integrates two types of model selection – one for determining the presence of a breakpoint and another for identifying the location of a breakpoint, based on the distance measure (1.10).

#### 1.3.3.1 SELECTION BETWEEN MODELS WITH OR WITHOUT A BREAK

The discussion starts by assuming there is potentially one breakpoint in any time domain of interest,  $\mathcal{I}$ , of length  $T$ . A model with a breakpoint will take a point  $t(\tau) = \lfloor \tau T \rfloor \in \mathcal{I}$  for some  $\tau \in (0, 1)$  and hypothesize that there are distinct factor spaces up to the point  $(\mathcal{I}_0(\tau))$  and after  $(\mathcal{I}_1(\tau))$  the point, respectively. Denote  $\hat{\mathcal{P}}_j(\tau)$  the estimated factor space from the window  $\mathcal{I}_j(\tau)$ .

The sample analogue  $\hat{d}(\tau) = \text{tr}[\hat{\mathcal{P}}_0^\perp(\tau)\hat{\mathcal{P}}_1(\tau)]$  measures the information gain by introducing a 'new' regime after  $t(\tau)$ . This gain should be penalized by the complexity of the model having distinct regimes before and after  $t(\tau)$ . Recall that the factor space  $\mathcal{P}_j(\tau)$  is estimated by minimizing  $\text{tr}[\hat{\Sigma}_{u,j}^{\text{sam}}(\tau)]$  in each supposed regime  $\mathcal{I}_j(\tau)$  by following the information criteria of [Bai and Ng, 2002](#). Denote  $T_j = \kappa_j T$  the length of the window  $\mathcal{I}_j(\tau)$  for some constant

$\kappa_j \in (0, 1)$ , omitting the dependence on  $\tau$  to simplify notations. The optimized penalty term of the information criteria of [Bai and Ng, 2002](#),

$$g_j \equiv \hat{K}_j \frac{N + T_j}{NT_j} \ln \left( \frac{NT_j}{N + T_j} \right), \quad (1.13)$$

which solves the optimal factor space  $\hat{\mathcal{P}}_j(\tau)$ , captures the complexity of having one factor model (1.7) in each supposed regime  $\mathcal{I}_j(\tau)$ . Hence, we propose the combined penalties,

$$G(\tau; 1) = G(\{N, T_j, K_j\}_{j \in \mathcal{J}}) = g_0 + g_1, \quad (1.14)$$

to construct the total information gain for having one break at  $t(\tau)$  as follows.

$$\mathcal{S}(\tau; 1) \equiv \ln \text{tr}[\hat{\mathcal{P}}_0^\perp(\tau) \hat{\mathcal{P}}_1(\tau)] - G(\tau; 1). \quad (1.15)$$

The statistic for the model without a breakpoint will be formulated by

$$\mathcal{S}(0) \equiv -G(0), \quad (1.16)$$

where  $G(0)$  denotes the optimized penalty term that fits one approximate factor model for the entire window  $\mathcal{I}$ , such that

$$G(0) \equiv \hat{K} \frac{N + T}{NT} \ln \left( \frac{NT}{N + T} \right).$$

To have a breakpoint at  $b = \tau^* T$  for certain  $\tau^* \in (0, 1)$ , the information gain  $\hat{d}(\tau^*) = \text{tr}[\hat{\mathcal{P}}_0^\perp(\tau^*) \hat{\mathcal{P}}_1(\tau^*)]$  should be sufficiently large to favor the existence of two distinct regimes within  $\mathcal{I}$ . That is, we require

$$\mathcal{S}(\tau^*; 1) > \mathcal{S}(0). \quad (1.17)$$

**Proposition 1.** Assume that there is no breakpoint in  $\mathcal{I}$ . Then for any  $\tau \in (0, 1)$ ,  $\Pr(\mathcal{S}(\tau; 1) < \mathcal{S}(0)) \rightarrow 1$  as  $N, T \rightarrow \infty$ .

The proof is in Appendix A.2. The intuition is as follows. When there is no breakpoint,  $\hat{d}$  approaches  $d = 0$  in probability, and it is stochastically bounded by the largest factor space error of the ones estimated from each of the two supposed regime intervals. We show that it leads to  $\ln \hat{d}$  being dominated by the level of the complexity  $g_j$  of the factor model in the corresponding interval  $\mathcal{I}_j$  of the largest error, almost surely for large  $N, T$ . Besides, as one approximate factor model truly governs the whole time period, the estimated dimensions of factor spaces (number of factors) in any separated windows will be asymptotically the same as the number of factors estimated in the whole window  $\mathcal{I}$ . That is,  $-g_j + G(0)$  is negative

almost surely for large  $N, T$  for any  $j$ . Combined, it concludes that  $\mathcal{S}(\tau; 1) + G(0) < 0$  holds asymptotically almost surely if there is no breakpoint.

### 1.3.3.2 EARLY WARNINGS OF STRUCTURAL BREAKS

Conditional on the existence of a breakpoint, consider the following object  $\underline{\tau}$  maximizing the left side of (1.17), or

$$\underline{\tau} = \operatorname{argmax}_{\tau \in (0,1)} \mathcal{S}(\tau; 1). \quad (1.18)$$

The component  $G(0)$  is omitted from the left side of (1.17) as it is for global information, not depending on local parameters such as  $\tau$ .

The maximum point  $\underline{\tau}$  is the earliest possible location of a breakpoint in a given interval. To elaborate, for the potential existence of a single breakpoint, the maximum point  $\underline{\tau}$  satisfying  $\mathcal{S}(\underline{\tau}; 1) > \mathcal{S}(0)$  indicates the existence of a breakpoint  $\tau^*$  in the location at or after  $\underline{\tau}T$ . Recall that, from the previous subsection,

$$\mathcal{S}(\underline{\tau}; 1) < \mathcal{S}(0), \quad (1.19)$$

implies that there is no breakpoint in the given interval.

As the dependence in  $\tau$  arises only conditional on the existence of a breakpoint, we abbreviate  $\mathcal{S}(\tau; 1) = \mathcal{S}(\tau)$  from now on. The maximum point  $\underline{\tau}$  with the condition  $\mathcal{S}(\underline{\tau}; 1) > \mathcal{S}(0)$  provides information on the existence of a breakpoint in a given interval and its earliest possible location.

**Proposition 2.** Assume that there exists a single breakpoint at  $b^* = \tau^*T$  for some  $\tau^* \in (0, 1)$  in a time window  $I$  of length  $T$ . Let  $\underline{\tau} = \operatorname{argmax}_{\tau \in (0,1)} \mathcal{S}(\tau)$ . Then  $\Pr[\tau^* \geq \underline{\tau}] \rightarrow 1$  in the large  $N, T$  limit.

A description of a perturbed factor space explains this result, which we refer to in Appendix A.2 for the details. When a supposed breakpoint  $\tau$  is later than the true breakpoint, the implied regime  $I_0(\tau)$  has a mixture of two processes. A misspecified factor space, which has a larger dimension than the true factor space, is identified in the large  $N, T$  limit. The implied distance from the wrongly presumed regimes will be zero for  $\tau > \tau^*$ , as the misspecified regime-0 factor space already captures all directional information of the true factor space  $\mathcal{P}_1$ . In addition, the penalty terms cost more in misspecified windows as the apparent dimension of the factor space is larger than the one from the true window.

The proposition extends to the cases with multiple breaks. We assume that as long as there are multiple breakpoints present in a given interval, the regimes are not totally recurrent in the following way:

**Assumption 12.** (NO TOTAL RECURRENCE) Let  $\{\tau_j^*\}_{j=1,\dots,J}$  be breakpoints separating regimes  $j = 0, \dots, J$ . For any partition of the regimes  $\mathcal{R}_0 = \{0, \dots, \underline{j}\}$  and  $\mathcal{R}_1 = \{\underline{j}+1, \dots, J\}$ , there is no total recurrence of the previous regimes  $\mathcal{R}_0$  in the latter regimes  $\mathcal{R}_1$ . That is, for any partition of regimes, there exists  $j \in \mathcal{R}_1$  such that  $\mathcal{P}_j$  was not a factor space of any regime in  $\mathcal{R}_0$ .

**Corollary 3.** Assume that there exists the first breakpoint at  $b^* = \tau_1^* T$  for some  $\tau_1^* \in (0, 1)$  in a time window  $I$  of length  $T$ . Let  $\underline{\tau} = \operatorname{argmax}_{\tau \in (0,1)} \mathcal{S}(\tau)$ . Under Assumption 11,  $\Pr[\tau_1^* \geq \underline{\tau}] \rightarrow 1$  in the large  $N, T$  limit.

Consider two windows  $I_0$  and  $I_1(\tau_1^*)$ , up to and after the first breakpoint  $\tau_1^*$ . The distance between  $\mathcal{P}_0$  and the mixed factor space in  $I_1(\tau_1^*)$  is  $d(\tau_1^*) = \operatorname{tr}[\mathcal{P}_0^\perp \oplus_{j=1}^J \mathcal{P}_j]$ . In comparison, for any  $\tau > \tau_1^*$ , the distance between mixed factor spaces in  $I_0(\tau)$  and  $I_1(\tau)$  is smaller than  $d(\tau_1^*)$ , as, intuitively, the first mixture factor space  $\mathcal{P}_0(\tau)$  captures more directional information as seen in Proposition 2.

Hence, the maximum points  $\underline{\tau}$  can serve as early warnings of structural breaks. Moreover, a subsequent search over the early warning points can locate the breakpoints. In the next subsection, we introduce the algorithm to detect the exact location of multiple breakpoints.

### 1.3.3.3 BREAKPOINT DETECTION ALGORITHM

The following algorithm yields the detection and the locations of the existing unknown number of breakpoints, combining the findings of Propositions 1,2, and Corollary 3.

To simplify notations, for given  $I$  of the length  $T$ , we consider any  $\tau \in (0, 1)$  satisfying  $\tau T \in \mathbb{N}$ , which yields practically the relevant points of inspection. Denote  $\mathcal{S}(\tau|I)$  for the statistics  $\mathcal{S}$  calculated for a supposed breakpoint  $\tau T$  and the subintervals  $I_0(\tau)$  and  $I_1(\tau)$  up to and after the inspected point  $\tau T$ , such that  $I_0(\tau) \sqcup I_1(\tau) = I$ . The maximum point among all such relevant values of  $\tau$  given  $I_j$  will be denoted as  $\underline{\tau}_j = \operatorname{argmax}_{\tau T \in I_j} \mathcal{S}(\tau)$ .

The algorithm starts by examining the maximum point  $\underline{\tau}$  for given  $I$ . If the maximum point  $\underline{\tau}_I$  indicates the existence of a breakpoint in this time period by holding  $\mathcal{S}(\tau|I) > \mathcal{S}(0|I)$ , its location informs the earliest possible time point to have a break. A breakpoint is located at  $\tau^* T \in I$  if the existence of a breakpoint is implied in a given time period  $I$  and there is no breakpoint in either of the intervals up to and after  $\tau^* T$ .

### DETECTION ALGORITHM (MAIN)

**STEP A.** An interval  $I$  of the length  $|I| = T$  is given. For any  $\tau \in (0, 1)$  such that  $\tau T \in \mathbb{N}$ , take the subintervals  $I_0(\tau) = [1, \tau T]$  and  $I_1(\tau) = [\tau T + 1, T]$ , separated by the supposed breakpoint  $\tau T$ . Calculate  $\mathcal{S}(\tau|I)$  for every point  $\tau T \in [L, T - L] \subset I$  for some  $L > 0$ .

Set  $\underline{\tau} = \operatorname{argmax}_{\tau \in (0,1)} \mathcal{S}(\tau|I)$ .

A1. If  $\mathcal{S}(\underline{\tau}|\mathbf{I}) < \mathcal{S}(0|\mathbf{I})$ , conclude that there is no breakpoint in  $\mathbf{I}$ .

A2. If  $\mathcal{S}(\underline{\tau}|\mathbf{I}) > \mathcal{S}(0|\mathbf{I})$ , move on to the next Step B.

STEP B. Set  $\tilde{\mathbf{I}}_1 = [\underline{\tau}T + 1, T]$  and  $\underline{\tau}_1 = \operatorname{argmax}_{\tau \in \tilde{\mathbf{I}}_1} \mathcal{S}(\tau|\tilde{\mathbf{I}}_1)$ . Inspect the interval  $\tilde{\mathbf{I}}_1$ .

B1. If  $\mathcal{S}(\underline{\tau}_1|\tilde{\mathbf{I}}_1) < \mathcal{S}(0|\tilde{\mathbf{I}}_1)$ , there exists no breakpoint later than  $\underline{\tau}$ . Conclude that the interval  $\mathbf{I}$  has a single breakpoint at  $\hat{\tau}^* = \underline{\tau}$ .

B2. If  $\mathcal{S}(\underline{\tau}_1|\tilde{\mathbf{I}}_1) > \mathcal{S}(0|\tilde{\mathbf{I}}_1)$ , inspect  $\tilde{\mathbf{I}}_0 = [1, \underline{\tau}_1 T]$ .

B2-1. If  $\mathcal{S}(\underline{\tau}|\tilde{\mathbf{I}}_0) < \mathcal{S}(0|\tilde{\mathbf{I}}_0)$ , inspect  $\underline{\tau}_0 = \operatorname{argmax}_{\tau \in \tilde{\mathbf{I}}'_0} \mathcal{S}(\tau|\tilde{\mathbf{I}}_0)$  for  $\tilde{\mathbf{I}}'_0 = [\underline{\tau}T, \underline{\tau}_1 T]$ .

B2-1-1. If  $\mathcal{S}(\underline{\tau}_0|\tilde{\mathbf{I}}_0) < \mathcal{S}(0|\tilde{\mathbf{I}}_0)$ , conclude no breakpoint in  $\tilde{\mathbf{I}}_0$ . Repeat the process from Step B with updated  $\tilde{\mathbf{I}}_1 = [\underline{\tau}_1 T + 1, T]$ .

B2-1-2. If  $\mathcal{S}(\underline{\tau}_0|\tilde{\mathbf{I}}_0) > \mathcal{S}(0|\tilde{\mathbf{I}}_0)$ , take  $\tau_1^* = \underline{\tau}_0$  and update  $\tilde{\mathbf{I}}_1 = [\underline{\tau}_0 T + 1, T]$ . Check whether  $\mathcal{S}(\underline{\tau}_1|\tilde{\mathbf{I}}_1) > \mathcal{S}(0|\tilde{\mathbf{I}}_1)$ . If it is true, the process repeats from Step B for the updated  $\tilde{\mathbf{I}}_1 = [\underline{\tau}_1 T + 1, T]$ . If this is not the case, the process repeats from Step A for the updated  $\mathbf{I} = [\underline{\tau}_0 T + 1, T]$ .

B2-2. If  $\mathcal{S}(\underline{\tau}|\tilde{\mathbf{I}}_0) > 0$ , conclude that the location of the first breakpoint  $\tau_1^* = \underline{\tau}$ . Repeat the process from Step B with the updated  $\tilde{\mathbf{I}}_1 = [\underline{\tau}_1 T + 1, T]$ .

Continued from Step B2-1 or Step B2-2, repeat the algorithm by taking new inspected windows to locate the first breakpoint (the case of B2-1-1) or the second or the next breakpoint (the case of B2-1-2 or B2-2).

We break down the algorithm. A given interval  $\mathbf{I}$  is concluded to have no breakpoint in Step A1, following Proposition 1. Step A2 determines the existence of a breakpoint, combining Propositions 1 and 2, as discussed in the previous subsection. The location of the first breakpoint can be concluded by inspecting the later intervals after the early warning points. For example, in the case of a single breakpoint, the location is the same as one of the early warning points if the time window after a certain warning point has no breakpoint, as seen in Step B1. Step B2 primarily considers whether the warning point identified in Step A was too early. If there is another warning point ( $\underline{\tau}_1$ ) in the later window  $\mathbf{I}_1$ , it can be the case that either the previous warning point ( $\underline{\tau}_0$ ) was too early or there are multiple breakpoints. These cases can be distinguished by examining the previous window  $\tilde{\mathbf{I}}_0$ . As a breakpoint in  $\tilde{\mathbf{I}}_0$  is also a breakpoint in  $\mathbf{I}$ , and Step A guarantees that there is no breakpoint before  $\underline{\tau}$ , hence we examine only the points from  $\underline{\tau}$  in Step B2-1. In Step B2-1-1, if  $\mathcal{S}(\underline{\tau}_0|\tilde{\mathbf{I}}_0) < \mathcal{S}(0|\tilde{\mathbf{I}}_0)$ , there is no breakpoint among the points  $\tau \geq \underline{\tau}$ , hence no breakpoint in  $\tilde{\mathbf{I}}_0$ .

If  $\mathcal{S}(\underline{\tau}_0|\tilde{\mathbf{I}}_0) > \mathcal{S}(0|\tilde{\mathbf{I}}_0)$ , it indicates a breakpoint in  $\tilde{\mathbf{I}}_0$  which is later than  $\underline{\tau}$ . The existence of such  $\underline{\tau}_0 \geq \underline{\tau}$  implies that  $\underline{\tau}$  cannot be a breakpoint by Propositions 1 and 2. It also implies that this location of the breakpoint was missed by the next warning point  $\underline{\tau}_1$ . These cases deviate

from the asymptotic property of the maximum points (Proposition 2 and Corollary 3). Step B2-1-2 is necessary only due to the potential presence of a weak factor structure in a small  $N, T$  environment. We will demonstrate in the next section that the frequency of such occurrences converges to zero, given the presence of a strong factor structure in the simulations.

The location of  $\underline{\tau}_0$  is a refinement of the previous early warning point  $\underline{\tau}$ . Once refined, the warning point is taken as the breakpoint of  $\tilde{\mathbf{I}}_0$  in Step B2-1-2. In principle, the location of the breakpoint in  $\tilde{\mathbf{I}}_0$  can be further refined by re-examining the location of  $\underline{\tau}_1$  subsequently. However, the total re-inspection of subsequent windows will be an expensive calculation. The location of the subsequent warning point  $\underline{\tau}_1$  is also re-examined if necessary, but considering relative positions with the next warning point, not with the previous warning points, to minimize the number of repeated backward inspections. In the results, the algorithm refines the location of each warning point at most once. In the simulation, we demonstrate that the proposed algorithm performs effectively.

As discussed, Step B2-1-2 will unlikely occur with the assumed strong factor structure. If the condition  $\mathcal{S}(\underline{\tau}|\tilde{\mathbf{I}}_0) < \mathcal{S}(0|\tilde{\mathbf{I}}_0)$  of Step B2-1 is met, it implies that  $\underline{\tau}$  was a too-early warning point, and it is  $\underline{\tau}_1$  that informs the location closer to the actual breakpoint. The entire process of recalculation in Steps B2-1-1 and B2-1-2 is unnecessary, as the conclusion reached with or without re-examination will be the same.

Hence, with an assumed strong factor structure, the proposed algorithm will perform as the following simplified process:

#### DETECTION ALGORITHM (SIMPLIFIED)

STEP A. An interval  $\mathbf{I}$  of the length  $|\mathbf{I}| = T$  is given. For any  $\tau \in (0, 1)$  such that  $\tau T \in \mathbb{N}$ , take the subintervals  $\mathbf{I}_0(\tau) = [1, \tau T]$  and  $\mathbf{I}_1(\tau) = [\tau T + 1, T]$ , separated by the supposed breakpoint  $\tau T$ . Calculate  $\mathcal{S}(\tau|\mathbf{I})$  for every point  $\tau T \in [L, T - L] \subset \mathbf{I}$  for some  $L > 0$ .

Set  $\underline{\tau} = \operatorname{argmax}_{\tau \in (0, 1)} \mathcal{S}(\tau|\mathbf{I})$ .

A1. If  $\mathcal{S}(\underline{\tau}|\mathbf{I}) < \mathcal{S}(0|\mathbf{I})$ , conclude that there is no breakpoint existing in  $\mathbf{I}$ .

A2. If  $\mathcal{S}(\underline{\tau}|\mathbf{I}) > \mathcal{S}(0|\mathbf{I})$ , move on to the next step B.

STEP B. Set  $\tilde{\mathbf{I}}_1 = [\underline{\tau}T + 1, T]$  and  $\underline{\tau}_1 = \operatorname{argmax}_{\tau T \in \tilde{\mathbf{I}}_1} \mathcal{S}(\tau|\tilde{\mathbf{I}}_1)$ . Inspect the interval  $\tilde{\mathbf{I}}_1$ .

B1. If  $\mathcal{S}(\underline{\tau}_1|\tilde{\mathbf{I}}_1) < \mathcal{S}(0)$ , there exists no breakpoint later than  $\underline{\tau}$ . Conclude that the interval  $\mathbf{I}$  has a single breakpoint at  $\hat{\tau}^* = \underline{\tau}$ .

B2. If  $\mathcal{S}(\underline{\tau}_1|\tilde{\mathbf{I}}_1) > \mathcal{S}(0)$ , inspect  $\tilde{\mathbf{I}}_0 = [1, \underline{\tau}_1 T]$ .

B2-1. If  $\mathcal{S}(\underline{\tau}|\tilde{\mathbf{I}}_0) < 0$ , conclude that there is no breakpoint in  $\tilde{\mathbf{I}}_0$ .

B2-2. If  $\mathcal{S}(\underline{\tau}|\tilde{\mathbf{I}}_0) > 0$ , conclude that the location of the first breakpoint  $\tau_1^* = \underline{\tau}$ .

Continued from Step B2-1 or Step B2-2, repeat the algorithm by taking  $\mathbf{I} = [\underline{\tau}_1 T + 1, T]$ , to locate the first breakpoint (the case of B2-1) or the second or the next breakpoint (the case of B2-2).

The reasoning of taking  $\tau_1^* = \underline{\tau}$  is straightforward. By Proposition 1, there can be no breakpoint before  $\underline{\tau}$  in  $\tilde{\mathbf{I}}_0$  or in  $\mathbf{I}$ . There can be no breakpoint after  $\underline{\tau}$  as well, otherwise it contradicts  $\underline{\tau}_1$  is the earliest point of break in  $\tilde{\mathbf{I}}_1$ . The repeated algorithm will settle the location of the consecutive breakpoints. The proposed algorithm with refinement steps performs by approximating the same line of logic as this simplified version.

## 1.4 SIMULATIONS

We present the results of the detection of single or double breakpoints applying the main detection algorithm in Section 1.3.3.3. The entire available length of time periods is denoted as  $T = \sum_j T_j$ , the sum of the length of all supposed regimes  $T_j$ . The cross-sectional dimension is fixed to  $N = 100$  in any regime. Each regime has  $K_j = 3$  dimension of the factor space. We assume  $\mathbf{f}_t \sim \mathcal{N}(\mathbf{0}_{3 \times 1}, \sigma_f^2 I_3)$ , loaded by  $P_0$  during the first regime, and  $\mathbf{u}_t \sim \mathcal{N}(\mathbf{0}_{N \times 1}, \sigma_u^2 I_N)$ . In the following exposition, we fix  $\sigma_u^2 = 2$  and vary  $\sigma_f^2$ . The seeds of the random signal draw are fixed for entire 500 trials. The underlying sequence of the factor spaces is fixed as well.  $\text{span}(P_0)$ ,  $\text{span}(P_1)$  and  $\text{span}(P_2)$  are constructed from a randomly chosen orthonormal  $N \times K_0$  matrix  $P_0$  fixing the distances between two subsequent factor spaces, based on the distance measure (1.10). The caption numbers of the figures in this section indicate the corresponding scenarios they represent.

### 1.4.1 ESTIMATION OF SINGLE BREAKPOINT LOCATIONS

We first present how the maximization of the statistics (1.15) performs in the cases of existing single breakpoints in various relative locations, accompanied by the criteria for the existence of a breakpoint (1.17). We inspect the stride-1 grid in the window of inspection that consists of 20 time points before and after the true location of the breakpoint ('BP'),  $[BP - 20, BP + 20]$ . The following relative locations of the breakpoint are considered:

- (a) A breakpoint located centrally at  $BP = 100$ , with  $T_0 = 100$  and  $T_1 = 100$  before and after the break.
- (b) A central breakpoint at  $BP = 50$ , with shorter time spans before and after the break,  $T_0 = 50$  and  $T_1 = 50$ , than case (a).
- (c) A breakpoint located on the left side of the entire time window ( $T$ ) at  $BP = 50$ , with a shorter time span before ( $T_0 = 50$ ) than after ( $T_1 = 100$ ) the break.

- (d) A breakpoint located on the right side of the entire time window ( $T$ ) at  $BP = 100$ , with a shorter time span after ( $T_1 = 50$ ) than before ( $T_0 = 100$ ) the break.

The table below shows the number of trials that correctly conclude a single breakpoint at the exact location out of 500 total number of trials. The inspected range of the relative intensity of the factor signals  $SN \equiv \sigma_f^2/\sigma_u^2$  is from 10 to 30. In the application to the high-dimensional data, we found that the relative strength of the factor signals easily exceeds 10 for regimes before and after the structural breakpoints of interest.

$SN = \sigma_f^2/\sigma_u^2$	10	12.5	15	17.5	20	22.5	25	27.5	30
(a) BP = 100, center	37.8	75.2	85	88.2	90.8	93	93.4	94.2	95
(b) BP = 50, center	5.6	15.8	34.2	54.8	70.2	78.4	84	86.4	88
(c) BP = 50, left	14	20.8	36.6	53.6	66	76.4	81.8	85.2	86.6
(d) BP = 100, right	14	42.6	63.2	72.2	78	79.4	81.6	83.4	84.8

Table 1.1: Success rate of detecting a single breakpoint at the exact location  
(%, out of 500 trials)

The results for the central breakpoints (a) and (b) in Table 1.1 suggest that the detection scheme will successfully detect a breakpoint with higher probability when there is a longer duration of the time window before and after the breakpoint. The detection criteria conclude the single breakpoint at the exact location for 75% of the trials with relatively less intense factor signals ( $SN = 12.5$ ) for scenario (a), where the durations of the before and after regimes are comparable to the size of the cross-section  $N = 100$  as shown in Figure 1.2.

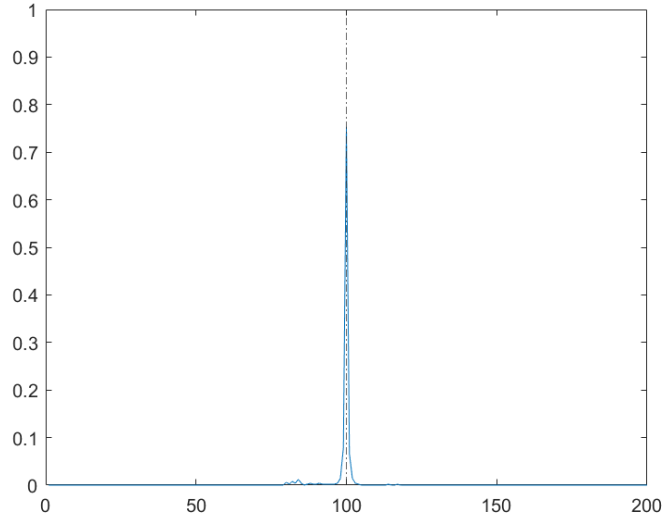
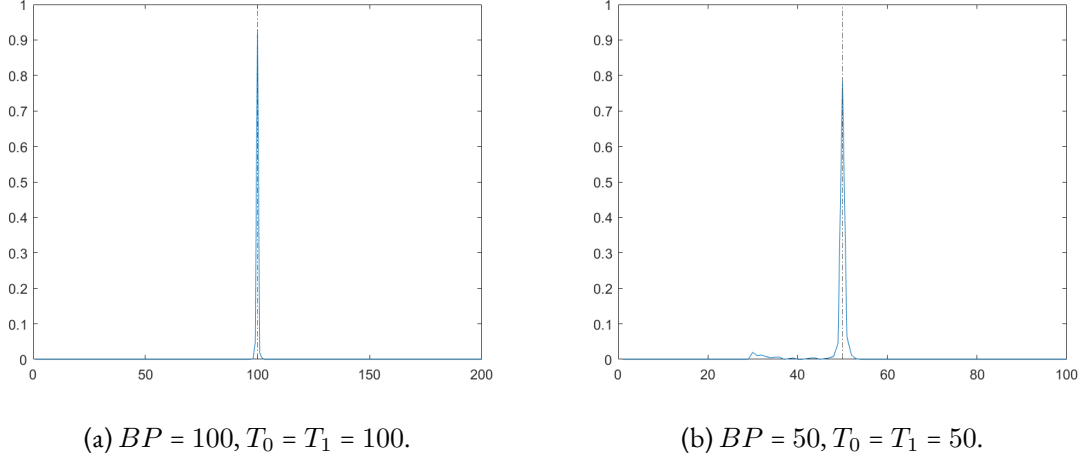
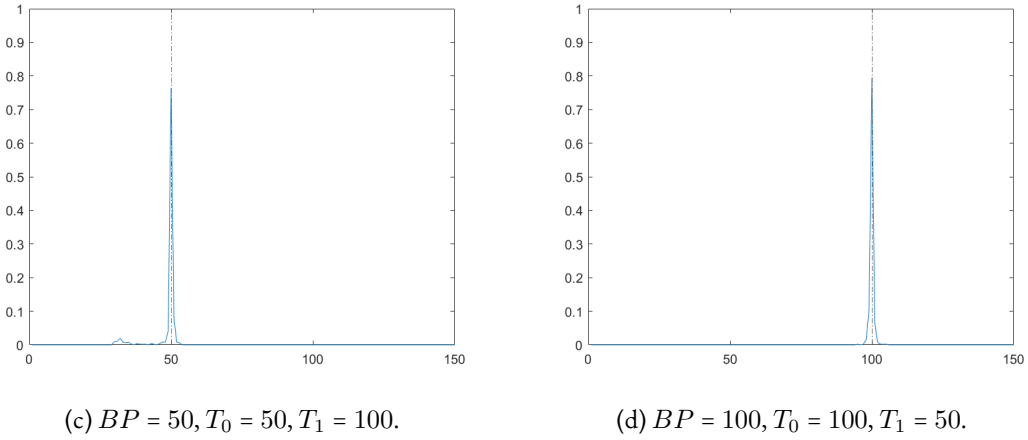


Figure 1.2: (a)  $BP = 100$ ,  $T_0 = T_1 = 100$  ( $SN = 12.5$ ).

The examples for  $SN$  over 20 in Figure 1.3 and Figure 1.4 indicate the performance of the detection for the various scenarios. In particular, when the durations of two regimes are

asymmetric, having a shorter time span after a break (scenario (d)) performs better than having a shorter time span before a break (scenario (c)) for cases of low or moderate relative signal strength of the factors ( $SN$ ). Given the lengths of the subsequent regimes, the results for varying  $SN$  for all scenarios indicate that the performance of the detection of a single breakpoint will improve under the presence of sufficiently intense factor signals.

Figure 1.3: Central Breakpoints,  $SN = 22.5$ .Figure 1.4: Side Breakpoints,  $SN = 22.5$ .

### 1.4.2 DETECTION OF NO BREAKPOINT

Now, consider the case where there is no breakpoint in the entire window of the length  $|I| = 100$ . The same settings generate the data as in the previous subsection, but the directional factor loading  $P$  is fixed to  $P_0$ . In this simulation, it is the stride-1 grid in the window  $[20, 80]$  inspected, that is, the entire  $I$  except the first and last 20 time points. For cases with relatively weak factor structures  $SN \leq 10$ , the factor space estimation becomes noisy for points closer to the beginning and end of the inspection windows. We perform the detection by imposing the maximum number of BPs as simply 1 and we count the number of trials that correctly

detected no breakpoint out of  $M = 500$  trials for each setup. The following Table 1.2 presents the results from  $SN > 10$ .

$SN = \sigma_f^2 / \sigma_u^2$	12.5	15	17.5	20	22.5	25	27.5	30	32.5	35
Success Rate	4.4	16.4	35.2	59.2	75.4	88.6	95.6	98.8	99.8	100

Table 1.2: Success rate of concluding No BP  
(%, out of 500 trials)

The success rate increases as the  $SN$  ratio increases. The performances for different settings of the maximum BP are identical.

### 1.4.3 MULTIPLE BREAKPOINTS

Now, let us discuss the result of the detection of multiple breakpoints. Consider two breakpoints with different time spans before and after as the following scenarios,

(A)  $BP_1 = 50$  and  $BP_2 = 100$  in the entire time window of length  $T = 150$ .

(B)  $BP_1 = 70$  and  $BP_2 = 140$  in the entire time window of length  $T = 210$ .

Again, the finest grid with stride 1 will be inspected, yet without restricting the window of inspection in a neighborhood of the true breakpoints. The inspection covers the whole window except the first and last 20 time points, which is less than 15% of the shortest entire window length  $T = 150$  of scenario (A). For each scenario, the detection proceeds to find maximum 5 breakpoints.

Table 1.3 below shows the number of detections across 500 trials counted as successful, based on the following criteria. First, it should conclude the existence of the correct number of breakpoints, two. Second, the estimated breakpoints concluded as either the first (out of two breakpoints) or the second (out of two breakpoints) are located within the neighborhood  $[BP_t - a, BP_t + a]$  of the true breakpoint  $BP_t$  of radius  $a$ , which is 10% of the duration of one regime;  $a = 5$  in case (A) and  $a = 7$  in case (B). The success rate is reported separately for each breakpoint and jointly as well. We present the range of the  $SN$  from over 10 to over 30 in the following table. The existence of multiple breakpoints undermines the performance of the detection for relatively low  $SN$ . For example, in case (A) with a shorter window size, the success rate of locating the first or second BP in the target neighborhood is less than 1% when  $SN = 10$ .

$SN = \sigma_f^2 / \sigma_u^2$			12.5	15	17.5	20	22.5	25	27.5	30	32.5
(A)	$(BP_1, BP_2)$ $= (50, 100)$	$BP_1$	2.4	5.6	8.6	16.8	31.2	45	59.2	75.4	84.2
		$BP_2$	5.6	7.4	16.2	27.8	45.4	55.6	65.2	77.6	80.4
		Joint	1	1.4	5.8	14.4	28.8	43.2	56.6	70.6	76.4
(B)	$(BP_1, BP_2)$ $= (70, 140)$	$BP_1$	4.8	4.4	11.4	18.4	40.2	61.4	73	85.4	92.8
		$BP_2$	3.2	5.8	15.8	29.2	50.4	67.6	77	85.8	88.6
		Joint	1	1.6	7.6	16.2	37.8	59.4	70.2	82.6	87.2

Table 1.3: Success rate of detecting two BPs located in the target neighborhoods  
(%, out of 500 trials)

The correct detection rates are higher in case (B), which features a longer duration of subsequent regimes. The success rate for case (B) is still higher when we narrow down the target neighborhood to match that of case (A). Figure 1.5 shows a comparison of the success rates calculated separately for two breakpoints.

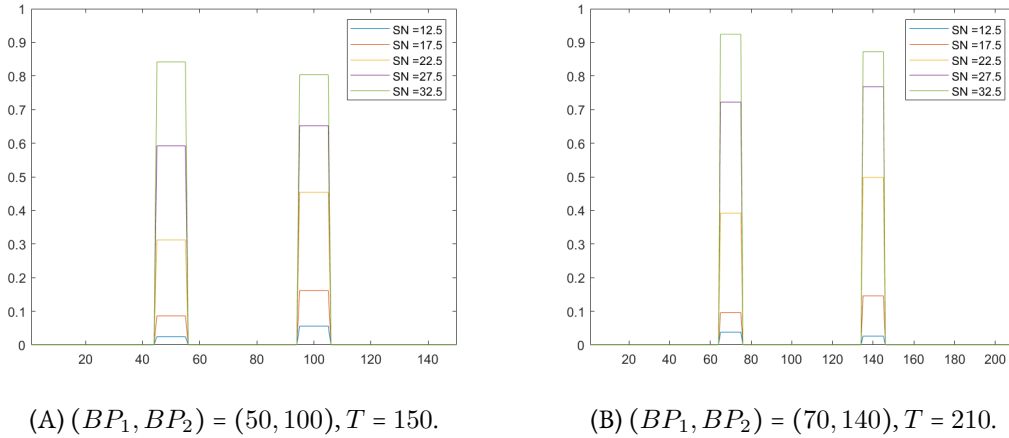


Figure 1.5: Success rates for the target neighborhoods of radius 5 (separately for each BP)

The success rates of detecting two breakpoints jointly within the target neighborhoods are shown in Figure 1.6. The results show improved performance in the joint detection where there is a strong enough factor structure within each regime.

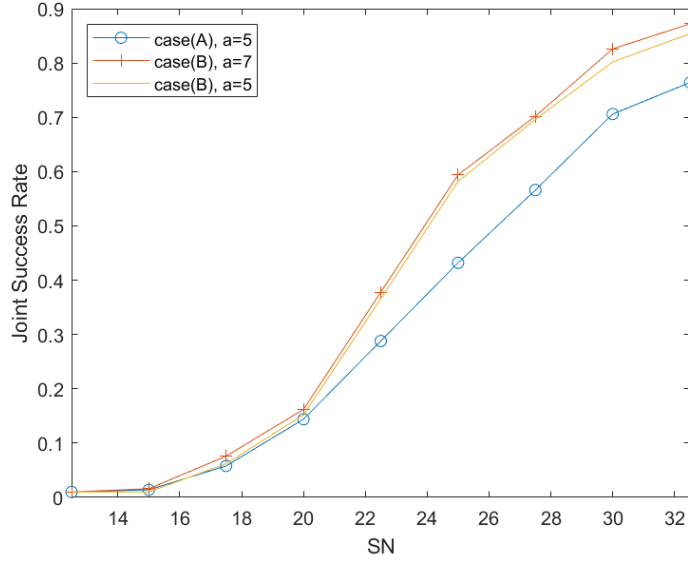


Figure 1.6: Joint Success Rates

#### 1.4.4 THE MAIN TO THE SIMPLIFIED ALGORITHM

As discussed in Section 1.3.3.3, the main algorithm can be simplified. We present how frequently the refinement steps in Step B2-1-2 of the main algorithm were activated out of 500 trials in varying scenarios of breakpoint locations. Note that any steps in the algorithm, including Step B2-1-2, can be activated multiple times in each trial during the grid search. The counts in Figure 1.7 reflect all such multiple activations. It shows that with a stronger factor structure (higher  $SN$ ), the activation of the refinement steps becomes increasingly rare across all scenarios considered. The main algorithm can be simplified under the assumption of a strong factor structure.

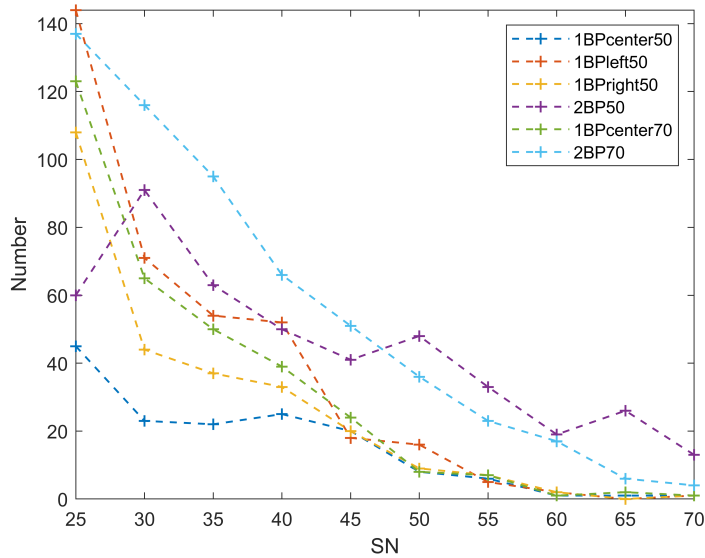


Figure 1.7: Number of Refinement Steps Activated

## 1.5 APPLICATIONS

The proposed method of structural breakpoint estimation will be applied to two different environments. The first application is to the S&P 500 daily return panel to analyze early instabilities relevant to the early developments of the global financial crisis. The second application is to a collection of macroeconomic and financial variables at monthly frequency introduced in [McCracken and Ng, 2016](#). An EM algorithm ([Stock and M. W. Watson, 2002a](#)) is performed to approximate PCA with missing values.

### 1.5.1 INSTABILITIES IN THE STOCK MARKET DURING THE EARLY STAGES OF THE GLOBAL FINANCIAL CRISIS

It is widely accepted that the global financial crisis started in mid-2007. We examined the structural breaks in the correlation structure of the panel of S&P 500 daily returns (log price differences) from the CRSP database, for the trading days from January 2, 2004 to June 1, 2007. The constituent list is based on July 31, 2007.

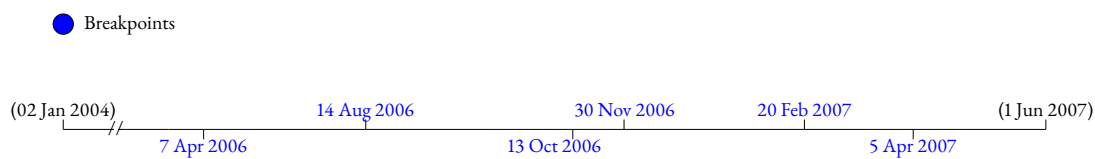


Figure 1.8: Instabilities in 2006 to mid 2007, S&P 500 Panel

The earliest breakpoint is estimated to be in early April of 2006. The locations of the breakpoints are consistent with the development of the subprime mortgage crisis behind the economic landscape from early 2006, which was still perceived as optimistic at the time. During the early to mid-2006, the housing price bubble peaked ([Phillips and J. Yu, 2011](#)), and the lowest credit score mortgages showed the fastest growth in the second and third quarters of 2006 ([Albanesi et al., 2022](#)). By the end of 2006, precursors of financial market instability had already emerged, including an increasing delinquency rate of subprime loans reported by several lenders, such as Ownit, New Century, and Novastar ([Mayer et al., 2009](#)). These lenders subsequently reported losses or filed for bankruptcy between the end of 2006 and early April 2007. Novastar reported "a surprise loss" on February 20, and New Century Financial filed for Chapter 11 bankruptcy protection on April 3rd, following the timeline sources from [Guillén, 2015](#) and the Joint Economic Committee report of the United States Congress, 2008 ([JEC, 2008](#)).

## 1.5.2 STRUCTURAL BREAKS IN CROSS-VARIABLE CORRELATIONS AMONG MACROECONOMIC AND FINANCIAL INDICATORS

The data collection first introduced in [McCracken and Ng, 2016](#) is a set of macroeconomic and financial variables at a monthly frequency. Among the continuously updated data vintages, we use the vintage of February 2025, which contains  $N = 126$  macro-financial variables from January 1959 to February 2025. The variables are normalized following various schemes, reported in detail in the database <sup>4</sup>. Over the entire time span, we found two breakpoints at **1998 December** and **2018 December**. Although it can only be speculative without further investigation, we suggest the following possible factors behind these breakpoints.



Figure 1.9: Instabilities in Macro-Financial Variables, 1959 - 2025 February

**DECEMBER 1998** One possible factor of structural break is the repeal of the Glass-Steagall Act in 1999. The Glass-Steagall legislation, enacted in 1933 after the financial market crash during the Great Depression, introduced provisions that separated commercial and investment banking. It came under critical pressure in 1998 during the merger of Travelers Group and Citicorp ([Sherman, 2009](#)). The systemic impact of this repeal has been studied widely before and after the global financial crisis (for example, [Stiroh and Rumble, 2006](#), [Laeven and Levine, 2009](#), [Schmid and Walter, 2009](#), [Acharya et al., 2006](#), [Demirgüç-Kunt and Huizinga, 2010](#), [DeYoung and Torna, 2013](#), and [Shleifer and Vishny, 2010](#)).

**DECEMBER 2018** There are several potential factors for a structural break around December 2018. One possible speculation relates to the policy shifts in the United States during President Trump's first term. The trade war between the U.S. and China began and escalated throughout 2018, while economic nationalism gained popularity worldwide. The potential structural impact of these developments has been explored in various studies, including [Fajgelbaum et al., 2020](#), [Amiti et al., 2019](#), [Amiti et al., 2020](#), [Freund et al., 2021](#), and [Dinopoulos et al., 2024](#).

In both of the empirical exercises, we found that once a breakpoint is detected at a certain location, the result is not overly sensitive to a reduced number of post-break data points. Although the proposed detection method is not a fully sequential or online method, it can enable a semi-real-time application.

<sup>4</sup><https://www.stlouisfed.org/research/economists/mccracken/fred-databases>

## 1.6 CONCLUDING REMARKS

We present a novel method for detecting instabilities in cross-correlation structures using a latent factor model framework. The proposed method is built on an intuitive distance between the column spaces of the loading matrix. It provides a measure of structural correlation changes free from the inherent identification issue of latent factor models. The proposed information criterion and algorithm integrate both the detection and localization of structural breakpoints. Our method also provides a framework for identifying the earliest possible point of structural change.

In applications to a stock return panel and a macro-financial variable collection, our methods detect early instability points preceding the global financial crisis, as well as major policy shifts that can reasonably be expected to lead to structural changes, consistent with the historical developments.

# APPENDIX TO CHAPTER 1

## A.1 EXTENDED DISCUSSION ON COVARIANCE DYNAMICS AND FACTOR SPACE CHANGE

### A.1.1 SECTION 1.2.1

**Properties 1.** Assume the decomposability (1.3) is guaranteed.  $\mathcal{P}$  is invariant under any rank preserving change of  $\Sigma_f = E[\mathbf{f}_t \mathbf{f}_t']$ .

*Proof.* Let  $\mathring{\mathbf{f}}_t$  be a stationary  $K$ -dimensional process with  $E[\mathring{\mathbf{f}}_t \mathring{\mathbf{f}}_t'] = I_K$ . First, we emphasize that any possible  $\Sigma_f - K(K + 1)/2$ -dimensional object – is fully parametrized by two operations:  $\mathcal{D} : \mathring{f}_t \mapsto D \mathring{f}_t$  for any diagonal matrix  $D$  ( $K$ -dimension), a variance change from the hypothetical  $\mathring{f}_t$ , and  $\mathcal{Q} : \mathring{f}_t \mapsto Q \mathring{f}_t$  for any orthonormal matrix  $Q$  ( $QQ' = Q'Q = I_K$ ,  $K(K - 1)/2$  dimension) that is, a correlation structure change from  $\mathring{f}_t$ . Observe that the object  $\mathcal{P} = PP'$  is invariant under transformation  $\mathcal{Q}$  due to orthonormality. Moreover,  $\mathcal{P} = PP'$  is invariant under  $\mathcal{D}$  as the eigenvector information  $P$  is not affected by the change of the diagonal scales. It implies as well,  $\mathcal{P}$  is invariant under a change from any  $\Sigma_f \mapsto I_K$ . Second, any change  $\Sigma_f \rightarrow \tilde{\Sigma}_f$  is a composition of a change  $\Sigma_f \mapsto I_K$  and  $I_K \mapsto \tilde{\Sigma}_f$ . Then the arguments we have just made conclude  $\mathcal{P}$  is invariant under  $\Sigma_f \rightarrow \tilde{\Sigma}_f$ , as it is invariant under both parts of the composition.  $\square$

### A.1.2 SECTION 1.2.2

#### A.1.2.1 BENCHMARK ASSUMPTIONS

This section aims to provide extended comments on the benchmark model Section 1.2.2. We discuss how the characteristic of covariance dynamics stated in Assumption 4 is aligned with the hypothesized factor structures in both regimes stated in Assumptions 1 and 2. Especially the substantiality of the off-diagonal perturbation can be, in fact, proven, although it was simply stated as an assumption to avoid lengthy extra discussions in the main section.

Let us first recall some facts on the subspace representation to assist our discussion. As employed in [Davis and Kahan, 1970](#) as well, one of the most popular ways of identifying a linear space  $\text{span}(P_j)$  is to identify it by  $P_j P_j'$ , the projector operator on the space  $\text{span}(P_j)$  itself.

In practice, it is convenient to identify  $\text{span}(P_j)$  by any chosen column orthonormal basis  $P_j$  (i.e.,  $P_j' P_j = I_{K_j}$ ) up to  $K_j$ -dimensional orthogonal transformation  $\mathcal{O}$ ; the projector operator is invariant under any internal rotation done by  $O \in \mathcal{O}$ , such that  $P_j O O' P_j' = P_j P_j'$  as  $O' O = O O' = I_{K_j}$ .  $P_j$  is called a *Stiefel* matrix and extensively studied; we refer [Edelman et al., 1998](#) or [Chikuse, 2003](#) for a short or an extensive introduction, respectively.

For a pair of Stiefel matrices  $P_0$  and  $P_1$ , we can decompose  $P_1$  into the direction of the  $\text{span}(P_0)$  and the  $\text{span}(P_0)^\perp$ , as in Section 3.2.1 of [Chikuse, 2003](#). As  $K_j \ll N$ , we state for the cases (i)  $K_1 \leq K_0 < N - K_0$  and (ii)  $K_0 < K_1 < N - K_0$ .

**Properties 2.** [Theorem 3.2.1 (i),(ii) of [Chikuse, 2003](#)]

- (i) Let  $K_1 \leq K_0 < N - K_0$ . Then there exists Stiefel matrices  $H_{K_0 \times K_1}$  and  $V_{N \times K_1}$ , a diagonal matrix  $T_{K_1 \times K_1}$  with each diagonal element  $t_h \in (0, 1)$ , an orthogonal transformation  $O \in \mathcal{O}(K_1)$  such that

$$P_1 = P_0 H T O' + V S O' \quad (\text{A.20})$$

where  $S \equiv (I - T^2)^{1/2}$  and  $P_0' V = \mathbf{0}_{K_0 \times K_1}$ .

- (ii) Let  $K_0 < K_1 < N - K_0$ . Then there exists a Stiefel matrix  $V_{N \times K_1}$ , a diagonal matrix  $T_{K_0 \times K_0}$  with each diagonal element  $t_h \in (0, 1)$ , orthogonal transformations  $H \in \mathcal{O}(K_0)$  and  $O \in \mathcal{O}(K_1)$  such that,

$$P_1 = P_0 [H \ \mathbf{0}_{K_0 \times (K_1 - K_0)}] \text{diag}(T, \mathbf{0}_{K_0 \times (K_1 - K_0)}) O' + V S O' \quad (\text{A.21})$$

where  $S \equiv \text{diag}((I - T^2)^{1/2}, I_{K_1 - K_0})$  and  $P_0' V = \mathbf{0}_{K_0 \times K_1}$ . ( $\text{diag}(A, B)$  denotes a block diagonal matrix with matrices A and B on the diagonal.)

What matters to measure the distance of the factor spaces is the component of  $P_1$  – up to orthogonal transformation  $\mathcal{O}(K_1)$  – that is orthogonal to  $\text{span}(P_0)$ . The expressions (A.20) and (A.21) provide enough to describe the necessary information of factor space dynamics. In other words, one can derive the expression of the factor space change invariant under the choice of basis  $P_0$  and  $P_1$  from (A.20) or (A.21). First, let us note that the original result Theorem 3.2.1 of [Chikuse, 2003](#) is about the decomposition of a Stiefel matrix  $P_1$  on  $\text{span}(P_0)$  and  $\text{span}(P_0)^\perp$ . The results are meant to be universal under the choice of basis  $P_0$ . For an arbitrarily chosen basis  $P_0$ , the second component in (A.20) or (A.21) corresponds to the projection of  $P_1$  on  $P_0^\perp P_0^{\perp'} \equiv I - P_0 P_0'$ , that is,  $V S O' = P_0^\perp P_0^{\perp'} P_1 = P_0^\perp P_0^{\perp'} V S O'$  where  $S$  is defined respectively for case (i) and (ii). In any cases,  $P_0^\perp P_0^{\perp'} V = V$  and the expression of  $V$  is invariant of the choice of the regime 0 basis  $P_0$ .

Besides, (A.20) and (A.21) lead universal results for the decomposition of *any* column orthonormal basis representation  $P_1$  of  $\text{span}(P_1)$ . If one considers a basis representation

$\tilde{P}_1 = P_1 \bar{O} \in \mathcal{O}(K_1)$ , the decompositions will remain fundamentally the same, with  $\tilde{O} \equiv O' \bar{O} \in \mathcal{O}(K_1)$  multiplied on the right end of the each terms of (A.20) and (A.21). It gives  $P_0^\perp P_0^{\perp'} P_1 P_1' P_0^\perp P_0^{\perp'} = V S^2 V'$  which is invariant under this internal symmetry  $\mathcal{O}(K_1)$  as it is indeed supposed to be as a measure of factor space change.

Hence we can take (A.20) or (A.21) as the model of factor space dynamics. The resulting dynamics resembles a rotating position vector in Euclidean space, in a sense that there are the direction of change  $V$  and the size of the change  $S$  governing the motion from  $\text{span}(P_0)$  to  $\text{span}(P_1)$ . Analogous to the motion of a rotating vector,  $S$  captures the information of the principal angles ( $\Theta$ ) between two subspaces;  $S = \sin \Theta$ , more precisely. Accordingly,  $T$  or  $\text{diag}(T, \mathbf{0}_{K_0 \times (K_1 - K_0)})$  in (A.20) or (A.21) squares to  $C \equiv \cos \Theta = (I - S^2)^{1/2}$ . We refer to [Davis and Kahan, 1970](#) for an extensive discussion and interpretation.

In a matrix form, (A.20) or (A.21) can be written as follows:

$$P_1 = \begin{bmatrix} P_0 & P_0^\perp \end{bmatrix} \begin{bmatrix} \tilde{H} C O' \\ \tilde{V} S O' \end{bmatrix} \quad (\text{A.22})$$

where  $\tilde{V} \equiv P_0^{\perp'} V$ , and  $\tilde{H} \equiv H$  for the case (i) and  $\tilde{H} \equiv [H \ \mathbf{0}]$  for the case (ii). Together with Assumptions 1 to 3 in the model in Section 1.2.2, it implies that up to  $o(1)$  error, the regime 1 covariance matrix will be written in terms of  $[P_0 \ P_0^\perp]$  basis such that

$$\begin{aligned} \Sigma_{y,1} &\simeq \begin{bmatrix} P_1 & P_1^\perp \end{bmatrix} \begin{bmatrix} \Lambda_{1,1} & \mathbf{0}_{K_1, N-K_1} \\ \mathbf{0}_{N-K_1, K_1} & \Lambda_{2,1} \end{bmatrix} \begin{bmatrix} P_1' \\ P_1^{\perp'} \end{bmatrix} \\ &= \begin{bmatrix} P_0 & P_0^\perp \end{bmatrix} \begin{bmatrix} \tilde{H} C O' & F_1 \\ \tilde{V} S O' & F_2 \end{bmatrix} \begin{bmatrix} \Lambda_{1,1} & \mathbf{0} \\ \mathbf{0}' & \Lambda_{2,1} \end{bmatrix} \begin{bmatrix} O C \tilde{H}' & O S \tilde{V}' \\ F_1' & F_2' \end{bmatrix} \begin{bmatrix} P_0' \\ P_0^{\perp'} \end{bmatrix}. \end{aligned} \quad (\text{A.23})$$

where  $P_1^\perp = [P_0 \ P_0^\perp] [F_1' \ F_2']'$  for some bounded operator  $F_1$  and  $F_2$ . That is, for the perturbation  $Z$  which is assumed to exist in Assumption 4 of Section 1.2.2, its off-diagonal component  $P_0' Z P_0^\perp$  is of size  $O(N)$  to generate the size  $O(N)$  dominating eigenvalues in regime 1 in the  $P_1$  direction.

**Properties 3.** Let the benchmark Assumptions 1 to 3 hold. Assume there exists a perturbation  $Z$  such that  $\Sigma_{y,1} = \Sigma_{y,0} + Z$ . Then  $\|P_0' Z P_0^\perp\|_F = O(N)$ .

*Proof.* The upper right block of the off-diagonal perturbation with respect to the  $P_0$  basis is  $P_0' Z P_0^\perp = \tilde{H} C O' \Lambda_{1,1} O S \tilde{V}' + F_1 \Lambda_{2,1} F_2'$  from (A.23). Let us denote  $A \equiv \tilde{H} C O' \Lambda_{1,1} O S \tilde{V}'$  for simplicity. By Assumptions 1 to 3,  $\|\Lambda_{1,1}\| = O(N)$  and  $\|\Lambda_{2,1}\| = O(1)$ . By Triangle inequality

$$\|A\|_F - \|F_1 \Lambda_{2,1} F_2'\|_F \leq \|P_0' Z P_0^\perp\|_F \leq \|A\|_F + \|F_1 \Lambda_{2,1} F_2'\|_F. \quad (\text{A.24})$$

Observe that

$$\text{tr}(A'A) = \text{tr}(\tilde{V}SO'\Lambda_{1,1}OC^2O'\Lambda_{1,1}OS\tilde{V}') = \text{tr}(O'\Lambda_{1,1}OC^2O'\Lambda_{1,1}OS^2)$$

due to the cyclic invariance of the trace operator and the orthonormality of  $\tilde{H}$  and  $\tilde{V}$ . It gives that

$$\min_h(\sin^2 \theta_h) \text{tr}(O'\Lambda_{1,1}OC^2O'\Lambda_{1,1}O) \leq \text{tr}(A'A) \leq \max_h(\sin^2 \theta_h) \text{tr}(O'\Lambda_{1,1}OC^2O'\Lambda_{1,1}O),$$

which leads to

$$\min_h(\sin^2 \theta_h) \min_k(\lambda_k^2) \text{tr}(C^2) \leq \text{tr}(A'A) \leq \max_h(\sin^2 \theta_h) \max_k(\lambda_k^2) \text{tr}(C^2),$$

where  $\lambda_k$  is the  $k$ -th diagonal element of  $\Lambda_{1,1}$ . Under the assumed factor structure of regime 1,  $\min_k(\lambda_k^2)$  and  $\max_k(\lambda_k^2)$  are  $O(N^2)$ . By Properties 2,  $\min_h(\sin^2 \theta_h) > 0$  and  $\text{tr}(C^2) > 0$ . Hence  $\|A\|_F = O(N)$  and so is  $\|P_0'ZP_0^\perp\|_F$  as in (A.24). □

#### A.1.2.2 MODEL EXTENSION

The benchmark model in Section 1.2.2 can be extended to allow certain types of non-stationarity within regimes. The generalized model is stated as follows:

For each  $j \in \{0, 1\}$ ,  $\mathbf{y}_{t,j}$  is decomposed into common component  $\boldsymbol{\chi}_{t,j}$  and idiosyncratic component  $\mathbf{u}_{t,j}$ , such that

$$\mathbf{y}_{t,j} = \boldsymbol{\chi}_{t,j} + \mathbf{u}_{t,j}, \quad \text{for all } t \in \mathbb{I}_j \quad (2.1')$$

All processes  $\mathbf{y}_{t,j}$ ,  $\boldsymbol{\chi}_{t,j}$  and  $\mathbf{u}_{t,j}$  are centered.  $\mathbf{u}_{t,j}$  is allowed to be regime specific as well. We will impose the following extended assumptions for each  $j \in \{0, 1\}$ :

**ASSUMPTION A.1.** For any  $t \in \mathbb{I}_j$ ,  $\Sigma_{y,t,j} = \Sigma_{\chi,t,j} + \Sigma_{u,t,j}$ , where  $\Sigma_{\chi,t,j} = P_{t,j}\Lambda_{\chi,t,j}P_{t,j}'$  satisfies the following:

- a.  $\Lambda_{\chi,t,j} = \text{diag}(\lambda_{\chi,t,j}^k)_{k=1,\dots,K_j}$ , for  $K_j \ll N$  non-zero eigenvalues  $\lambda_{\chi,t,j}^k$  satisfying

$$\inf_{t \in \mathbb{I}_j} \lambda_{\chi,t,j}^k = O(N).$$

- b.  $P_{t,j} = P_j \mathcal{O}_t$  for some orthonormal  $\mathcal{O}_t$  and  $P_j'P_j = I_{K_j}$ .

**ASSUMPTION A.2.** There exists a constant  $q_j \in [0, 1]$  such that

$$c_{u,j} \equiv \sup_{t \in \mathbb{I}_j} \max_{i=1,\dots,N} \sum_{i'=1,\dots,N} |\text{cov}(u_{it}, u_{i't})|^{q_j} = O(1).$$

ASSUMPTION A.3.  $\sup_{t \in \mathcal{I}_0} \|P_0 P_0' \Sigma_{u,t} P_0^\perp P_0^{\perp'}\|_F = o(1)$ .

ASSUMPTION A.4. Denote  $t = t_j$  if  $t \in \mathcal{I}_j$ . For any pair  $t_0$  and  $t_1$ ,  $\Sigma_{y,t_1} = \Sigma_{y,t_0} + Z_{t_0,t_1}$ , where

$$\inf_{t_0, t_1} \|P_0' Z_{t_0, t_1} P_0^\perp\|_F = O(N).$$

In a concise version, Assumption A.1 can be rewritten as follows:

ASSUMPTION A.1\*.  $\Sigma_{y,t,j} = \Sigma_{\chi,t,j} + \Sigma_{u,t}$ , where  $\Sigma_{\chi,t,j} = P_j \tilde{\Lambda}_{\chi,t,j} P_j'$ , for a symmetric matrix  $\tilde{\Lambda}_{\chi,t,j}$  with its  $K_j \ll N$  non-zero eigenvalues  $\lambda_{\chi,t,j}^k$  satisfying

$$\inf_{t \in \mathcal{I}_j} \lambda_{\chi,t,j}^k = O(N),$$

and  $P_j' P_j = I_{K_j}$ .

## A.2 PROOFS

**Proposition 1.** Assume that there is no breakpoint in  $\mathcal{I}$ . Then for any  $\tau \in (0, 1)$ ,

$$\Pr(S(\tau; 1) < S(0)) \rightarrow 1$$

as  $N, T \rightarrow \infty$ .

*Proof.* We can write  $\hat{d}(\tau) = \text{tr}[\hat{\mathcal{P}}_0^\perp(\tau) \hat{\mathcal{P}}_1(\tau)]$  as

$$\begin{aligned} \text{tr}[\hat{\mathcal{P}}_0^\perp \hat{\mathcal{P}}_1] &= \text{tr}[\hat{\mathcal{P}}_0^\perp (\mathcal{P}_1 - \mathcal{P}_1 + \hat{\mathcal{P}}_1)] = \text{tr}[(\mathcal{P}_0^\perp + \mathcal{P}_0 - \hat{\mathcal{P}}_0) \mathcal{P}_1] + \text{tr}[(I_N - \hat{\mathcal{P}}_0)(\hat{\mathcal{P}}_1 - \mathcal{P}_1)] \\ &= \text{tr}[\mathcal{P}_0^\perp \mathcal{P}_1] + \hat{K}_1 - K_1 + \text{tr}[(\mathcal{P}_0 - \hat{\mathcal{P}}_0) \mathcal{P}_1] + \text{tr}[\hat{\mathcal{P}}_0(\mathcal{P}_1 - \hat{\mathcal{P}}_1)], \end{aligned} \quad (\text{A.25})$$

where the dependence in  $\tau$  omitted for simple exposition.

We only need to examine the latter two terms of (A.25). Without a breakpoint, the first term  $\text{tr}[\mathcal{P}_0^\perp \mathcal{P}_1] = 0$ . Throughout this discussion,  $\hat{K}_j - K_j$  will be treated as zero by considering sufficiently large  $N$  and  $T$  that guarantee the two integers to be the same for an arbitrarily high probability.

Having no break implies either  $\mathcal{P}_1 = \mathcal{P}_0$  or that  $\text{span}(\mathcal{P}_1)$  is a strict subspace of  $\text{span}(\mathcal{P}_0)$ , hence  $\text{tr}[\mathcal{P}_0^\perp \mathcal{P}_1] = 0$  and  $K_1 < K_0$ . The third term  $\text{tr}[(\mathcal{P}_0 - \hat{\mathcal{P}}_0) \mathcal{P}_1]$  achieves its maximum when  $\mathcal{P}_1 = \mathcal{P}_0$ . That is,

$$\text{tr}[(\mathcal{P}_0 - \hat{\mathcal{P}}_0) \mathcal{P}_1] \leq \text{tr}[(\mathcal{P}_0 - \hat{\mathcal{P}}_0) \mathcal{P}_0] = \text{tr}[(I_{K_0} - \hat{\mathcal{P}}_0) \mathcal{P}_0] = \text{tr}[\hat{\mathcal{P}}_0^\perp \mathcal{P}_0],$$

where the equalities are guaranteed as the projectors are idempotent.

The last term of (A.25) can be rewritten as

$$\text{tr}[\hat{\mathcal{P}}_0(\mathcal{P}_1 - \hat{\mathcal{P}}_1)] = \text{tr}[\mathcal{P}_0(\mathcal{P}_1 - \hat{\mathcal{P}}_1)] + \text{tr}[(\hat{\mathcal{P}}_0 - \mathcal{P}_0)(\mathcal{P}_1 - \hat{\mathcal{P}}_1)]. \quad (\text{A.26})$$

The first term  $\text{tr}[\mathcal{P}_0(\mathcal{P}_1 - \hat{\mathcal{P}}_1)] \leq \text{tr}[\mathcal{P}_1(\mathcal{P}_1 - \hat{\mathcal{P}}_1)] = \text{tr}[\hat{\mathcal{P}}_1^\perp \mathcal{P}_1]$ : as there is no break,  $\text{tr}[\mathcal{P}_0 \mathcal{P}_1] = K_1 = \text{tr}[\mathcal{P}_1 \mathcal{P}_1]$ , and  $(0 \leq) \text{tr}[\mathcal{P}_1 \hat{\mathcal{P}}_1] \leq \text{tr}[\mathcal{P}_0 \hat{\mathcal{P}}_1]$ .

The second term of (A.26) is bounded as

$$|\text{tr}[(\hat{\mathcal{P}}_0 - \mathcal{P}_0)(\mathcal{P}_1 - \hat{\mathcal{P}}_1)]| \leq \|\hat{\mathcal{P}}_0 - \mathcal{P}_0\|_F \|\mathcal{P}_1 - \hat{\mathcal{P}}_1\|_F \leq 2(\text{tr}[\mathcal{P}_0^\perp \hat{\mathcal{P}}_0] \text{tr}[\mathcal{P}_1^\perp \hat{\mathcal{P}}_1])^{1/2}.$$

The first inequality comes from the Matrix Cauchy-Schwarz Inequality, and the second inequality comes as  $\|\hat{\mathcal{P}}_j - \mathcal{P}_j\|_F = \sqrt{2}(\text{tr}[\mathcal{P}_j^\perp \hat{\mathcal{P}}_j])^{1/2}$ . Note that, for large  $N, T$  guarantees  $\hat{K}_j = K_j$ ,  $\text{tr}[\hat{\mathcal{P}}_j^\perp \mathcal{P}_j] = \text{tr}[\mathcal{P}_j^\perp \hat{\mathcal{P}}_j]$ . Hence, combining the above observations, we have

$$\hat{d}(\tau) \lesssim \max_j \text{tr}[\mathcal{P}_j^\perp \hat{\mathcal{P}}_j].$$

Remind that  $\text{tr}[\mathcal{P}_j^\perp \hat{\mathcal{P}}_j] = \|\mathcal{P}_j^\perp \hat{\mathcal{P}}_j\|_F^2$ . From now on, let  $j \equiv \arg\max_{j'} \text{tr}[\mathcal{P}_{j'}^\perp \hat{\mathcal{P}}_{j'}]$ .

The first inequality of the following expression,

$$\begin{aligned} \|\mathcal{P}_j^\perp \hat{\mathcal{P}}_j\|_F &\leq \frac{\sqrt{K_j} \|\hat{\Sigma}_{\mathcal{X},j} - \Sigma_{\mathcal{X},j}\|}{\lambda_{\mathcal{X}}^{K_j}} \leq \frac{\sqrt{K_j} (\|\hat{\Sigma}_{\mathcal{X},j} - \Sigma_{y,j}\| + \|\Sigma_{y,j} - \Sigma_{\mathcal{X},j}\|)}{\lambda_{\mathcal{X}}^{K_j}} \\ &= \frac{\sqrt{K_j} \|\hat{\Sigma}_j^{\text{sam}} - \Sigma_{y,j}\|}{\lambda_{K_j}^{\mathcal{X}}} + O(1/N), \end{aligned} \quad (\text{A.27})$$

follows the sin  $\Theta$  theorem (Davis and Kahan, 1970). The theorem guarantees that  $\|\mathcal{P}_j^\perp \hat{\mathcal{P}}_j\|_F \leq \|(\hat{\Sigma}_{\mathcal{X},j} - \Sigma_{\mathcal{X},j})\mathcal{P}_j\|_F / |\hat{\lambda}_{\mathcal{X},j}^{K_j+1} - \lambda_{\mathcal{X},j}^{K_j}|$ . As the perturbation  $\hat{\Sigma}_{\mathcal{X},j}$  is of the same rank as that of  $\Sigma_{\mathcal{X},j}$ , the denominator equals  $\lambda_{\mathcal{X},j}^{K_j}$ . The numerator,

$$\begin{aligned} \|(\hat{\Sigma}_{\mathcal{X},j} - \Sigma_{\mathcal{X},j})\mathcal{P}_j\|_F &= (\text{tr}[P_j'(\hat{\Sigma}_{\mathcal{X},j} - \Sigma_{\mathcal{X},j})^2 P_j])^{1/2} \\ &\leq \sqrt{K_j} (\lambda_{\max}(\hat{\Sigma}_{\mathcal{X},j} - \Sigma_{\mathcal{X},j})'(\hat{\Sigma}_{\mathcal{X},j} - \Sigma_{\mathcal{X},j}))^{1/2} \\ &= \sqrt{K_j} \|\hat{\Sigma}_{\mathcal{X},j} - \Sigma_{\mathcal{X},j}\|. \end{aligned}$$

By Assumption 1,  $\lambda_{\mathcal{X},j}^{K_j} \asymp N$ . Then the last part of the line (A.27) follows as  $\|\Sigma_{y,j} - \Sigma_{\mathcal{X},j}\| = O(1)$  by Assumption 2. The first part of the line comes as  $\|\hat{\Sigma}_{\mathcal{X},j} - \Sigma_{y,j}\| \leq \|\hat{\Sigma}_{y,j}^{\text{sam}} - \Sigma_{y,j}\|$ , which is  $O_p(N\sqrt{(\ln N)/T_j})$  by Assumptions 1, 2 and 6 to 10. It gives  $\hat{d}(\tau) = O_p((\ln N)/T_j)$ .

For any  $\epsilon > 0$ ,

$$\Pr\left(\ln \hat{d}_{N,T}(\tau) < \delta_\epsilon \ln((\ln N)/T_j)\right) > 1 - \epsilon,$$

for some  $\delta_\epsilon > 0$ , for sufficiently large  $N, T$ . As  $(\ln N)/T_j = o(1)$  under Assumption 11, for any  $\delta > 0$ ,  $\delta_\epsilon \ln((\ln N)/T_j) < \delta(\ln N)/T_j$  for sufficiently large  $N, T$ . That is, for any  $\epsilon > 0$  and any  $\delta > 0$ ,

$$\Pr\left(\ln \hat{d}_{N,T}(\tau) < \delta(\ln N)/T_j\right) > 1 - \epsilon, \quad (\text{A.28})$$

for large  $N, T$ . Observe that, for  $r \geq 1$ ,  $g_j \simeq K_0(1/T_j + 1/N) \ln N$  for sufficiently large  $N$ , which is larger than  $(\ln N)/T_j$ . For this case, the argument for  $\delta = K_j$  above is sufficient to show that  $\ln \hat{d}_{N,T}(\tau) < g_j$  asymptotically almost surely.

Recall that  $T_j \geq \tilde{\kappa}_j N^r$  for some  $\tilde{\kappa}_j > 0$ , by Assumption 11 and  $T_j = \kappa_j T$  for some  $\kappa_j \in (0, 1)$ . For  $r < 1$ ,  $g_j \simeq K_j[(r/T_j) \ln N + (1/T_j) \ln \tilde{\kappa}_j + \Delta]$  for sufficiently large  $N$ , for  $\Delta > 0$ . In the case  $\tilde{\kappa} \geq 1$ , the above boundedness (A.28) for  $\delta = rK_j$  guarantees that asymptotically  $\ln \hat{d}_{N,T}(\tau) < g_j$  almost surely. For  $\tilde{\kappa} < 1$ , there exists large enough  $\underline{N} \in \mathbb{N}$  such that  $1/\tilde{\kappa}_j < \underline{N}^r$ . That is,  $1/\tilde{\kappa}_j = \underline{N}^{\tilde{\epsilon}}$  for  $\tilde{\epsilon} = (\ln(1/\tilde{\kappa}_j))/\ln \underline{N} < r$ . Take  $\delta = (r - \tilde{\epsilon})K_j$ . Then again the boundedness (A.28) guarantees that  $g_j \geq (\delta/T_j) \ln N$  is almost surely larger than  $\ln \hat{d}(\tau)$  for large  $N, T$ . In other words, combining the arguments, for any  $\epsilon > 0$ , there exist  $N_\epsilon$  and  $T_\epsilon \in \mathbb{N}$  such that

$$\Pr\left(\ln \hat{d}_{N,T}(\tau) < g_j\right) > 1 - \epsilon,$$

for all  $N \geq N_\epsilon$  and  $T \geq T_\epsilon$ . Moreover, since  $K_0 = K_1 = K$  without breakpoint, and as  $\{g_j\}_{j \in \mathcal{J}}$  and  $G(0)$  are decreasing functions in  $T$ ,  $-g_{j'} < -G(0)$  as  $T_{j'} < T$ , for any  $j' \neq j$ . Hence,  $\Pr\left(\ln \hat{d} - g_0 - g_1 < -G(0)\right) \rightarrow 1$  in large  $N, T$  limit.  $\square$

**Proposition 2.** Assume that there exists a single breakpoint at  $b^* = \tau^* T$  for some  $\tau^* \in (0, 1)$  in the entire time window  $\mathbf{I}$  of length  $T$ . Let  $\underline{\tau} = \operatorname{argmax}_{\tau \in (0,1)} \mathcal{S}(\tau)$ . Then  $\Pr[\tau^* \geq \underline{\tau}] \rightarrow 1$  in the large  $N, T$  limit.

*Proof.* We will show that for any  $\tau > \tau^*$ ,  $\Pr[\mathcal{S}(\tau) < \mathcal{S}(\tau^*)] \rightarrow 1$  in large  $N, T$  limit. It implies that the maximum point  $\underline{\tau} \leq \tau^*$  asymptotically almost surely.

For some  $\tau > \tau^*$ , one supposed a window  $\mathbf{I}_0(\tau) = [1, \tau T]^5$  to follow one static factor model while the true process has a break at  $\tau^* T$ . In  $\mathbf{I}_0(\tau)$ , the process follows that

$$\mathbf{y}_t = \begin{cases} P_0 \mathbf{f}_{0,t} + \mathbf{u}_{0,t} & t \in \mathbf{I}_0, \\ P_1 \mathbf{f}_{1,t} + \mathbf{u}_{1,t} & t \in \mathbf{I}_0(\tau) \setminus \mathbf{I}_0 \subset \mathbf{I}_1, \end{cases} \quad (\text{A.29})$$

where the windows corresponding to the true regimes are denoted as  $\mathbf{I}_j = \mathbf{I}_j(\tau^*)$ . The expression (A.29) takes the natural loading-signal specification (1.2) discussed in Section 1.2.1. The true factor space basis  $P_1$  of regime 1 can be expressed as follows:

$$P_1 = \begin{bmatrix} P_0 & P_0^\perp \end{bmatrix} \begin{bmatrix} \tilde{H} C O' \\ \tilde{V} S O' \end{bmatrix}, \quad (\text{A.30})$$

<sup>5</sup>Assume that the one knows the realization of the data is indexed by  $\mathbb{N}$ , and expect  $\tau T \in \mathbb{N}$ .

for some  $\tilde{H}_{K_0 \times K_1}$ , diagonal matrices  $C_{K_1 \times K_1}$  and  $S_{K_1 \times K_1}$ , and  $\tilde{V} \equiv P_0^{\perp'} V$  for some column-orthonormal matrix  $V_{N \times K_1}$  such that  $P_0' V = \mathbf{0}$ . Then (A.29) can be represented as

$$\mathbf{y}_t = P(\tau) \tilde{\mathbf{f}}_t + \tilde{\mathbf{u}}_t = \begin{bmatrix} P_0 & V \end{bmatrix} \begin{bmatrix} \mathbf{f}_{0,t} 1_{t \in I_0} + \tilde{H} C O' \mathbf{f}_{1,t} 1_{t \in I_1} \\ S O' \mathbf{f}_{1,t} 1_{t \in I_1} \end{bmatrix} + \tilde{\mathbf{u}}_t \quad \forall t \in I_0(\tau), \quad (\text{A.31})$$

where  $\tilde{\mathbf{u}}_t = \mathbf{u}_{0,t} 1_{t \in I_0} + \mathbf{u}_{1,t} 1_{t \in I_1}$ .

The wrongly included regime 1 common component (or  $\mathbf{f}_{1,t}$  in current specification) becomes a source of perturbation on the true regime-0 factor signal covariance  $E[\mathbf{f}_{0,t} \mathbf{f}_{0,t}'] = \Lambda_{\chi,0}$ . The size of perturbation is proportional to  $\alpha \|\Lambda_{\chi,1}\|$  where  $\alpha = E[1_{t \in I_0(\tau) \setminus I_0}]$ . As  $\|E[\tilde{\mathbf{u}}_t \tilde{\mathbf{u}}_t']\|$  is bounded as  $\|\Sigma_{u,j}\|$  bounded, for large  $N$ , the perturbation is substantial enough to identify the misspecified factor space  $\mathcal{P}_0(\tau) = P_0(\tau) P_0(\tau)'$  in population level. Then

$$\text{tr}[\mathcal{P}_0(\tau)^\perp \mathcal{P}_1] = 0, \quad (\text{A.32})$$

as  $\mathcal{P}_0(\tau)$  spanned by the spaces  $\mathcal{P}_0$  and  $\mathcal{V} \equiv V V' (\mathcal{P}_0(\tau) = \mathcal{P}_0 \oplus \mathcal{V})$  whose composition generates  $\mathcal{P}_1 = \mathcal{P}_1(\tau)$ . In other words, the supposed next regime  $I_1(\tau) = [\tau T + 1, T]$  shows no new directional information compared to  $I_0(\tau)$ .

In the sample level, similar as discussed in the proof of Proposition 1,  $\hat{d}(\tau)$  is composed of the factor space estimation errors of  $I_0(\tau)$  and  $I_1(\tau)$  supposed by  $\tau$ . The size of the overall errors will be dominated by the errors in  $I_0(\tau)$ , where the actual process contains mixed factor spaces. The dominating error will be of order  $O_p(\sqrt{(\ln N)/(\tau - \tau^*)T})$  and it is again dominated by  $g_0(\tau)$ , by a similar argument as in Proposition 1. Then  $\ln \hat{d}(\tau) - g_0(\tau) < 0$  and decreases to negative infinity asymptotically almost surely as the errors converge to zero. Compared to this side,  $\ln d(\tau^*) - g_0$  in  $\mathcal{S}(\tau^*)$  side converges to a fixed value  $\ln d(\tau^*)$  asymptotically. Furthermore, for large  $N, T$ ,  $-g_1(\tau) < -g_1(\tau^*)$  as  $\hat{K}_1(\tau) = K_1 = \hat{K}_1(\tau^*)$  and  $T_1(\tau) < T_1(\tau^*)$ . Hence  $\Pr[\mathcal{S}(\tau) < \mathcal{S}(\tau^*)] \rightarrow 1$ .  $\square$

**Corollary 3.** Assume that there exists a breakpoint at  $b^* = \tau^* T$  for some  $\tau^* \in (0, 1)$  in the entire time window  $I$  of length  $T$ . Let  $\underline{\tau} = \arg\max_{\tau \in (0,1)} \mathcal{S}(\tau)$ . Then  $\Pr[\tau^* \geq \underline{\tau}] \rightarrow 1$  in large  $N, T$  limit.

*Proof.* Let  $\{\tau_j^*\}_{j=1,\dots,J}$  be  $J$  breakpoints separating regimes  $j = 0, \dots, J$ . In the large  $N, T$  limit, the penalty terms converge to zero, and mixed factor spaces are identifiable. Hence, it is sufficient to compare the size of the true distances. Consider two windows  $I_0$  and  $I_1(\tau_1^*)$ , up to and after the first breakpoint  $\tau_1^*$ . The distance between  $\mathcal{P}_0$  and the mixed factor space in  $I_1(\tau_1^*)$  is  $d(\tau_1^*) = \text{tr}[\mathcal{P}_0^\perp \oplus_{j=1}^J \mathcal{P}_j]$ . In comparison, consider  $\tau \in (\tau_1^*, \tau_2^*)$  and corresponding windows  $I_0(\tau)$  and  $I_1(\tau)$  segregated by  $\tau$ , for example. The distance between the mixed factor spaces in  $I_0(\tau)$  and  $I_1(\tau)$  can be written as  $d(\tau) = \text{tr}[\mathcal{P}_0(\tau)^\perp \oplus_{j=2}^J \mathcal{P}_j]$ , as there is no

additional directional information from the mixed factor space  $\mathcal{P}_0(\tau)$  to  $\mathcal{P}_1$  as in Proposition

2. Then  $d(\tau_1^*) > d(\tau)$  for any  $\tau \in (\tau_1^*, \tau_2^*]$ .

This applies to  $\tau$  in any location. Let  $\tau \in (\tau_{\underline{j}}^*, \tau_{\underline{j}+1}^*]$  for some  $\underline{j} = 1, \dots, J$ . Then the distance between the mixed factor space  $d(\tau)$  presents the following inequalities:

$$d(\tau) = \text{tr}\left[\mathcal{P}_0(\tau)^\perp \bigoplus_{j=\underline{j}+1}^J \mathcal{P}_j\right] \leq \text{tr}\left[\mathcal{P}_0^\perp \bigoplus_{j=\underline{j}+1}^J \mathcal{P}_j\right] < \text{tr}\left[\mathcal{P}_0^\perp \bigoplus_{j=1}^J \mathcal{P}_j\right] = d(\tau_1^*).$$

The first inequality holds as the argument within the trace operator  $d(\tau)$  extracts the components of  $\bigoplus_{j=\underline{j}+1}^J \mathcal{P}_j$  orthogonal to all directional information of  $\mathcal{P}_0(\tau)$ , which is larger than that of  $\mathcal{P}_0$  in the second information. In other words,  $\mathcal{P}_0(\tau)^\perp$  is a smaller space than  $\mathcal{P}_0^\perp$ . The second inequality holds as the size of components orthogonal to  $\mathcal{P}_0$  strictly increases as the space to be projected becomes strictly enlarged. Unless the factor spaces  $\{\mathcal{P}_j\}_{j=\underline{j}+1, \dots, J}$  are complete recurrence of  $\{\mathcal{P}_j\}_{j \in 0, 1, \dots, J}$  (Assumption 12), the strict inequality holds. Therefore, the maximum point gives  $\mathcal{S}(\tau) \geq \mathcal{S}(\tau_1^*)$  is almost surely equals to or precedes  $\tau_1^*$ .  $\square$

# 2 SYSTEMIC INFLUENCE IN STRUCTURAL BREAKS: GRANULAR TIME SERIES DETECTION

## 2.1 INTRODUCTION

Modern socio-economic systems experience crises of varying scales. The origins of crises can differ. Some crises can be considered originating locally, such as the bankruptcy of Lehman Brothers for the global financial crisis, and some crises can originate globally, such as the COVID-19 pandemic. Regardless, the fluctuations from different individual entities of a system have different implications for crisis development. In particular, idiosyncratic volatilities of key entities – such as big firms or major financial institutions – are not diversified and propagate throughout the entire system ([Acemoglu, Carvalho, et al., 2012](#), [Baqaee, 2018](#), [Gaubert and Itskhoki, 2021](#)) by influencing the existing network of relationships ([Acemoglu and Tahbaz-Salehi, 2020](#), [Taschereau-Dumouchel, 2019](#), [Heipertz et al., 2019](#)). The pioneering work of [Gabaix, 2011](#) termed an economic system under the systemic influence of such entities as a *granular economy*. We thus label these individuals *granular units*, and aim to detect them from a large panel.

Understanding micro-originated volatility transmission is crucial in the context of systemic risk, as it can trigger or amplify system-wide instabilities, potentially causing or deepening crises. However, the true mechanism of the volatility transmission can be complex. Approaches to fully model and analyze the true mechanism can often be time- or data-intensive, making them suboptimal for timely crisis signaling. Hence, instead, our aim is to propose an early detection framework for systemic risk that is agnostic to the likely unknown transmission mechanism, and straightforward to implement.

We consider a panel with a large number of cross-sectional units for a single economic variable, such as stock returns. In a system represented by panel data, without presuming the true propagation mechanism, a change in the cross-correlation structure remains identifiable and can empirically indicate ongoing volatility transmission from the individual (idiosyncratic) level to the system level. Therefore, we focus on a large break in the system cross-correlation structure and identify the individual units contributing most to this structural break as the systemic

risk components. In application to daily stock return data across historical economic crises, our detection framework demonstrates the potential for real-time application by identifying likely key actors – such as Lehman Brothers – from the early stages of each crisis.

This project makes three key contributions. First, it provides a novel, straightforward analysis of the second-moment effects from the micro level to the system level. Implementation is also straightforward, utilizing well-established methods of principal component analysis (PCA). Second, our framework operates on a clear and conservative definition of systemic influence: a micro-level effect is deemed systemic if it substantially contributes to system-wide instability (structural breaks). This definition minimizes debates about whether certain individual units' influences are truly system-wide. Finally, we establish a clear connection between a standard latent factor model and a network model. From this perspective, our criterion of detection identifies individuals who shape overall equilibrium actions through an underlying latent network.

From a methodological standpoint, we model system covariance dynamics agnostically, employing a standard approximate latent factor model, a prominent workhorse in the field of macroeconomics and finance (e.g., [Ross, 1976](#), [Chamberlain and Rothschild, 1983](#), [Stock and M. W. Watson, 2002b](#), [Stock and M. W. Watson, 2002a](#), and [Bernanke et al., 2005](#)). In this model, the cross-correlation structure is governed by a small number of latent common factor signals and their loadings – the transmission rule of how the common factors are transmitted and affect all cross-sectional units. While common factors are macro-level and detached from micro-level characteristics, the transmission rule – encoded in the loadings – can still communicate with the micro-level. Idiosyncratic fluctuations of important units can reshape the underlying microstructure through which the common factors are transmitted to the entire units of the system. Hence, we further specify system-wide instabilities of our focus as a large break in the transmission rule. Granular units will be the main contributors to this structural break.

Our framework introduces a technical innovation to disentangle the dynamics of the transmission rule from those of the latent common factor signals – an inherently non-trivial task due to their assumed latent nature. In technical terms, we represent the transmission rule by the column space of the factor loading (the *factor space* in our terminology) whose dynamics are straightforwardly identifiable by standard methods (PCA) and remain robust to the potential dynamics of the latent common factor signals. While more abstract initially, this approach facilitates a more straightforward second-moment-level analysis. Through this approach, the contribution of each unit can be easily analyzed by the first-order effect of their idiosyncratic second moments on the magnitude of the structural break. This results in a comprehensive systemic influence measure that captures both the direct and indirect roles of each unit in transmitting both idiosyncratic and common sources of fluctuations to the entire system.

There are two branches of studies related to the aim and the theme of this project. The first branch primarily studies group identification via systemic influence in a stationary environment, e.g., [Diebold and Yilmaz, 2014](#), [Basu, Shojai, et al., 2015](#), [Parker and Sul, 2016](#), [Barigozzi](#)

and Hallin, 2017, Barigozzi and Brownlees, 2019, Brownlees and Mesters, 2021, Guðmundsson and Brownlees, 2021, Brownlees, Guðmundsson, et al., 2022. Departing from this literature, this project focuses on a distribution-changing effect from the "individual" (idiosyncratic) dimension. The second branch of the studies connects group identity to potentially non-stationary system-wide changes, e.g., Billio et al., 2012, Bianchi et al., 2019, Basu and Rao, 2021. Modeling and methods for addressing non-stationarity can be complex in this branch of literature compared to our proposed framework.

Our detection scheme is applicable when reliable breakpoint information is available, whether acquired directly or estimated. We introduce a new structural breakpoint estimation method developed in a separate project. In applications, our granular unit detection scheme effectively identifies likely sources of well-known economic crises—such as the dot-com bubble and the 2007-2008 financial crisis—from their early stages, implementing our breakpoint estimation method developed in the first chapter together. Our framework demonstrates the potential for real-time applications. Points of system-wide instability often precede the major collapses, and the identification of the granular units remains robust with limited post-break data points.

This paper is organized as follows. In Section 2.2, we recall the model of dynamic system covariance introduced in Chapter 1, incorporating a generic connection to mechanisms of volatility transmission. Our measure of systemic influence is introduced in Section 2.3, where we also propose the detection criteria. Section 2.4 details the estimation strategy for constructing the proposed influence measure, followed by implementation using simulated data. Applications to daily stock return data, considering both known and unknown structural breakpoints, are discussed in Section 2.5. Finally, Section 2.6 concludes with closing remarks.

## 2.2 STRUCTURAL BREAKS IN A SYSTEM WITH LATENT FACTORS

Systemic influence can be understood as a factor behind large breaks in the system cross-correlation structure. Types of idiosyncratic second moments – such as the idiosyncratic volatilities, the cross-sectional or partial correlations – can represent the individual-originated sources that contribute to a structural break in the system's second moments. We aim for a straightforward analysis of a second-moment to second-moment effect from individual units to the system without specifying the factors of the system covariance. Such analysis is enabled by employing the latent factor model as an intrinsic tool for modeling the structure of system cross-correlations, as we suggest in this section. Additionally, we will discuss how a structural break, captured by changes in the factor space, has a natural interpretation within the context of a generic latent network model.

### 2.2.1 COVARIANCE DYNAMICS AND FACTOR SPACE CHANGES

Consider a system of  $N$  time series,  $\mathbf{y}_t = [y_{1t}, \dots, y_{Nt}]'$ , of a single economic variable,  $y$ , of interest, e.g., sales or stock returns. Assume that there is a single set of  $H$  important cross-sectional units, referred to as the *granular units*. We aim to identify this set of granular units,  $\mathcal{G}$ . For simplicity, we can write  $\mathbf{y}_t = [\mathbf{y}_{1:H,t}, \mathbf{y}_{H+1:N,t}]'$ , where  $\mathbf{y}_{1:H,t}$  refers to the values of  $y_t$  for the granular units (re-indexed as  $\mathcal{G} = \{1, \dots, H\} \subset \mathcal{N}$ ), and  $\mathbf{y}_{H+1:N,t}$  refers to the values of the remaining, i.e., the non-granular units.

The system covariance evolves in discrete steps. There are two regimes before and after one break, respectively: the present (regime 0) and the future (regime 1). Let  $\mathbf{I}_0$  denote the time window of the present regime, and  $\mathbf{I}_1$  the time window of the future regime. We can now formalize our benchmark model. The modeling shares the major part of the model in the first chapter.

#### 2.2.1.1 BENCHMARK MODEL AND ASSUMPTIONS

For each  $j \in \{0, 1\}$ , let  $\mathbf{y}_t$  be decomposed into common component  $\boldsymbol{\chi}_{j,t}$  and idiosyncratic component  $\mathbf{u}_t$ , such that:

$$\mathbf{y}_t = \boldsymbol{\chi}_{j,t} + \mathbf{u}_t, \quad \text{where} \quad \mathbf{u}_t = [\mathbf{g}_t \quad \boldsymbol{\epsilon}_t]' \quad \text{for all } t \in \mathbf{I}_j. \quad (2.1)$$

Here,  $\mathbf{g}_t$  denotes idiosyncratic components of the granular units, and  $\boldsymbol{\epsilon}_t$  denotes idiosyncratic components of the non-granular units. Further,  $\mathbf{y}_t$ ,  $\boldsymbol{\chi}_{j,t}$  and  $\mathbf{u}_t$  are all mean-zero objects, specific to regime  $j$ . We impose the following assumptions:

**Assumption 1.**  $\Sigma_{y,j} = \Sigma_{\chi,j} + \Sigma_{u,j}$ , where  $\Sigma_{\chi,j} = P_j \Lambda_{\chi,j} P_j'$  with  $K_j \ll N$  non-zero eigenvalues  $\lambda_{\chi,j,k} = O(N)$  for  $\Lambda_{\chi,j} = \text{diag}(\lambda_{\chi,j,k})_{k=1,\dots,K_j}$ , and  $P_j' P_j = I_{K_j}$ .

**Assumption 2.** There exists a constant  $q_j \in [0, 1]$  such that

$$c_{u,j} \equiv \max_{i=1,\dots,N} \sum_{i'=1,\dots,N} |\text{cov}(u_{it}, u_{i't})|^{q_j} = O(1).$$

**Assumption 3.**  $\|P_0 P_0' \Sigma_{u,0} P_0^\perp P_0^{\perp'}\|_F = o(1)$ .

**Assumption 4.**  $\Sigma_{y,1} = \Sigma_{y,0} + Z$ , where  $\|P_0' Z P_0^\perp\|_F = O(N)$ .

The expression (2.1), supported by Assumptions 1 and 2, states that, in each regime,  $\mathbf{y}_t$  is decomposed into two components: the common component with low dimensional large and dominant variances and the idiosyncratic component with bounded variances. A system has a factor structure if it has this decomposability.

Assumptions 1 and 2 are standard conditions for the approximate factor model that guarantee the decomposability. The idiosyncratic components can be correlated but in a bounded fashion for any size of the cross-sectional dimension  $N$ , as stated in Assumption 2. On the other hand, the common components prevail no matter how large the system is, following Assumption 1.  $\Sigma_{\chi,j} = P_j \Lambda_{\chi,j} P_j'$  is the spectral decomposition of the common component covariance.<sup>1</sup> As captured by the unbounded non-zero eigenvalues of  $\Sigma_{\chi,j}$ , the size of common component covariance is not dissipating in large  $N$  limit.<sup>2</sup>

The major correlation structure of the system is captured by a small number,  $K_j$ , of important directions  $\{\mathbf{p}_j^k\}_{k=1,\dots,K_j}$ , which load the non-dissipating eigenvalues. If we assume there are  $K_j$  independent signals of strength  $\{\lambda_{\chi,j,k}\}_{k=1,\dots,K_j}$ , these directions represent how those signals are distributed to the entire  $N$ -dimensional cross-sectional units. When the signals are unobservable, this directional information<sup>3</sup> is encapsulated by the factor space, as defined below.

**FACTOR SPACE.** The factor space of regime  $j$  is the eigenspace of the common component covariance  $\Sigma_{\chi,j}$  in  $N$ -dimension, that is,

$$\text{span}(P_j) \equiv \text{Col}(P_j) = \left\{ \sum_{k=1}^{K_j} r_k \mathbf{p}_j^k \mid r_k \in \mathbb{R} \right\}. \quad (2.2)$$

In the next subsection, we review how focusing on the factor space provides a straightforward way to analyze factor loading dynamics, aligned with the standard specification of the common component –  $\chi_{j,t} = B_j \mathbf{f}_{t,j}$ , where  $f_{t,j}$  denotes common latent factor signals and  $B_j$  represents a static rule of loading the common signals onto the system.<sup>4</sup> Later, in Section 2.4, we will explain the model estimation using this conventional loading-signal specification as well. For now, we continue our discussion of the benchmark assumptions for model identification at the population level, for which a description of the conventional specification is not strictly necessary.

Under Assumptions 1 and 2 with a perturbation bound result (the  $\sin \theta$  theorem) of [Davis and Kahan, 1970](#), the eigenspace of the  $K_j$ -leading eigenvalues of the system covariance  $\Sigma_{y,j}$  is consistent with the factor space at the population level.

Assumption 3 guarantees that  $\Sigma_{y,j}$  is asymptotically block diagonal with respect to the factor space basis. Assumption 4 hypothesizes that the regime-0 covariance experiences a substantial

<sup>1</sup>Equivalently, it is the (thin) singular value decomposition of  $\Sigma_{\chi,j}$ .

<sup>2</sup>Although there is a natural explanation – [Wang and Fan, 2017](#) equation (1.1) – the rate is assumed to be linear in  $N$  mainly to simplify the later discussion. This can be easily generalized.

<sup>3</sup>Such directional information can be interpreted in terms of network centrality. We will discuss this further in a later part of the section.

<sup>4</sup>The static representation can also allow for a latent dynamic factor signal process with a finite lag under standard regularity conditions, see [Forni et al., 2009](#).

perturbation that is off-diagonal with respect to the previous basis  $[P_0 \ P_0^\perp]$ . Let  $P_j^\perp$  denote the column augmentation of  $N - K_j$  basis vectors of the space  $\text{span}(P_j)^\perp = \{v \in \mathbb{R}^N \mid v'p = 0, \forall p \in \text{span}(P_j)\}$ , the orthogonal complement of the factor space  $\text{span}(P_j)$ . Then, up to an error  $E$  of order  $o(1)$  (note that  $\|E\|_{\max} = \max_{i,i'} |E_{ii'}| = o(1)$  by Assumption 3) for large  $N$ , the regime-0 covariance can be written in terms of  $P_0$  as

$$\Sigma_{y,0} \simeq \begin{bmatrix} P_0 & P_0^\perp \end{bmatrix} \begin{bmatrix} \Lambda_{1,0} & \mathbf{0}_{K_0, N-K_0} \\ \mathbf{0}_{N-K_0, K_0} & \Lambda_{2,0} \end{bmatrix} \begin{bmatrix} P_0' \\ P_0^{\perp'} \end{bmatrix}. \quad (2.3)$$

Due to the assumed perturbation, a sizable perturbation  $P_0' Z P_0^\perp$  (and  $P_0^{\perp'} Z P_0$ ) will be added to the initially zero off-diagonal blocks in the expression (2.3). After such a perturbation, the previous important directions (or a basis of the regime-0 factor space)  $P_0$  can no longer explain the system's major correlation structure. The new regime will thus admit a new set of important directions represented by  $P_1$  such that

$$\Sigma_{y,1} \simeq \begin{bmatrix} P_1 & P_1^\perp \end{bmatrix} \begin{bmatrix} \Lambda_{1,1} & \mathbf{0}_{K_1, N-K_1} \\ \mathbf{0}_{N-K_1, K_1} & \Lambda_{2,1} \end{bmatrix} \begin{bmatrix} P_1' \\ P_1^{\perp'} \end{bmatrix}, \quad (2.4)$$

which implies that the factor space has changed from  $\text{span}(P_0)$  to  $\text{span}(P_1)$ . As discussed in the first chapter, the existence of the factor structure in both regimes (Assumptions 1 and 2) also suggests the type of perturbation characterized in Assumption 4. We refer to Appendix A.1.2.1 of the first chapter for full discussion.

### 2.2.1.2 IDENTIFIABLE CHANGES IN THE UNOBSERVABLE FACTOR LOADINGS

Focusing on the factor space (2.2) provides a straightforward way to disentangle a structural change of the latent transmission rule (the factor loading) from that of the latent signals (the factors) it carries to the entire  $N$ -dimensional system. In the conventional specification,

$$\mathbf{x}_{j,t} = B_j \mathbf{f}_{j,t}, \quad (2.5)$$

the unobservable factor loading  $B_j$  and the signals  $\mathbf{f}_{j,t}$  can be identified up to invertible linear transformations. In many studies, substantial breaks in the factor loading matrix have been naturally interpreted as structural changes in the system, reflecting changes in how common macroeconomic (systematic) factors transmit to the entire system.<sup>5</sup> However, as both the factor signals and their loadings are unobservable, dynamics of the factor (signal)

<sup>5</sup>For instance, breakpoints correspond to important economic events such as the 1979-1980 oil price shock or the Great Moderation, e.g., in [Stock and M. Watson, 2009](#), [Chen et al., 2014](#), [Ma and Su, 2018](#), and [Baltagi et al., 2021](#). [Banerjee et al., 2008](#) and [Yamamoto, 2016](#) have provided evidence that consideration of such breaks is important in forecasting.

covariance  $E[\mathbf{f}_{j,t}\mathbf{f}_{j,t}']$  cannot be distinguished from that of the transmission rule without extra restrictions.

In our view, it is the directional information of the transmission rule – the way latent common factors of unit signal strengths are loaded to the entire units of the system – and its dynamics that can truly capture the underlying mechanism of volatility transmission. In other words, the directional information represents the distributive characteristic of the transmission rule, regardless of the size of the latent factor signals. While the nature of the common factor factors – including their signal strengths or dynamics – is macro, systematic, or market-level, detached from micro-level characteristics, the idiosyncratic volatilities of the granular units may propagate by shifting this distributive characteristic of the transmission rule. In addition, notably, the dynamics of this directional information of the factor loading can be disentangled from the latent dynamics of the factor signals.

To clarify this, let us recall the representation. The natural way to capture this directional information is to take a column-orthonormal representation of the factor loading matrix, which corresponds to  $P_j$  in Assumption 1, up to orthonormal transformations to guarantee invariance under the unobservability. In other words, due to the latent nature of the factor signals, the directional information is represented by a ( $K_j$ –dimensional) subspace of the entire  $N$ –dimension, the factor space (2.2). It guarantees the necessary invariance, for the representation of which we take the projector  $\mathcal{P}_j \equiv P_j P_j'$ . Indeed, any linear space can be identified by the projector operator that projects any vector onto that space.

A change of the factor space is defined independently from changes in the factor covariance structure. Note that a structural change in the factor covariance, while keeping the number of factors constant, will occur in one of the following two types or as a combination of both. The first type involves a change resulting from a different linear combination of the factors. This is captured by the eigenvector changes of the factor covariance matrix, which corresponds to an internal rotation within the  $K_j$ –dimensional subspace. The factor model should remain invariant under this type of change as long as the signals are assumed to be latent. The second type is a change in the factor signal strengths captured by a change in eigenvalues of the factor covariance. Both of the characteristics can be seen as structural changes in the factor signals rather than a change in the transmission rule.

Neither the factor space nor its representation,  $\mathcal{P}_j = P_j P_j'$  is affected by these types of changes. Projectors remain invariant under the internal rotations – rotations within the  $K_j$  dimensional subspace – and the normalization separates out the factor signal strengths. However, the factor space will be affected by a change in the number of factors, which is conceptually expected. An introduction or removal of a factor necessitates an emergence or disappearance of specific pathways of transmission. Hence, the dynamics of the identifiable directional information of the factor loading matrix, as carried by the factor space, can be disentangled from those of the factor signal covariance without requiring additional restrictions.

### 2.2.2 INTERPRETING STRUCTURAL BREAKS: FACTOR SPACE, NETWORK CENTRALITY, AND EQUILIBRIUM

To provide a more tangible and interesting interpretation of the structural break that is captured by the factor space change, let us make a slight digression to zoom in on a connection between the standard factor model and a generic network model.<sup>6</sup> Consider a simple network model where  $\{y_{it}\}$  are cross-sectionally interconnected by  $\Omega$ , net of idiosyncratic components during  $t \in \mathcal{I}_0$ , such that

$$y_{it} - u_{it} = r_t + \sum_{i'} \Omega_{ii'}(y_{i't} - u_{i't}), \quad \text{or equivalently,}$$

$$\mathbf{y}_t = (I_N - \Omega)^{-1} \mathbf{1} r_t + \mathbf{u}_t = \mathbf{b} r_t + \mathbf{u}_t, \quad (2.6)$$

where we assume the invertibility of  $(I_N - \Omega)$ . The marginal benefits of exposure to  $r$  are assumed to be  $\alpha_{N \times 1} = \mathbf{1}$ . The general model with multiple common exposures  $\{r_k\}_{k=1, \dots, K}$  with corresponding heterogeneous marginal returns  $\{\alpha^k \neq \mathbf{1}\}_{k=1, \dots, K}$  will be discussed soon. This class of models can cover broad scenarios of interconnected economic activities. For instance,  $\mathbf{y}_t$  can be investment returns balanced with a common return  $r$  – from a safe asset investment or a final good demand depending on the context – where  $\Omega$  can represent mutual investments through a production network or borrower-lender relationships.

There are conceptual links among the factor model, network centrality, and equilibrium actions. On the one hand, one can see in the simple case (2.6) of a single common exposure  $r$  with homogeneous marginal returns,

$$\mathbf{b} = (I_N - \Omega)^{-1} \mathbf{1}, \quad (2.7)$$

which equals the Bonacich centrality of the cross-sectional units in the constant network  $\Omega$  (Ballester et al., 2006). When the common source of exposure and the network structure  $\Omega$  are not observable, one can describe (2.6) by a one-dimensional factor model,

$$\mathbf{y}_t = \tilde{B} f_t + \mathbf{u}_t,$$

where the factor loading  $\tilde{B}_{N \times 1}$  amounts to the centrality vector  $\mathbf{b}$ , and the common factor  $f_t$  corresponds to the common source of exposure  $r_t$ , up to a unknown scaling. From this point of view, a change of the factor space will be incurred by a structurally substantial change of the centrality, which is more than just a change in the scaling.

On the other hand, Bonacich centrality is a concept closely related to the equilibrium exposure to  $r$  given the network structure and the marginal returns (Ballester et al., 2006, Galeotti et al., 2020). With marginal benefits  $\alpha = [\alpha_i]_{i=1, \dots, N}$  potentially heterogeneous across  $i$  for the

<sup>6</sup>Appendix B.2 provides an extended discussion.

single exposure  $r$ , the weighted Bonacich centrality  $\mathbf{b} = [\beta_i]_{i=1,\dots,N} = (I_N - \Omega)^{-1}\boldsymbol{\alpha}$  depicts the equilibrium actions solving

$$\max U_i(b_i) = \max [b_i\alpha_i - (1/2)b_i^2 + b_i \sum_{i'} \Omega_{ii'} b_{i'}]. \quad (2.8)$$

In line with this conceptual Bonacich-Nash linkage, the factor space change can be interpreted as a change in equilibrium actions, and the granular units as the main contributors to the change in the equilibrium. We discuss this perspective in more detail in Appendix B.2 for general cases with multiple sources of common exposure  $\{r_k\}$  and corresponding marginal benefits  $\boldsymbol{\alpha}^k$ . In a nutshell, the generic model can be written as

$$\mathbf{y}_t = [(I_N - \Omega)^{-1}\boldsymbol{\alpha}^1 | \dots | (I_N - \Omega)^{-1}\boldsymbol{\alpha}^K] \mathbf{r}_t + \mathbf{u}_t = B\mathbf{r}_t + \mathbf{u}_t, \quad (2.9)$$

where each column of  $B$  consists of a weighted Bonacich centrality  $\mathbf{b}^k \equiv (I_N - \Omega)^{-1}\boldsymbol{\alpha}^k$  capturing the equilibrium actions of exposure to  $r_k$ . When  $\Omega, \{\boldsymbol{\alpha}^k\}$  and  $\{r_k\}$  are latent and  $K_0 (\leq K)$  signals of  $\{r_k\}$  are strong, (2.9) will be described by the  $K_0$  dimensional factor model  $\mathbf{y}_t = \tilde{B}_{N \times K_0} \mathbf{f}_t + \mathbf{u}_t$ , and the factor space carries information of the latent centrality or the equilibrium actions.

## 2.3 SYSTEMIC INFLUENCE IN STRUCTURAL BREAKS

For the granular units, idiosyncratic disturbances they experience – whether through their own volatilities or correlations with other units – can trigger a viable adjustment of existing relationships, leading to a change in the major cross-correlation structure. Such adjustments may take time and occur infrequently rather than gradually due to the necessary process of learning, assessment, and implementation. As a result, these adjustments manifest as structural breaks in our framework, identified as discrete changes in the factor space, while remaining agnostic about the exact mechanisms driving them. The systemic importance of the idiosyncratic disturbances of granular units becomes more apparent through these breaks. Within a regime, such disturbances may initially appear sparse and weakly correlated, offering little indication of their potential importance.

The second-moment-to-second-moment effect, from the idiosyncratic dimension to the system, can identify the granular units. We propose a straightforward approach to analyze this effect. First, we show that the idiosyncratic second moments and the concentration matrix (the partial correlation network) factor the magnitude of the structural break. Subsequently, the systemic influence of each unit can be evaluated by the first-order effect of its idiosyncratic second moments on the magnitude of the structural break via a straightforward application of matrix calculus. In addition, we discuss systemic importance analysis based on the partial

correlation network or concentration matrix, comparing it to our approach. Finally, the criteria for detecting the granular unit will be proposed.

### 2.3.1 BRIDGING THE IDIOSYNCRATIC DIMENSION AND THE STRUCTURAL BREAK

The magnitude of the structural break – captured by the change of the factor space – can be measured using the following metric introduced in Chapter 1 (Section 1.3):

PROJECTION METRIC (Edelman et al., 1998)

$$d(\text{span}(P_0), \text{span}(P_1)) \equiv \text{tr}[\mathcal{P}_0^\perp \mathcal{P}_1]. \quad (2.10)$$

It is a distance between two spaces  $\text{span}(P_0)$  and  $\text{span}(P_1)$ . To be precise, in (2.10), we take the square of the original projection metric as the distance measure. Recall that the spaces are represented by a form of projectors  $\mathcal{P}_j = P_j P_j'$ , free from any identification issues, as the expressions  $P_j P_j'$  are invariant under any choice of the representation of the column orthonormal basis  $P_j$ . We use the terms factor space ( $\text{span}(P_j)$ ) and its projector representation  $\mathcal{P}_j$  interchangeably.

The idiosyncratic dimension bridges into a change in the common ("systematic") dimension through the measure (2.10). Under the benchmark model in Section 2.2.1.1, the following proposition shows that for a given system with a large cross-sectional dimension  $N$ , the size of the break measured by (2.10) can be expressed as a composition involving the idiosyncratic covariance. Once translated in this way, the contribution of the idiosyncratic second moments to the change in the system's second moments, resulting in the structural break, can be straightforwardly analyzed by applying matrix calculus.

**Proposition 1.** Under the benchmark model, for large  $N$ ,

$$d(\text{span}(P_0), \text{span}(P_1)) = \text{tr}(\Sigma_{u,0} \Sigma_{y,0}^{-1} \mathcal{P}_1 \Sigma_{y,0}^{-1} \Sigma_{u,0}) + o(1). \quad (2.11)$$

The proof is in Appendix B.1. An intuitive argument is as follows. In a large  $N$  limit, the approximate factor model is compatible with PCA representation. For the decomposition  $\Sigma_{y,0} = \Sigma_{\chi,0} + \Sigma_{u,0}$ , the factor space  $\mathcal{P}_0$  is close to the first (in descending order of eigenvalues)  $K_0$ -principal eigenspace of  $\Sigma_{y,0}$ . The orthogonal directions of  $\mathcal{P}_0$  mainly capture the idiosyncratic covariance,

$$(I_N - \mathcal{P}_0) \Sigma_{y,0} \simeq \Sigma_{u,0}.$$

Then,

$$\begin{aligned} (I_N - \mathcal{P}_0)\mathcal{P}_1(I_N - \mathcal{P}_0) &= (I_N - \mathcal{P}_0)\Sigma_{y,0}\Sigma_{y,0}^{-1}\mathcal{P}_1\Sigma_{y,0}^{-1}\Sigma_{y,0}(I_N - \mathcal{P}_0) \\ &\simeq \Sigma_{u,0}\Sigma_{y,0}^{-1}\mathcal{P}_1\Sigma_{y,0}^{-1}\Sigma_{u,0}. \end{aligned}$$

The expression (2.11) will be utilized to construct a measure of the systemic influence of cross-sectional units in the next section. To simplify the exposition, in the rest of this section, *let us omit the present regime subscripts 0* (except for the case of the regime-0 factor space or its basis) unless otherwise stated. That is, expressions such as  $\Sigma_y^{-1}$ ,  $\Sigma_u$ , or any subcollections of their entries without subscripts will indicate regime-0 objects.

### 2.3.2 A MEASURE OF SYSTEMIC INFLUENCE

An individual unit's systemic influence can be measured by the contribution of its idiosyncratic second moments to the factor space change. The most straightforward way to capture this contribution is through the first-order effect of  $\Sigma_u$  on the magnitude of the factor space change. As the idiosyncratic covariance factors the size of the structural break as in (2.11), it is simply the partial derivative of the expression (2.11) with respect to  $\Sigma_u$ ,

$$\partial_{\Sigma_u} d(\text{span}(P_0), \text{span}(P_1)) = 2\Sigma_y^{-1}\mathcal{P}_1\Sigma_y^{-1}\Sigma_u, \quad (2.12)$$

that captures the contribution. This simple application is enabled by the characteristic of the trace operator, the summation of the diagonal elements of the matrix products.

The adjusted factor space  $\mathcal{P}_1$  is assumed to have no direct (first-order) effect from a hypothetical perturbation on  $\Sigma_u$ . The idiosyncratic disturbances may demand the adjustment of the existing relationships between some or all cross-sectional units. For example, adjustment of the network structure  $\Omega$ , following the conceptual connection from the latent network model in Section 2.2.2. However, the result of the adjustment – the new relationships  $\Omega_1$  or the corresponding new factor space  $\mathcal{P}_1$  – may have a functional dependence on the parameters that enable the adjustment, for example, the market or bargaining power, information superiority of certain units or system-wide asymmetries of those, rather than on the idiosyncratic disturbances that may demand an adjustment. A technical discussion for more general cases continues in Appendix B.3.

To make a straightforward interpretation of (2.12), let us assume that all idiosyncratic components are uncorrelated. As  $\Sigma_u$  is diagonal, it is only  $\sigma_{u,i}^2$  that matters among the idiosyncratic

second moments for given unit  $i$ . In this case, the share of unit  $i$  in the factor space adjustment is captured by

$$\mathcal{I}_i \equiv \frac{1}{2} \partial_{\sigma_{u,i}^2} d(\text{span}(P_0), \text{span}(P_1)) = \left[ \Sigma_y^{-1} \mathcal{P}_1 \Sigma_y^{-1} \Sigma_u \right]_{ii} = [\sigma_y^{i1} \dots \sigma_y^{iN}] \mathcal{P}_1 \begin{bmatrix} \sigma_y^{1i} \\ \vdots \\ \sigma_y^{Ni} \end{bmatrix} \sigma_{u,i}^2.$$

The contribution of unit  $i$  consists of three types of information. First, the size of the idiosyncratic shock faced by unit  $i$  ( $\sigma_{u,i}^2$ ) in regime-0. Second, the importance of unit  $i$  in terms of the structure of the partial correlation  $[\Sigma_y^{-1}]_i = [(\sigma_y^{in})_{n=1,\dots,N}]$  in regime-0.<sup>7</sup> Finally, how all other units connected to  $i$  through the partial correlation become important to explain the major cross-correlation structure of the next regime ( $\mathcal{P}_1$ ). Together, these three features convey a full picture of the systemic influence of individuals.

In other words,  $\mathcal{I}_i$  evaluates the distributive consequence ( $\mathcal{P}_1$ ) of the idiosyncratic second moments ( $\sigma_u^i = [\sigma_u^{i1}, \dots, \sigma_u^{iN}]'$ , for general cases) through an interconnected structure ( $\Sigma_y^{-1}$ ). This approach provides a more comprehensive perspective on systemic influence compared to methods that focus solely on the magnitude of the idiosyncratic volatilities or a network structure.

For a general structure of the idiosyncratic covariance, we define the contribution of unit  $i$  as a norm of the  $i$ th column of (2.12), that is:

$$\mathcal{I}_i \equiv \left\| \frac{1}{2} [\partial_{\Sigma_u} d(\text{span}(P_0), \text{span}(P_1))]^i \right\| = \left\| \Sigma_y^{-1} \mathcal{P}_1 \Sigma_y^{-1} \sigma_u^i \right\|, \quad (2.13)$$

where  $\sigma_u^i = [\sigma_u^{i1}, \dots, \sigma_u^{iN}]'$  acts as the source triggering the structural break.

### 2.3.2.1 THE CONCENTRATION MATRIX REVISITED

In a stationary environment, the concentration matrix alone can be utilized for the detection of granular units. [Brownlees and Mesters, 2021](#) showed that a column norm of the concentration matrix  $\Sigma_y^{-1}$  can provide a measure of systemic influence in a stationary environment under a certain type of static factor model.<sup>8</sup> The concentration matrix is a popular object of study in the literature, as it captures partial correlations among cross-sectional items of stationary panel data.<sup>9</sup> The granular units identified through the concentration matrix can be seen as the most central individuals in the stationary network of partial correlations. In contrast, our proposed modeling assumes a non-stationary environment, where the underlying latent

<sup>7</sup>In a stationary environment, the concentration matrix alone can be utilized for the detection of granular units. We will soon discuss this point before the end of this subsection.

<sup>8</sup>This expression does not have subscript because the discussion is independent of the existence of different regimes.

<sup>9</sup>A standard exposition can be found in [Pourahmadi, 2013](#), Chapter 5.

structure governing the cross-correlations is infrequently adjusting. This is as if the adjustment was carried out after assessing a situation by learning during a stationary time window.

Such a "slow" adjustment scenario is more adapted to a high-frequency data environment. In a low-frequency environment, one can assume that the data exhibits a certain static factor structure that already represents the systemic influence. The observations can be made by giving enough time to the system to absorb or get affected by the potential systemic influence. It may not be the case in a high-frequency environment. It can be the case that the effect of the influence is not realized in each high-frequency observation but is exhibited as a structural change after some period. From our point of view, this latter behavior provides a chance to distinguish a factor behind the perceived structure of correlations. Accordingly, the proposed measure of influence not only involves the partial correlation structure of the current regime but also considers the changed correlation structure of the next regime, realized through  $P_1$  or  $\mathcal{P}_1$ .

The concentration matrix itself is a form of a partial change of the system covariance as well. By the very nature of the symmetric operator inversion, the  $(i, i')$ -th component of  $\Sigma_y^{-1}$  equals (Horn and Johnson, 2013, equation (0.8.2.7))

$$[\Sigma_y^{-1}]^{ii'} = \frac{1}{\det \Sigma_y} \frac{\partial}{\partial \sigma_y^{ii'}} \det \Sigma_y = \frac{\partial}{\partial \sigma_y^{ii'}} \ln \det \Sigma_y. \quad (2.14)$$

It is the percentage partial change of the size of the dispersion of the system covariance measured by  $\det \Sigma_y = \prod_{i=1}^N \lambda_i$ <sup>10</sup>, due to a perturbation on  $\sigma_y^{ij}$ , fixing all other entries of the covariance. The  $i$ -th column norm of the concentration matrix corresponds to the sum of the partial effects (2.14) due to  $i$  across overall  $i'$ , for example,

$$\|\Sigma_y^{-1}\|^i = \sqrt{\sum_{i'=1}^N \left( \frac{\partial}{\partial \sigma_y^{ii'}} \ln \det \Sigma_y \right)^2}.$$

In this sense, the column norm of the concentration matrix does capture a kind of importance of each unit's second moments to the system's second moments. Assuming a factor structure, however, there are several aspects it does not capture. First, if there are idiosyncratic shocks that potentially communicate with the transmission rule of the common factors, their effects can not be fully captured by the partial derivatives. All other  $\{\sigma_y^{jk}\}$  will change according to the evolving transmission rule. By keeping them constant, the partial change (2.14) will miss such an indirect channel that may provide a fuller picture of systemic influence in the non-stationary environment on which we focus. Second, due to the nature of the determinant (defined by the eigenvalue information), a measure based on (2.14) does not actively exploit directional characteristics of the system covariance captured in eigenspaces, which may be informative under a factor structure.

<sup>10</sup> $\det \Sigma_y$  captures the volume of the image of the system covariance as an operator.

It is worth noting that the focus of current literature has been on the concentration matrix of the residual covariance ( $\Sigma_u^{-1}$ ) as well, to capture a conditional partial correlation structure of a system (e.g., [Dahlhaus, 2000](#), [Eichler, 2012](#), [Bianchi et al., 2019](#), and [Barigozzi and Brownlees, 2019](#)). It can represent a contemporaneous dependence conditional on the common factor dimension. When the *conditions* are changing, for example, due to a regime change represented by a change in the factor loading, a disparity between the conditional contemporaneous dependence in different regimes can be important and informative, as mentioned, e.g., in [Bianchi et al., 2019](#) and [Massacci, 2021](#). The way we perceive it is that such a change of *condition* will be informative for recognizing a group of systemic individuals.

We will now establish criteria for granular unit detection utilizing the proposed influence measure.

### 2.3.3 CRITERIA FOR DETECTING GRANULAR UNITS

We have discussed how systemic influence can be evaluated through the contributions of the idiosyncratic second moments to changes of the factor space. Granular units are naturally characterized as those that present the largest contributions. This provides the criterion for membership in  $\mathcal{G}$ , the set of granular units. What remains is to establish a criterion for the size of  $\mathcal{G}$ . To complete the detection criteria, we will utilize a comprehensive feature of the factor space dynamics.

Recall that granular units are those capable of altering existing relationships in ways that induce major changes in system correlations. The adjustment can be seen as changes of equilibrium exposures to common sources or in network centrality, given a network representing the existing relationships or the within-regime cross-sectional correlations, as discussed in Section 2.2.2.

When a granular unit adjusts, it induces a reconfiguration of the entire equilibrium actions of all units. For multiple common sources of exposure,  $\{r_k\}$ , the equilibrium actions ( $\mathbf{b}_{N \times 1}^k$ ) can be defined for each  $r_k$ . If the equilibrium actions change for  $H$  distinct common sources, we assume there are  $H$  granular units. Distinct granular units can be found responsible for changes in equilibrium exposure to each distinct common source. In its latent counterpart – involving the unobservable network, common sources, and potentially unit-specific marginal returns on these sources – this assumption will be framed as a feature of the factor space change, as follows.

**Assumption 5.** The number of granular units corresponds to the number of independent directions of a change of the factor space. That is,

$$H = \text{rank}(\mathcal{P}_0^\perp \mathcal{P}_1). \quad (2.15)$$

A geometric feature of the factor space dynamics illuminates this assumption. Under the benchmark model introduced in Section 2.2.1.1, the dynamics are conceptualized as a form of rotation of the regime-0 factor space to the regime-1 factor space.<sup>11</sup> If the factor spaces have a fixed dimension 1, the dynamics will be represented solely by a vector  $P_0$ , which, when rotated in a certain direction (say  $V$ , the *velocity*) yields another vector  $P_1$  in  $N$ -dimensional space. Similarly, the motion of a multi-dimensional subspace is described by a collection of rotations of its  $K$ -basis vectors, each rotating in a specific direction. The velocity also becomes a multidimensional object, represented as a collection of the directions for change.

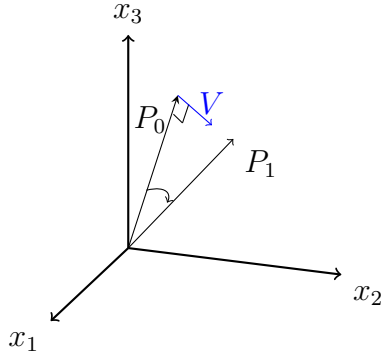


Figure 2.1: A rotating 1-dimensional factor space in  $N = 3$  dimension.  $P_0$  ( $P_1$ ) represents a basis of the regime 0 factor space  $\text{span}(P_0)$  ( $\text{span}(P_1)$ , resp.). (All vectors representing directional information ( $P_0, P_1$ , and  $V$ ) have their lengths normalized to 1.)

Let us recall that, as in the argument inside the trace of (2.10), the change of the factor space is measured by the component of  $\mathcal{P}_1$  that is perpendicular to  $\text{span}(P_0)$ , or  $\mathcal{P}_0^\perp$ . The directional information of this component equals exactly the velocity. The number of independent directions of change, or the rank of  $V$ , is a crucial characteristic determining the factor space dynamics, just as important as the overall magnitude of the change (2.10), which is employed to construct the criterion for membership detection. We assume that the number of granular units is equal to the number of directions constituting the velocity  $V$ . The factor space evolves as if each important unit selects an independent direction of change.

The choice of this velocity is the true latent source of factor space dynamics, which remains almost entirely model-free in our approach. Although we remain agnostic about the true process behind the directional choice, the rank of  $V$ , or the rank of the change, can be deduced as long as we have any factor space representations,  $\mathcal{P}_0$  and  $\mathcal{P}_1$ .

### 2.3.3.1 DETECTION CRITERIA

We can now summarize the criteria for detecting the size (how many granular units there are) and the membership (which the granular units are) of the set of granular units. The statement of the criteria has been assigned a new subsection number for ease of future reference.

NUMBER OF GRANULAR UNITS  $H = \text{rank}(\mathcal{P}_0^\perp \mathcal{P}_1)$ .

<sup>11</sup>Refer to Appendix A.1.2.1 for a detailed discussion.

**MEMBERSHIP OF THE SET OF GRANULAR UNITS** The set  $\mathcal{G}$  of granular units consists of  $H$  cross-sectional units which present the highest column norms,

$$\mathcal{I}_i \equiv \left\| \frac{1}{2} [\partial_{\Sigma_u} d(\text{span}(P_0), \text{span}(P_1))]^i \right\| = \left\| \Sigma_y^{-1} \mathcal{P}_1 \Sigma_y^{-1} \boldsymbol{\sigma}_u^i \right\|, \quad (2.13)$$

where  $\Sigma_y^{-1}$  is the regime-0 concentration matrix and  $\boldsymbol{\sigma}_u^i = [\sigma_u^{i1}, \dots, \sigma_u^{iN}]'$  is the  $i$ -th column of the regime-0 idiosyncratic covariance.

The sample analogue of (2.13) will be utilized in practice. In Appendix B.4, we provide a more detailed explanation of the geometric aspects of the detection criteria.

## 2.4 ESTIMATION

The proposed detection scheme exploits a structural break, characterized as a change of the factor space. Although detecting the breakpoint is necessary in principle, the main focus of our discussion, presented in the first section, is on the case where the breakpoints are known. We also address the estimation of breakpoints in the second section. The systematic analysis of cases involving unknown breakpoints will be explored in detail in a separate project.

### 2.4.1 ESTIMATION WITH A KNOWN BREAKPOINT

Assume that we know one break point that separates two windows of the present and future regimes,  $\mathbf{I}_0$  and  $\mathbf{I}_1$ . The length of each regime is given as  $|\mathbf{I}_j| = \kappa_j T$ , for some constant  $\kappa_j \in (0, 1)$ , for the entire time period  $T$ . The sample analogue of the proposed influence measure,

$$\hat{\mathcal{I}}_i = \left\| \hat{\Sigma}_{y,0}^{-1} \hat{P}_1 \hat{P}_1' \hat{\Sigma}_{y,0}^{-1} \hat{\boldsymbol{\sigma}}_{u,0}^i \right\|, \quad (2.16)$$

consists of the  $i$ -th column  $\hat{\boldsymbol{\sigma}}_{u,0}^i$  of idiosyncratic covariance matrix  $\hat{\Sigma}_{u,0}$ , the concentration matrix  $\hat{\Sigma}_{y,0}^{-1}$  of the present regime, and the factor space in future  $\hat{P}_1 \hat{P}_1'$ .<sup>12</sup> The dimensions of the factor spaces in both windows also need to be estimated during the procedure. Consistent estimations of these objects have been studied extensively. We mainly adopt the estimation procedures proposed in [Fan et al., 2013](#), which provide consistent estimations of the factor space, the concentration matrix, and the idiosyncratic covariance simultaneously. Classical studies [Stock and M. W. Watson, 2002b](#), [Bai and Ng, 2002](#) are also closely related. For a complete exposition, we refer to the original papers.

Recall from the benchmark model in Section 2.2.1.1 that we have  $T_j$  data for regime- $j$ , following

$$\mathbf{y}_{t,j} = \boldsymbol{\chi}_{j,t} + \mathbf{u}_{t,j}, \quad \text{for } t \in \mathbf{I}_j, \quad (2.1)$$

<sup>12</sup>Recall that this is the projector representation of the factor space  $\text{span}(\hat{P}_1)$ .

where  $\Sigma_{\chi,j} = P_j \Lambda_{\chi,j} P_j'$  has all nonzero  $K_j$  eigenvalues diverging at the rate  $O(N)$  (Assumption 1). For optimal access to the references mentioned above, we explain the estimation procedures in accordance with the standard specification of the low-rank part  $\chi_{j,t}$ ,

$$\chi_{j,t} = B_j \mathbf{f}_{t,j}, \quad \text{for } t \in \mathcal{I}_j, \quad (2.5)$$

where  $B_j$  denotes the factor loading matrix fixed within regime for given  $N$ , and  $\mathbf{f}_{t,j}$  denotes  $K_j$  factor signals. By augmenting the  $T_j$  data in columns, the data  $Y_j$  of the given regime is represented as an  $N$  by  $T_j$  matrix,

$$Y_j = B_j F_j + U_j, \quad (2.17)$$

where  $F_j$  is a  $K_j \times T_j$  matrix of factors and  $U_j$  is an  $N \times T_j$  matrix of idiosyncratic errors. Under this specification, the benchmark model in Section 2.2.1.1 can be conditioned on  $B_j$  to absorb the linearly growing eigenvalues of  $\Sigma_{\chi,j}$ , while  $\text{var}(\mathbf{f}_{t,j})$  remains finite. The contents of the following Assumptions 6 to 11 closely resemble Assumptions 1 to 4 of [Fan et al., 2013](#), Section 3.

**Assumption 6.** For each  $j \in \{0, 1\}$ ,  $B_j' B_j / N \rightarrow D_j$  as  $N \rightarrow \infty$  for some full  $K_j$ -rank diagonal matrix  $D_j$ .

**Assumption 7.** For each  $j \in \{0, 1\}$ ,  $(\mathbf{f}_{t,j}, \mathbf{u}_{t,j})$  is stationary,  $E[\mathbf{f}_{t,j}] = E[\mathbf{u}_{t,j}] = \mathbf{0}$ , and  $E[f_{kt} u_{it}] = 0$  for all  $i \in \mathcal{N}$  and  $k = 1, \dots, K_j$ .

There are additional distributional assumptions on  $\mathbf{f}_t$  and  $\mathbf{u}_t$ : exponential tail behaviors (Assumption 8), a strong mixing condition (Assumption 9), and appropriate moment conditions (Assumption 10). For Assumption 9, denote the  $\sigma$ -fields

$$\mathcal{F}_{L_1}^{L_2} \equiv \sigma(\{(\mathbf{f}_t, \mathbf{u}_t) \mid t \in [L_1, L_2]\})$$

and let the mixing coefficient be

$$\alpha(T) \equiv \sup_{\ell \in \mathbb{Z}} \sup_{A \in \mathcal{F}_{-\infty}^\ell, B \in \mathcal{F}_{\ell+T}^\infty} |\Pr(A \cap B) - \Pr(A) \Pr(B)|. \quad (2.18)$$

**Assumption 8.** There exist constants  $r_1, r_2, b_1, b_2 > 0$  such that for all  $j \in \{0, 1\}$ , for any  $s > 0$ ,  $i \in \mathcal{N}$  and  $k = 1, \dots, K_j$ ,

$$\begin{aligned} \sup_{t \in \mathcal{I}_j} \Pr(|u_{it,j}| > s) &\leq \exp\{-s/b_1\}^{r_1}, \\ \sup_{t \in \mathcal{I}_j} \Pr(|f_{kt,j}| > s) &\leq \exp\{-s/b_2\}^{r_2}. \end{aligned}$$

**Assumption 9.** There exist  $C_r > 0$  and  $r_3 > 0$  such that  $3r_1^{-1} + (3/2)r_2^{-1} + r_3^{-1} > 1$ , satisfying  $\alpha(T) < \exp(-C_r T^{r_3})$  for all  $T \in \mathbb{Z}_+$ .

**Assumption 10.** There exists  $C > 0$  such that, for all  $j \in \{0, 1\}$ , for any  $i \in \mathcal{N}$ ,  $s, t \in \mathcal{I}_j$ ,

(a)  $\|\mathbf{b}_{i,j}\|_{max} < C$ , for the  $i$ -th row vector  $\mathbf{b}_{i,j}$  of  $B_j$ .

(b)  $E\left[\left(N^{-1/2}\left\{\mathbf{u}_{s,j}'\mathbf{u}_{t,j} - E[\mathbf{u}_{s,j}'\mathbf{u}_{t,j}]\right\}\right)^4\right] < C$ ,

(c)  $E\left[\|N^{-1/2}B_j'\mathbf{u}_{t,j}\|^4\right] < C$ .

**Assumption 11.**  $\ln(N) = o(T^{\gamma/6})$  for  $\gamma^{-1} \equiv 3r_1^{-1} + (3/2)r_2^{-1} + r_3^{-1} + 1$ , and  $T = o(N^2)$ .

The assumption of strict stationarity in [Fan et al., 2013](#) (Assumption 2(a)) can be relaxed. The weak stationarity with uniform tail behaviors is sufficient to apply Bernstein's inequality in [Merlevède et al., 2011](#) (Theorem 1), by which the necessary results in [Fan et al., 2013](#) are produced to guarantee consistency. The strong mixing condition is on the entire time period combining regimes. The rate of  $N$  and  $T$  is assumed to guarantee consistency, following the original paper.

Under Assumptions 1-2 in Section 2.2.1.1 and Assumptions 6-11 above, first, the dimension of the factor space in each regime can be consistently estimated following [Bai and Ng, 2002](#). A consistent estimate  $\hat{K}_j$  of the factor space dimension minimizes the following information criteria

$$IC_{K_j} = \ln V(K_j) + K_j g(N, T_j), \quad (2.19)$$

where  $V(K_j) = \text{tr}(U_j U_j') / NT_j$ . The penalty function  $g(N, T)$  for any given size  $(N, T)$  of the cross-sectional and time dimensions needs to converge to zero slower than the rate  $(\min\{N, T\})^{-1}$  (Theorem 2, [Bai and Ng, 2002](#)). The same asymptotic property is required by the given regularity conditions based on [Fan et al., 2013](#). We employ the following functions

$$g(N, T) = \frac{N+T}{NT} \ln\left[\frac{NT}{N+T}\right] \quad \text{or} \quad g(N, T) = \frac{N+T}{NT} \ln[\min\{N, T\}], \quad (2.20)$$

introduced in [Bai and Ng, 2002](#) and adopted in [Fan et al., 2013](#).

Second, after the consistent estimation of the factor space dimension, the common component  $\chi_{j,t}$  is estimated by projecting  $Y_j$  on the  $K_j$ -leading principal subspace of the sample covariance  $\hat{\Sigma}_{y,j}^{\text{sam}} = Y_j Y_j' / T_j$ , or on that of the right Gram-matrix  $\hat{\Sigma}_{y,j}^N = Y_j' Y_j / N$ . For  $\hat{P}_j = [\hat{e}_j^1 | \dots | \hat{e}_j^{K_j}]$ , orthonormalized  $K_j$ -leading eigenvectors  $\{\hat{e}_j^k\}_{k=1, \dots, K_j}$  of  $\hat{\Sigma}_{y,j}^{\text{sam}}$ ,  $\hat{\chi}_j = \hat{P}_j \hat{P}_j' Y_j$  by augmenting the time dimension of  $\hat{\chi}_{j,t}$  column-wise. For the cross-sectional dimension  $N > T_j$ , utilizing  $K_j$ -leading eigenvectors  $\hat{P}_{T_j}$  of  $T_j \times T_j$  matrix  $Y_j' Y_j / N$  can be computationally efficient ([Stock and M. W. Watson, 2002b](#), [Bai and Ng, 2002](#)). In this case,

$\hat{\chi}_j = Y_j \hat{P}_{T_j} \hat{P}_{T_j}'$ . Those are standard and identical methods under the presence of a small number of unobservable factors  $K \ll N$ .

Third, the factor space information is fully captured by the eigenvectors  $\hat{P}_j = [\hat{e}_j^1 | \dots | \hat{e}_j^{K_j}]$  of the sample covariance matrix. Note that the estimated common component covariance is  $\hat{\Sigma}_{\chi,j} = \hat{\chi}_j \hat{\chi}_j' / T = \hat{P}_j \hat{\Lambda}_{K_j} \hat{P}_j'$ , the spectral decomposition of the sample covariance up to  $K_j$ th eigenvalue and the corresponding eigenspace, regardless of which method estimates  $\hat{\chi}_j$  in the second task. The leading  $K_j$ -principal subspace  $\text{span}(\hat{P}_j)$  of  $\hat{\Sigma}_{y,j}^{\text{sam}}$  deviates from  $\text{span}(P_j)$  by  $o_p(1)$  mainly due to the following reasons:  $\|\hat{\Sigma}_{\chi,j} - \Sigma_{\chi,j}\| = o_p(N)$  (due to Lemma 4 of Fan et al., 2013), the factor prevalence with the rate  $O(N)$  (Assumption 1 of 2.2.1.1 and Assumption 6), and because the common component covariance  $\Sigma_{\chi,j}$  is estimated by  $\hat{\Sigma}_{\chi,j}$  of the same rank. We explain in detail the contributions of these terms in Appendix B.1.

Fourth, Fan et al., 2013 introduced a thresholding method ('POET') to consistently estimate the idiosyncratic covariance under the above set of conditions. The thresholding parameter needs to be gauged with the sparsity parameter  $c_{u,j}$  and  $q_j$  of  $\Sigma_{u,j}$  to secure consistency. Recall from Assumption 2 that  $c_{u,j} \equiv \max_{i=1,\dots,N} \sum_{i'=1,\dots,N} |\text{cov}(u_{it,j}, u_{i't,j})|^{q_j} = O(1)$  for some constant  $q_j \in [0, 1]$ . The empirical correlation estimator of  $i, i' \in \mathcal{N}$  – the time average of the product of  $i$ -th and  $i'$ -th residuals  $\hat{u}_{i,j}$  and  $\hat{u}_{i',j}$  – will be adaptively thresholded proportional to

$$\omega_{T,j} \equiv 1/\sqrt{N} + \sqrt{(\ln N)/T_j}, \quad (2.21)$$

where  $c_{u,j} \omega_{T,j}^{1-q_j} = o(1)$ . Under our simple benchmark assumption  $c_{u,j} = O(1)$ , it is sufficient to have  $\omega_{T,j} = o(1)$  for consistency of the idiosyncratic covariance. Assumptions 9 and 11 assure this rate as  $\gamma < 1/2$  and  $T_j$  is a fixed portion of the entire  $T$ .

Fifth, it is also proven in the same paper that the estimates of idiosyncratic covariance  $\hat{\Sigma}_{u,j}$  and the common component covariance estimator  $\hat{\Sigma}_{\chi,j} = \hat{\Gamma}_{\chi,j} \hat{\Gamma}_{\chi,j}'$  can be plugged into the Sherman-Morrison-Woodbury formula

$$\hat{\Sigma}_{y,j}^{-1} \equiv \hat{\Sigma}_{u,j}^{-1} - \hat{\Sigma}_{u,j}^{-1} \hat{\Gamma}_{\chi,j} (I_K + \hat{\Gamma}_{\chi,j}' \hat{\Sigma}_{u,j}^{-1} \hat{\Gamma}_{\chi,j})^{-1} \hat{\Gamma}_{\chi,j}' \hat{\Sigma}_{u,j}^{-1}, \quad (2.22)$$

where  $\hat{\Gamma}_{\chi,j} = \hat{P}_j \hat{\Lambda}_{K_j}^{1/2}$ , to give a consistent estimation of the concentration matrix of  $\mathbf{y}_{t,j}$ . The rate  $\|\hat{\Sigma}_{y,j}^{-1} - \Sigma_{y,j}^{-1}\| = \|\hat{\Sigma}_{u,j} - \Sigma_{u,j}\| = O_p(c_{u,j} \omega_{T,j}^{1-q})$ .

Finally, the number of granular units  $H \equiv \text{rank}(W)$  for  $W \equiv P_0^\perp P_0^\perp' P_1 P_1'$  can be decided by the number of nonzero eigenvalues of its sample analogue

$$\hat{W} \equiv \hat{P}_0^\perp \hat{P}_0^{\perp'} \hat{P}_1 \hat{P}_1'.$$

Although numerous sophisticated methods can be applied, in applications, a check on the eigenvalue gap through the scree plot of the matrix  $\hat{W}$  will be the most uncomplicated yet acceptable procedure.

## RANKING CONSISTENCY OF THE INFLUENCE MEASURE

The proposed measure  $\mathcal{I}_i \equiv \left\| \Sigma_{y,0}^{-1} P_1 P_1' \Sigma_{y,0}^{-1} \sigma_{u,0}^i \right\|$  is a norm of each column of

$$\mathcal{I} \equiv \Sigma_{y,0}^{-1} P_1 P_1' \Sigma_{y,0}^{-1} \Sigma_{u,0}. \quad (2.23)$$

The membership detection based on ranking  $\{\mathcal{I}_i\}_{i \in \mathcal{N}}$  can be proven to be valid by showing consistency of the ranking of  $\{\hat{\mathcal{I}}_i\}_{i \in \mathcal{N}}$  between the granular and the non-granular units. The consistency can be proven in a similar way as in [Brownlees and Mesters, 2021](#), exploiting the consistency of  $\mathcal{I}$  estimation.

Define event  $\Upsilon$ , where the estimated influence measures are indeed higher for the granular units than those for the non-granular units, that is,

$$\Upsilon \equiv \left\{ \|\hat{\mathcal{I}}_g\| > \|\hat{\mathcal{I}}_i\| \mid g \in \mathcal{G}, i \in \mathcal{G}^c \right\}. \quad (2.24)$$

**Proposition 2.** Under the Assumptions 1-2 in Section 2.2.1.1 and 6-11, event  $\Upsilon$  holds asymptotically almost surely.

The proof is left to Appendix B.1.

### 2.4.2 SIMULATION

This section contains the simulation results for the granular unit detection. The simulation for granular unit detection presents higher success rates in identifying true granular groups as those with larger gaps in their systemic influence relative to non-granular units.

Consider a system of  $N = 100$  cross-sectional units in two regimes ( $J = 2$ ). Each regime ( $j = 0, 1$ ) has  $T_j = 100$  data, both with  $K = 3$  dimension of the factor space. Assume that the breakpoint at  $T_1 = 100$  is known.

The regime change amounts to a change of factor space  $\text{span}(P_0)$  to  $\text{span}(P_1)$ .  $P_0$  is a randomly chosen orthonormal  $N \times K$  matrix whose column space equals the regime-0 factor space  $\text{span}(P_0)$ . We assume  $\mathbf{f}_t \sim \mathcal{N}(\mathbf{0}_{K \times 1}, \Sigma_{\chi} = \sigma_{\chi}^2 I_K)$  and loaded by  $P_0$  during the first regime, and  $\mathbf{u}_t \sim \mathcal{N}(\mathbf{0}_{N \times 1}, \Sigma_u = \sigma_u^2 I_N)$ . It is further assumed that  $\Sigma_{\chi}$  and  $\Sigma_u$  are fixed across regimes, with  $\sigma_{\chi} = 5$  and  $\sigma_u = \sqrt{2}$ . That is, for any  $j \in \{0, 1\}$ ,

$$\mathbf{y}_t = P_j \mathbf{f}_t + \mathbf{u}_t \quad \text{for } t \in \mathcal{I}_j.$$

The regime-1 factor space basis  $P_1$  is chosen so that combined with  $\Sigma_{y,0}^{-1}$ , the resulting  $\text{span}(P_1)$  implies a particular set  $\mathcal{G}$  of three units as the set of granular units based on the measure  $\mathcal{I}_i \equiv \left\| \Sigma_{y,0}^{-1} P_1 P_1' \Sigma_{y,0}^{-1} \sigma_{u,0}^i \right\|$  in equation (2.13). We present 48 different sets  $\mathcal{G}$  of granular units

(and the corresponding choices of  $P_1$ ), while keeping the distance  $d(\text{span}(P_0), \text{span}(P_1)) \equiv \text{tr}[P_0^\perp P_1]$  in (2.10) the same. Distinct choices of the  $P_1$  point in various directions and span different three-dimensional subspaces within the entire  $N = 100$  dimension. The different factor space dynamics – and the corresponding groups  $\mathcal{G}$  or  $\text{span}(P_1)$  – present different influence gaps between the granular units and the non-granular units. The groups are numbered by their rankings of the influence gap measured as the ratio of  $\mathcal{I}_H$  and  $\mathcal{I}_{H+1}$  in descending order.

Let us detail the construction of the sample granular groups. The collection is first randomly chosen among the groups with the influence gap ( $\equiv \mathcal{I}_H/\mathcal{I}_{H+1}$ ) in the range  $(1.10, 2.03)$  and the average group influence  $\bar{\mathcal{I}}_{\mathcal{G}} \equiv (\sum_{g=1}^H \mathcal{I}_g)/H > 0.1$ . By the design of the influence measure, some units can appear much more frequently in many different groups than other units. As discussed in Section 2.3.2, the units that have a relatively high centrality in regime-0 based on  $\Sigma_{y,0}^{-1}$  can appear as granular units in many different scenarios of factor space change; such as, for example, the units (65, 64, 47) that are the top 3 of the highest column norms of  $\Sigma_{y,0}^{-1}$  by 2-norm. Besides, due to the homogeneous and diagonal  $\Sigma_u$  in our setup, those who have more intense loads of the change  $P_1 P_1'$  from  $P_0 P_0'$  will also appear as granular units, for example, the units (1, 22, 63).

The group collection has been adjusted to encompass more than half of all 100 units in the group membership. The membership list of the 48 different groups is presented in Table 2.1 below.

Group Identities by $\mathcal{I}_H/\mathcal{I}_{H+1}$ ranking							
1	[43 92 13]	13	[43 63 96]	25	[21 63 18]	37	[22 55 3]
2	[79 65 1]	14	[100 90 29]	26	[79 65 5]	38	[7 65 84]
3	[47 57 1]	15	[22 77 64]	27	[12 57 29]	39	[63 57 62]
4	[77 47 42]	16	[59 81 65]	28	[47 77 96]	40	[63 21 90]
5	[68 73 69]	17	[73 88 68]	29	[47 17 96]	41	[9 10 90]
6	[22 65 25]	18	[99 85 1]	30	[13 22 81]	42	[63 62 55]
7	[22 88 59]	19	[21 17 7]	31	[1 57 16]	43	[6 29 8]
8	[23 63 66]	20	[45 57 16]	32	[17 45 16]	44	[13 73 20]
9	[79 45 59]	21	[79 88 5]	33	[69 67 64]	45	[10 12 9]
10	[79 77 11]	22	[1 9 6]	34	[23 7 20]	46	[56 11 60]
11	[23 44 5]	23	[56 7 60]	35	[13 7 81]	47	[11 36 5]
12	[42 69 1]	24	[92 47 5]	36	[22 75 25]	48	[6 69 59]

Table 2.1: Sample collection of granular groups

The sample analogue  $\hat{\mathcal{I}}_i = \left\| \hat{\Sigma}_{y,0}^{-1} \hat{P}_1 \hat{P}_1' \hat{\Sigma}_{y,0}^{-1} \hat{\sigma}_{u,0}^i \right\|$  is constructed following the estimation methods discussed in Section 2.4.1. We repeat the process  $M = 500$  times for each group  $\mathcal{G}$  and count the number of successful detection of the true membership of  $\mathcal{G}$ . A detection is considered successful only when it detects all three members correctly, while correct detection of only some of the members of  $\mathcal{G}$  is considered a failure. The random seeds for the draws of  $\mathbf{f}$  and  $\mathbf{u}$  are the same across the different sets of true granular units.

Figure 2.2 presents the results of this simulation exercise.

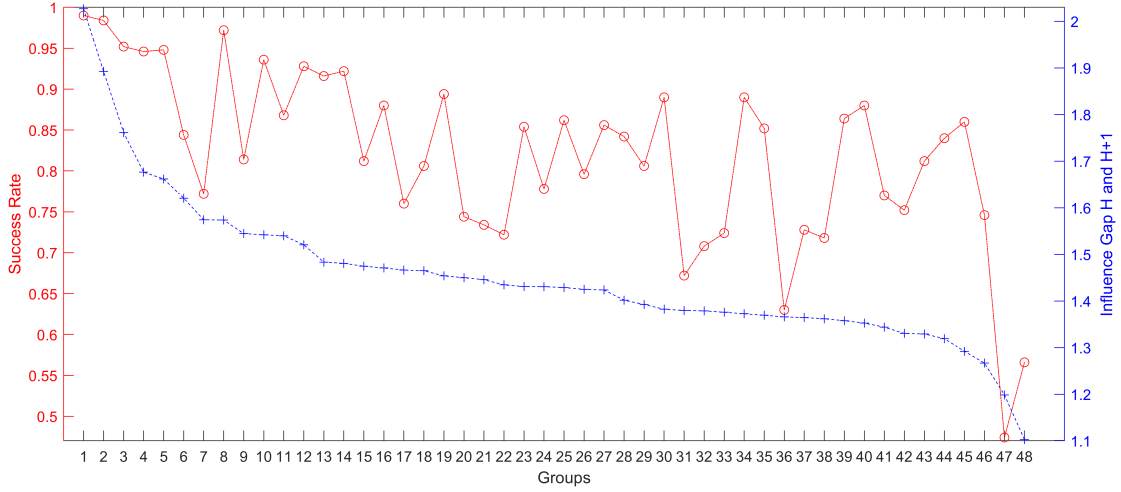


Figure 2.2: Success Rate of the Granular Unit Detection  
(by the influence Gap,  $\mathcal{I}_H/\mathcal{I}_{H+1}$ )

The rate of successful detection overall presents the anticipated decreasing trend as the influence of the granular units becomes less distinguished compared to non-granular units. In this trial, if the least essential granular unit is still 40% more influential than the non-granular units, the rate of successful detection of the granular units is higher than 72.2%.

The average group influence  $\bar{\mathcal{I}}_G \equiv (\sum_{g=1}^H \mathcal{I}_g)/H$  does explain some fluctuations. For example, groups [22 88 59] and [79 45 59] show the earliest drops in success rate while being in ranking 7 and 9 by the influence gap ( $\mathcal{I}_H/\mathcal{I}_{H+1}$ ), respectively. Those groups only come as the ranking 29th and the 45th in terms of the average group influence. On the contrary, groups [63 21 90] and [10 20 19] that show the latest peaks in ranking the 40th and the 45th by the influence gap will come earlier as the 15th and the 26th by the ranking of the average group influence ( $\bar{\mathcal{I}}_G$ ). A relatively strong systemic influence exerted collectively by the granular units contributes to improved detection performance.

## 2.5 APPLICATIONS

As long as there is reasonable information about a structural break, our method can be applied to screen for potential key players governing the dynamics of the second-moment structure of the system. We apply the proposed detection scheme for granular units from Section 2.3.3.1 and the breakpoint estimation method from the first chapter to a panel of the daily S&P 100 return (log price differences), utilizing the data shared in Barigozzi and Hallin, 2017.<sup>13</sup> The data contains daily closing prices of  $N = 90$  constituents of S&P 100 index traded from the period January 03, 2000 to September 30, 2013. We focus our analysis on the historical periods of the dot-com bubble burst (2000-2001) and the global financial crisis (2007-2008). The proposed granular detection scheme finds reasonable potential key actors from the early stages

<sup>13</sup>The data can be retrieved at <http://wileyonlinelibrary.com/journal/rss-datasets>.

of the crisis, featuring our own breakpoint estimation. The results will be discussed as well for extended panels, which also include notable companies that were delisted during or shortly after each crisis period. Especially for the period 2007-2008, the inclusion of the missing units substantially affects the breakpoint and, hence, the result of the granular unit detection.

Two studies provide reference points for comparison regarding granular unit detections and structural breakpoint dates. The primary objective of this exposition is to demonstrate the robustness of our granular detection results across deviating breakpoint dates. For structural breakpoints, we reference the common component breakpoint dates in [Barigozzi, Cho, et al., 2018](#) ('BCF2018') to compare with our estimated breakpoint dates. BCF2018 studied breakpoint estimation of the common and idiosyncratic components and applied the method to daily S&P 100 return data (differences of the log daily closing prices) of  $N = 88$  stocks traded from January 04, 2000, to August 10, 2016. We assume that the result of the common component breakpoints for the periods of interest (the years 2000 - 2001 and 2007 - 2008) in BCF2018 are not affected by minor differences in the datasets due to the potential delisting of constituents during the period from September 30, 2013, to August 10, 2016.<sup>14</sup> Breakpoints estimated using our method utilizing the data [Barigozzi and Hallin, 2017](#) show overall similarity with the common component breakpoints reported in BCF2018.

For granular unit detection, the method of [Brownlees and Mesters, 2021](#) will be the benchmark. The comparison will focus on membership detection. Let us recall the granular unit detection criteria in Section 2.3.3.1:

**DETECTION OF THE SET OF GRANULAR UNITS (SECTION 2.3.3.1)** The set  $\hat{\mathcal{G}}$  of granular units consists of  $\hat{H} = \text{rank}(\hat{\mathcal{P}}_0' \hat{\mathcal{P}}_1)$  cross-sectional units with the highest column norms,

$$\hat{\mathcal{I}}_i = \left\| \hat{\Sigma}_{y,0}^{-1} \hat{\mathcal{P}}_1 \hat{\mathcal{P}}_1' \hat{\Sigma}_{y,0}^{-1} \hat{\sigma}_{u,0}^i \right\|.$$

The benchmark reference for membership detection ([Brownlees and Mesters, 2021](#)) is based on the  $\hat{H}$ -highest column norms  $\|[\hat{\Sigma}_y^{-1}]^i\|$ ,<sup>15</sup> analyzed for both separate and combined regimes. The construction of the measures  $\hat{\mathcal{I}}_i$  and  $\|[\hat{\Sigma}_{y,j}^{-1}]^i\|$  follows the procedure described in Section 2.4.1. For breakpoints provided by [Barigozzi, Cho, et al., 2018](#) or estimated using our methods, the granular units detected through our proposed method are better interpreted as the potential key sources within the historical context of each crisis.

<sup>14</sup>From S&P 500 constituent list – the historical S&P 100 constituent list is licensed and was not available – in CRSP data (through WRDS), we found only DELL was delisted among the 90 stocks of [Barigozzi and Hallin, 2017](#) during the period from September 30, 2013, to August 10, 2016.

<sup>15</sup> $[\hat{\Sigma}_y^{-1}]^i$  denotes the  $i$ -th column of  $\hat{\Sigma}_y^{-1}$ .

### 2.5.1 DOT-COM BUBBLE

Figure 2.3 below summarizes the results of the granular unit detection based on the proposed criteria 2.3.3.1, applied to breakpoints obtained from our own estimations (indicated in blue) and from BCF2018 (indicated in black).

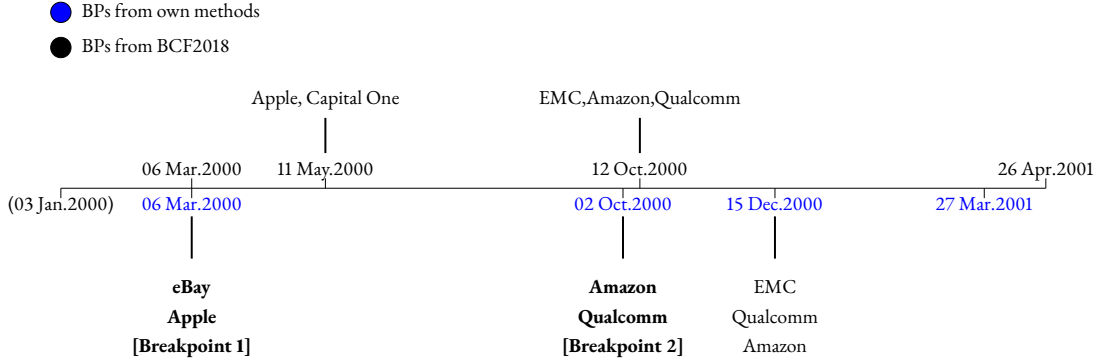


Figure 2.3: Granular Units in Dot-com bubble, based on  $\hat{\mathcal{L}}_i$

Overall, the detected granular units based on the estimated influence measure  $\hat{\mathcal{L}}_i$  are major players in e-commerce (eBay or Amazon) or big tech companies (Apple, Qualcomm, EMC), which are the reasonable key contributors in the onset of the dot-com bubble burst. The breakpoints of different resources mildly deviate; however, the detected granular units are not very sensitive to such deviations. The identity of the detected granular units is also not highly sensitive to the length of the post-break window. For instance, for the first breakpoint, eBay remains the top granular unit even when the post-break window is reduced to 20 days or shorter.

For comparison, Table 2.2 presents the results based on the concentration matrix for the windows before and after breakpoints 1 and 2.

$I_0$ : Jan 3, 2000 - Mar 6	$I_1$ : Mar 7 - Oct 2, 2000	$I_2$ : Oct 3 - Dec 15, 2001
Simons Property Group	ExxonMobil	Simons Property Group
General Electric	Chevron	Citigroup

Table 2.2: Granular Units in Dot-com bubble, based on  $\|[\hat{\Sigma}_{y,j}^{-1}]^i\|$

The detected granular units span the financial, industrial, and energy sectors and do not exhibit clear connections to the context of the dot-com bubble burst. When combining  $I_0$  and  $I_1$  ( $I_0 \cup I_1$ ) or  $I_1$  and  $I_2$  ( $I_1 \cup I_2$ ), the granular units identified include companies in the energy sector, such as ExxonMobil, Chevron, and ConocoPhillips. For the windows before and after the latest breakpoint (December 15), companies in similar sectors—industrial, finance, or energy—were also identified, as shown in the earlier windows presented in Table 2.2.

For the period surrounding the dot-com crash, the breakpoints and detected granular units do not change substantially when adding notable missing entities like Enron, Yahoo, WorldCom,

or Global Crossing to the panel. The most significant change occurs at the first breakpoint (March 6), which shifts 10 days earlier; however, eBay remains the top granular unit.

### 2.5.2 2007-2008 FINANCIAL CRISIS

The proposed granular unit detection identified notable companies in the financial sector at the given or estimated breakpoints. Our breakpoint estimation method detected a breakpoint in September 2008, coinciding with the historical peak of the global financial crisis, which aligns with the breakpoint found in BCF2018. The granular units at the September breakpoint are nearly identical across both sets of dates. In addition, our own estimation points to an earlier breakpoint in July 2008, which identified another set of notable financial institutions—Bank of America, Wells Fargo, and AIG—as the granular units.

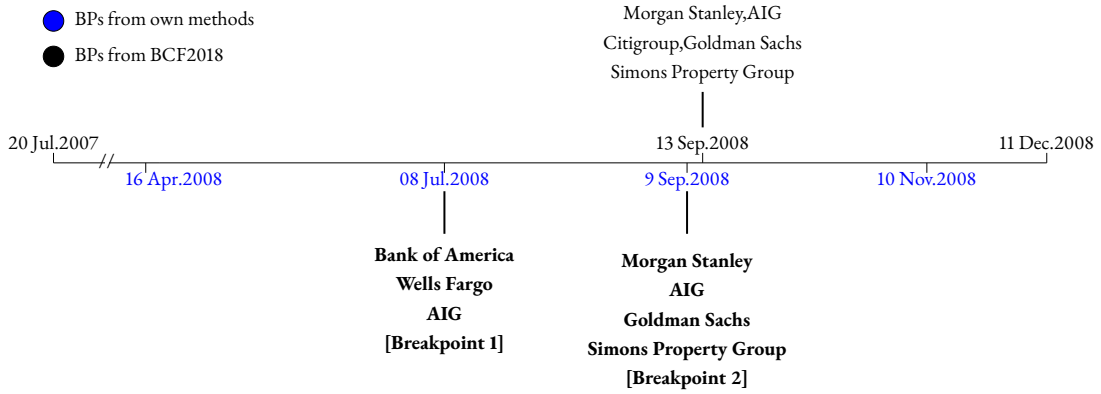


Figure 2.4: Granular Units in 2008 Financial Crisis, based on  $\hat{\mathcal{I}}_i$

The concentration matrix identifies companies in various sectors as granular units, as shown below for the top three granular units (the year '2008' is omitted in the first row of Table 2.3). The sectors are distributed across the healthcare, utilities, consumer discretionary, and energy for the separate windows. For the combined windows, companies in the industrial and telecommunications sectors are also included.

$I_0$ : Apr 16 - Jul 7	$I_1$ : Jul 8 - Sep 8	$I_2$ : Sep 9 - Nov 10
Johnson & Johnson	Allstate	McDonald's
Baxter	Eli Lilly and Company	The Walt Disney Company
Southern Company	Johnson & Johnson	Chevron

Table 2.3: Granular Units in the Global Financial Crisis, based on  $\|[\hat{\Sigma}_{y,j}^{-1}]^i\|$

Although the proposed granular unit detection captures relevant units in the context of the financial crisis during this period, some notable companies are missing in the current analysis, such as Lehman Brothers, Bear Stearns, Merrill Lynch, Washington Mutual, and General Motors. We examine earlier periods – 2006 to early 2008 – preceding and including the onset of the global financial crisis. The cross-sectional dimension is extended to  $N = 95$  by including

the initially missing constituents. The following Figure 2.5 presents the result of the detected breakpoints and the top granular units corresponding to each break from 2006 to early 2008. Note that Bear Stearns was delisted after May 30, 2008.

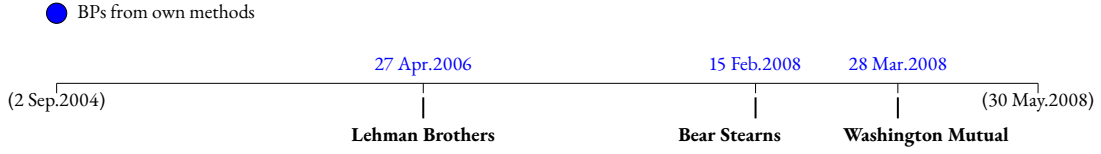


Figure 2.5: Top Granular Units from 2006 to early 2008, based on  $\hat{\mathcal{L}}_i$

The breakpoints occurred in late April 2006, as well as in February and March 2008. Lehman Brothers was the top granular unit at the breakpoint on April 27, 2006, during a period when the housing market prices peaked and financial risk in the subprime mortgage market began to escalate (Phillips and J. Yu, 2011, Albanesi et al., 2022). Bear Stearns was the top granular unit at the breakpoint on February 15, a month before its collapse on March 16, 2008. Washington Mutual, the parent company of the largest savings and loan association at the time, was the top granular unit at the March 28, 2008 breakpoint. It had already been the second most important granular unit next to Lehman Brothers at the April 27, 2006 breakpoint – years ahead of its collapse in September 2008 alongside Lehman Brothers. The identity of the granular units remains stable, even when the length of the post-break data is reduced or when there are slight changes in breakpoint locations.

The membership detection is based on the collective feature of systemic influence, as discussed in Section 2.3.2. The detected granular units do not necessarily exhibit the largest changes in their idiosyncratic volatility or correlations with other units. For the dot-com bubble period, nearly all of the detected granular units are far outside the Top 10 for idiosyncratic covariance change before and after the considered breakpoints, based on the column norm. Only Apple was within the Top 10, as it was ranked the 9th. In the case of the financial crisis, Bank of America, AIG, and Morgan Stanley are outside the Top 10, and none of the detected granular units are within the Top 3. The chosen granular units are not necessarily those that had the highest loadings of the common factors after the break, either. For instance, after the break during the dot-com crash, common factors loaded more heavily on Texas Instruments than on Qualcomm. Similarly, during the financial crisis, companies in the Energy (e.g., NOV, APC, OXY) or Materials (e.g., FCX) sectors had higher loadings than Goldman Sachs or Simons Property Group.

Through this application, we found that the proposed criteria and influence measure effectively capture reasonable potential sources of the known crises. Our method can be seen as providing a fairly conservative measure of systemic influence. By identifying individual-level effects during considerable system-wide breaks, our approach minimizes the debate about whether the influence of certain individuals is truly system-wide. Furthermore, while the detection

scheme is feasible after a break has occurred, the results show that the proposed method provides timely information about probable risk components at the early stages of each crisis. The detected instability points precede the major collapses of the crises, and the detected granular units are not overly sensitive to the length of the post-break data window.

Note that the assumption of a stationary factor structure underlying the concentration matrix-based measure becomes less plausible in a high-frequency data environment. A more appropriate comparison could be made with detection methods that model the dynamics of correlations, such as those described in [Basu and Rao, 2021](#) using a network model. However, our approach retains the advantage of simplicity compared to methods that involve the explicit modeling of a dynamic network of correlations.

## 2.6 CONCLUDING REMARKS

In socio-economic systems, micro-originated volatility translations can drive system-wide instabilities and further potential crises. We propose a novel detection scheme that directly incorporates system-wide instabilities and the identification of their main contributors in a panel. It is agnostic about the true volatility transmission mechanism yet provides a more straightforward analysis of the second-moment to second-moment effect from the micro-level to the system level compared to existing studies to the best of our knowledge. Our proposed method is straightforward to implement, utilizing the well-established theory of factor models and principal component analysis (PCA). Additionally, we provide insights into interpreting the latent factor model as a network model. Applied to daily stock return data, our scheme successfully identified plausible sources of well-known economic crises at relatively early stages, demonstrating its potential for real-time application.

The proposed granular unit detection scheme can have extended applications. While this paper interprets cross-sectional units as individual entities, such as firms or banks, in principle, the units can represent any collection of time-varying variables. For example, by including both real and financial variables, the detection scheme could identify which types of variables contribute most to system-wide instabilities.

Another potential extension relates to the literature on granular instrumental variables (IV). In [Gabaix and Koijen, 2021](#), the optimal weighting of idiosyncratic shocks for constructing granular IV is orthogonal to the factor loading. As discussed in Appendix B.4, these orthogonal directions in the factor loading represent the evolution of the factor space. A realized structural break can reveal the actual weight of idiosyncratic shocks, which may provide a clearer understanding of the true characteristics of granularity. While it is often natural to consider large actors as the most significant based on their size, size alone may not fully capture the fundamental characteristics driving their systemic importance. We plan to explore these extensions in future research.

# APPENDIX TO CHAPTER 2

## B.1 PROOFS

For a simple exposition, let us omit **all** the subscript '0' for the present regime.

### SECTION 2.3

**Proposition 1.** Under the model assumptions, for large  $N$ ,

$$d(\text{span}(P_0), \text{span}(P_1)) = \text{tr}(\Sigma_{u,0} \Sigma_{y,0}^{-1} P_1 P_1' \Sigma_{y,0}^{-1} \Sigma_{u,0}) + o(1). \quad (2.11)$$

*Proof.*

$$d(\text{span}(P), \text{span}(P_1)) = \text{tr}(P_{\perp} P_{\perp}' P_1 P_1' P_{\perp} P_{\perp}') = \text{tr}(P_{\perp} P_{\perp}' \Sigma_y \Sigma_y^{-1} P_1 P_1' \Sigma_y^{-1} \Sigma_y P_{\perp} P_{\perp}')$$

As  $\Sigma_y = \Sigma_{\chi} + \Sigma_u$  where the low dimensional component has orthogonal decomposition  $\Sigma_{\chi} = P \Sigma_f P'$ ,

$$\begin{aligned} \text{tr}(P_{\perp} P_{\perp}' \Sigma_y \Sigma_y^{-1} P_1 P_1' \Sigma_y^{-1} \Sigma_y P_{\perp} P_{\perp}') &= \text{tr}(P_{\perp} P_{\perp}' \Sigma_u \Sigma_y^{-1} P_1 P_1' \Sigma_y^{-1} \Sigma_u P_{\perp} P_{\perp}') \\ &= \text{tr}(\Sigma_u \Sigma_y^{-1} P_1 P_1' \Sigma_y^{-1} \Sigma_u P_{\perp} P_{\perp}') \end{aligned}$$

by the cyclic invariance of the trace. As  $P_{\perp} P_{\perp}' = I_N - P P'$ ,

$$d(\text{span}(P), \text{span}(P_1)) = \text{tr}(\Sigma_u \Sigma_y^{-1} P_1 P_1' \Sigma_y^{-1} \Sigma_u) - \text{tr}(\Sigma_u \Sigma_y^{-1} P_1 P_1' \Sigma_y^{-1} \Sigma_u P P'). \quad (\text{B.25})$$

The last term of (B.25) equals

$$\text{tr}(P_1' \Sigma_y^{-1} \Sigma_u P P' \Sigma_u \Sigma_y^{-1} P_1) = \text{tr}[\Sigma_y^{-1} \Sigma_u P P' \Sigma_u \Sigma_y^{-1} | \text{span}(P_1)],$$

the partial trace confining the domain of the quadratic operation of  $\Sigma_y^{-1} \Sigma_u P P' \Sigma_u \Sigma_y^{-1}$  to  $v \in \text{span}(P_1)$ . That is, it is defined for any orthonormal basis  $\{\mathbf{v}_k\}_{k=1, \dots, K_1}$  of  $\text{span}(P_1)$ ,

$$\text{tr}[\Sigma_y^{-1} \Sigma_u P P' \Sigma_u \Sigma_y^{-1} | \text{span}(P_1)] \equiv \sum_{k=1}^{K_1} \mathbf{v}_k' \Sigma_y^{-1} \Sigma_u P P' \Sigma_u \Sigma_y^{-1} \mathbf{v}_k.$$

It is bounded by the whole trace, as  $\text{tr}(\Sigma_y^{-1} \Sigma_u P P' \Sigma_u \Sigma_y^{-1}) \geq \sum_{\kappa=1}^{K_1} \lambda_\kappa$  for the eigenvalues  $\{\lambda_\kappa\}$  of  $\Sigma_y^{-1} \Sigma_u P P' \Sigma_u \Sigma_y^{-1}$  in descending order<sup>16</sup>, and the summation of the first  $K_1$  eigenvalues are the supremum of the partial trace confined to all possible subspaces  $V$  of dimension  $K_1$  in the entire  $N$  dimension (Tao, 2023 Proposition 1.3.4):

$$\sum_{\kappa=1}^{K_1} \lambda_\kappa = \sup_{V, \dim(V)=K_1} \text{tr}[\Sigma_y^{-1} \Sigma_u P P' \Sigma_u \Sigma_y^{-1} | V].$$

Now we focus on  $\text{tr}[\Sigma_y^{-1} \Sigma_u P P' \Sigma_u \Sigma_y^{-1}]$ . Let  $\tilde{P}$  be a column-augmented orthonormal basis of the principle subspace corresponding to the  $K$  largest eigenvalues of  $\Sigma_y$ . As the eigenvectors are invariant under the matrix inversion,  $\Sigma_y^{-1}$  has the orthogonal spectral decomposition with respect to  $\tilde{P}$ , such that  $\Sigma_y^{-1} = \tilde{P} \tilde{P}' \Sigma_y^{-1} \tilde{P} \tilde{P}' + \tilde{P}_\perp \tilde{P}_\perp' \Sigma_y^{-1} \tilde{P}_\perp \tilde{P}_\perp' (= \tilde{P} \tilde{\Lambda}_1 \tilde{P}' + \tilde{P}_\perp \tilde{\Lambda}_2 \tilde{P}_\perp')$ . Accordingly,  $\text{tr}[\Sigma_y^{-1} \Sigma_u P P' \Sigma_u \Sigma_y^{-1}] (= \boxed{1})$  can be decomposed as follows:

$$\begin{aligned} \boxed{1} = & \text{tr}[\Sigma_y^{-1} \tilde{P} \tilde{P}' \Sigma_u \tilde{P} \tilde{P}' P P' \tilde{P} \tilde{P}' \Sigma_u \tilde{P} \tilde{P}' \Sigma_y^{-1}] + 2\text{tr}[\Sigma_y^{-1} \tilde{P} \tilde{P}' \Sigma_u \tilde{P}_\perp \tilde{P}_\perp' P P' \tilde{P} \tilde{P}' \Sigma_u \tilde{P} \tilde{P}' \Sigma_y^{-1}] \\ & + 2\text{tr}[\Sigma_y^{-1} \tilde{P}_\perp \tilde{P}_\perp' \Sigma_u \tilde{P}_\perp \tilde{P}_\perp' P P' \tilde{P} \tilde{P}' \Sigma_u \tilde{P}_\perp \tilde{P}_\perp' \Sigma_y^{-1}] + \text{tr}[\Sigma_y^{-1} \tilde{P} \tilde{P}' \Sigma_u \tilde{P}_\perp \tilde{P}_\perp' P P' \tilde{P}_\perp \tilde{P}_\perp' \Sigma_u \tilde{P} \tilde{P}' \Sigma_y^{-1}] \\ & + \text{tr}[\Sigma_y^{-1} \tilde{P}_\perp \tilde{P}_\perp' \Sigma_u \tilde{P}_\perp \tilde{P}_\perp' P P' \tilde{P}_\perp \tilde{P}_\perp' \Sigma_u \tilde{P}_\perp \tilde{P}_\perp' \Sigma_y^{-1}] + \text{tr}[\Sigma_y^{-1} \tilde{P}_\perp \tilde{P}_\perp' \Sigma_u \tilde{P} \tilde{P}' P P' \tilde{P} \tilde{P}' \Sigma_u \tilde{P}_\perp \tilde{P}_\perp' \Sigma_y^{-1}], \end{aligned}$$

since any terms involving  $\tilde{P} \tilde{P}' \Sigma_y^{-2} \tilde{P}_\perp \tilde{P}_\perp'$  after a cyclic transformation of the argument of the trace operation vanish as  $\Sigma_y^{-2}$  shares the same basis of the spectral decomposition as  $\Sigma_y^{-1}$ .

Let us number the six terms of  $\boxed{1}$  as  $\boxed{1}$  -1 to  $\boxed{1}$  -6. The following properties will be repeatedly employed to give a bound on each term, mainly jointly applied with the matrix Cauchy-Schwarz inequality (stated below) on products of positive semidefinite matrices and the trace cyclicity.

### Properties 1.

- (a)  $\text{tr}[\tilde{P}' \Sigma_u^2 \tilde{P}] \leq K \|\Sigma_u^2\| = O(1)$ , by Assumption 2.
- (b)  $\text{tr}[\tilde{P} \tilde{P}' \Sigma_y^{-2} \tilde{P} \tilde{P}'] \leq K \|\tilde{\Lambda}_1^{-2}\| = o(1)$ , by Assumption 1.
- (c)  $\|\tilde{P}_\perp \tilde{P}_\perp' P P'\|_F^2 = O(N^{-2})$  by **The sin $\theta$  Theorem** (Davis and Kahan, 1970) with Assumptions 1 and 2.
- (d)  $\|\tilde{P}_\perp \tilde{P}_\perp' \Sigma_u \tilde{P} \tilde{P}'\|_F^2 = O(N^{-2})$ , by Assumptions 1-3, and the above property (c).

**MATRIX CAUCHY-SCHWARZ INEQUALITY** Let  $*$  denote the Hermitian operator (the transpose of the complex conjugation). For any complex (or real) matrices  $A, B$  of the same sizes, the

<sup>16</sup>  $\lambda_\kappa \geq 0, \forall \kappa = 1, \dots, N$  as the eigenvalues of a product of positive semidefinite matrices.

trace operation  $\text{tr}(B^* A) (= \text{tr}(A^* B))$  defines an inner product (the *Frobenius inner product*, [Horn and Johnson, 2013](#) (5.2.7))

$$\langle A, B \rangle_F \equiv \text{tr}(B^* A) (= \text{tr}(B' A) \text{ for real matrices}).$$

Hence, it equips an inner product on the space of complex (or real) matrices of the same sizes. The Cauchy-Schwarz inequality  $\langle A, B \rangle_F^2 \leq \langle A, A \rangle_F \langle B, B \rangle_F$  is naturally inherited on this inner product space. That is, for the case of the space of real matrices of the same sizes,

$$|\text{tr}(A' B)| \leq [\text{tr}(A' A)]^{1/2} [\text{tr}(B' B)]^{1/2} (= \|A\|_F \|B\|_F). \quad (\text{B.26})$$

(it implies that the trace is submultiplicative on positive semidefinite matrices.)

A term-by-term inspection of  $\boxed{1}$  follows.

$\boxed{1}$ -1:  $\text{tr}[\Sigma_y^{-1} \tilde{P} \tilde{P}' \Sigma_u \tilde{P} \tilde{P}' P P' \tilde{P} \tilde{P}' \Sigma_u \tilde{P} \tilde{P}' \Sigma_y^{-1}] = \text{tr}[\Sigma_u \tilde{P} \tilde{P}' P P' \tilde{P} \tilde{P}' \Sigma_u \tilde{P} \tilde{P}' \Sigma_y^{-2} \tilde{P} \tilde{P}']$  due to the cyclicity. As the trace is submultiplicative on positive semidefinite matrices, it is bounded as

$$\text{tr}[\Sigma_u \tilde{P} \tilde{P}' P P' \tilde{P} \tilde{P}' \Sigma_u \tilde{P} \tilde{P}' \Sigma_y^{-2} \tilde{P} \tilde{P}'] \leq \text{tr}[\Sigma_u \tilde{P} \tilde{P}' P P' \tilde{P} \tilde{P}' \Sigma_u] \text{tr}[\tilde{P} \tilde{P}' \Sigma_y^{-2} \tilde{P} \tilde{P}'] = o(1),$$

since  $\text{tr}[\Sigma_u \tilde{P} \tilde{P}' P P' \tilde{P} \tilde{P}' \Sigma_u] = \text{tr}[\tilde{P}' \Sigma_u^2 \tilde{P} | \text{span}(P)] \leq \text{tr}[\tilde{P}' \Sigma_u^2 \tilde{P}] = O(1)$  by (a), and  $\text{tr}[\tilde{P} \tilde{P}' \Sigma_y^{-2} \tilde{P} \tilde{P}'] = o(1)$  by (b).

$\boxed{1}$ -2:  $\text{tr}[\Sigma_y^{-1} \tilde{P} \tilde{P}' \Sigma_u \tilde{P}_\perp \tilde{P}_\perp' P P' \tilde{P} \tilde{P}' \Sigma_u \tilde{P} \tilde{P}' \Sigma_y^{-1}] = \text{tr}[\Sigma_u \tilde{P}_\perp \tilde{P}_\perp' P P' \tilde{P} \tilde{P}' \Sigma_u \tilde{P} \tilde{P}' \Sigma_y^{-2} \tilde{P} \tilde{P}']$  due to the cyclicity. Let us denote  $A := \Sigma_u \tilde{P}_\perp \tilde{P}_\perp' P P' \tilde{P} \tilde{P}' \Sigma_u$ . By the Cauchy-Schwarz (B.26),

$$\text{tr}[\Sigma_u \tilde{P}_\perp \tilde{P}_\perp' P P' \tilde{P} \tilde{P}' \Sigma_u \tilde{P} \tilde{P}' \Sigma_y^{-2} \tilde{P} \tilde{P}'] \leq [\text{tr}(A' A)]^{1/2} \text{tr}(\tilde{P} \tilde{P}' \Sigma_y^{-2} \tilde{P} \tilde{P}'). \quad (\text{B.27})$$

Let us observe that, by the cyclicity and the submultiplicativity of the trace,

$$\begin{aligned} \text{tr}(A' A) &= \text{tr}(\Sigma_u \tilde{P} \tilde{P}' P P' \tilde{P}_\perp \tilde{P}_\perp' \Sigma_u^2 \tilde{P}_\perp \tilde{P}_\perp' P P' \tilde{P} \tilde{P}' \Sigma_u) \\ &\leq \text{tr}[P P' \tilde{P}_\perp \tilde{P}_\perp' \Sigma_u^2 \tilde{P}_\perp \tilde{P}_\perp' P P'] \text{tr}(\tilde{P} \tilde{P}' \Sigma_u^2 \tilde{P} \tilde{P}'). \end{aligned} \quad (\text{B.28})$$

The last component  $\text{tr}(\tilde{P} \tilde{P}' \Sigma_u^2 \tilde{P} \tilde{P}') = O(1)$  by (a). The other part,

$$\text{tr}[P P' \tilde{P}_\perp \tilde{P}_\perp' \Sigma_u^2 \tilde{P}_\perp \tilde{P}_\perp' P P'] \leq \|P P' \tilde{P}_\perp \tilde{P}_\perp'\|_F^2 \text{tr}(\Sigma_u^2) = O(N^{-1}) = o(1), \quad (\text{B.29})$$

since  $\|PP'\tilde{P}_\perp\tilde{P}_\perp'\|_F^2 = O(N^{-2})$  by (c) and  $\text{tr}(\Sigma_u^2) \leq N\|\Sigma_u^2\| = O(N)$  by Assumption 2. Hence  $\text{tr}(A'A) = o(1)$  in (B.28). As the last component in (B.27),  $\text{tr}(\tilde{P}\tilde{P}'\Sigma_y^{-2}\tilde{P}\tilde{P}') = o(1)$  by (b),  $\boxed{1}$ -2 (up to the factor 2) is bounded by  $o(1)$ .

$\boxed{1}$ -3: By the cyclicity, the orthonormality  $\tilde{P}_\perp'\tilde{P}_\perp = I_{N-K}$ , and (B.26),  $\boxed{1}$ -3 is bounded (up to the factor 2) such as

$$\text{tr}[\Sigma_y^{-1}\tilde{P}_\perp\tilde{P}_\perp'\Sigma_u\tilde{P}_\perp\tilde{P}_\perp'PP'\tilde{P}\tilde{P}'\Sigma_u\tilde{P}_\perp\tilde{P}_\perp'\tilde{P}_\perp\tilde{P}_\perp'\Sigma_y^{-1}] \leq [\text{tr}(B'B)]^{1/2}\text{tr}(\tilde{P}_\perp\tilde{P}_\perp'\Sigma_y^{-2}\tilde{P}_\perp\tilde{P}_\perp'), \quad (\text{B.30})$$

where  $B := \Sigma_u\tilde{P}_\perp\tilde{P}_\perp'PP'\tilde{P}\tilde{P}'\Sigma_u\tilde{P}_\perp\tilde{P}_\perp'$ . Then due to (B.29) above and (d),

$$\begin{aligned} \text{tr}(B'B) &= \text{tr}[\tilde{P}_\perp\tilde{P}_\perp'\Sigma_u\tilde{P}\tilde{P}'PP'\tilde{P}_\perp\tilde{P}_\perp'\Sigma_u^2\tilde{P}_\perp\tilde{P}_\perp'PP'\tilde{P}\tilde{P}'\Sigma_u\tilde{P}_\perp\tilde{P}_\perp'] \\ &\leq \text{tr}[PP'\tilde{P}_\perp\tilde{P}_\perp'\Sigma_u^2\tilde{P}_\perp\tilde{P}_\perp'PP']\|\tilde{P}\tilde{P}'\Sigma_u\tilde{P}_\perp\tilde{P}_\perp'\|_F^2 = O(N^{-3}). \end{aligned}$$

Alongside with  $\text{tr}(\tilde{P}_\perp\tilde{P}_\perp'\Sigma_y^{-2}\tilde{P}_\perp\tilde{P}_\perp') \leq (N-K)\|\Sigma_y^{-2}\| = O(N-K)$ , (B.30) gives an  $o(1)$  bound.

$\boxed{1}$ -4: By the trace cyclicity and the submultiplicativity, (B.29), and (b),

$$\begin{aligned} &\text{tr}[\Sigma_y^{-1}\tilde{P}\tilde{P}'\Sigma_u\tilde{P}_\perp\tilde{P}_\perp'PP'\tilde{P}_\perp\tilde{P}_\perp'\Sigma_u\tilde{P}\tilde{P}'\Sigma_y^{-1}] + \text{tr}[\Sigma_u\tilde{P}_\perp\tilde{P}_\perp'PP'\tilde{P}_\perp\tilde{P}_\perp'\Sigma_u\tilde{P}\tilde{P}'\Sigma_y^{-2}\tilde{P}\tilde{P}'] \\ &\leq \text{tr}[\Sigma_u\tilde{P}_\perp\tilde{P}_\perp'PP'\tilde{P}_\perp\tilde{P}_\perp'\Sigma_u]\text{tr}[\tilde{P}\tilde{P}'\Sigma_y^{-2}\tilde{P}\tilde{P}'] \\ &= \text{tr}[PP'\tilde{P}_\perp\tilde{P}_\perp'\Sigma_u^2\tilde{P}_\perp\tilde{P}_\perp'PP']\text{tr}[\tilde{P}\tilde{P}'\Sigma_y^{-2}\tilde{P}\tilde{P}'] = o(1), \end{aligned}$$

$\boxed{1}$ -5: By the trace cyclicity and the submultiplicativity and (c),

$$\begin{aligned} &\text{tr}[\Sigma_y^{-1}\tilde{P}_\perp\tilde{P}_\perp'\Sigma_u\tilde{P}_\perp\tilde{P}_\perp'PP'\tilde{P}_\perp\tilde{P}_\perp'\Sigma_u\tilde{P}_\perp\tilde{P}_\perp'\Sigma_y^{-1}] \\ &\leq \text{tr}[\tilde{P}_\perp\tilde{P}_\perp'PP'\tilde{P}_\perp\tilde{P}_\perp']\text{tr}[\Sigma_u\tilde{P}_\perp\tilde{P}_\perp'\Sigma_y^{-2}\tilde{P}_\perp\tilde{P}_\perp'\Sigma_u] = O(N^{-2})\text{tr}[\Sigma_u\tilde{P}_\perp\tilde{P}_\perp'\Sigma_y^{-2}\tilde{P}_\perp\tilde{P}_\perp'\Sigma_u]. \end{aligned} \quad (\text{B.31})$$

Again by the cyclicity,  $\text{tr}[\Sigma_u\tilde{P}_\perp\tilde{P}_\perp'\Sigma_y^{-2}\tilde{P}_\perp\tilde{P}_\perp'\Sigma_u] = \text{tr}[\tilde{P}_\perp'\Sigma_y^{-2}\tilde{P}_\perp\tilde{P}_\perp'\Sigma_u^2\tilde{P}_\perp]$   
 $\leq \text{tr}[\Sigma_y^{-2}\tilde{P}_\perp\tilde{P}_\perp'\Sigma_u^2 | \text{span}(\tilde{P}_\perp)] \leq \text{tr}[\Sigma_y^{-2}\tilde{P}_\perp\tilde{P}_\perp'\Sigma_u^2] \leq (N-K)\|\Sigma_u^2\Sigma_y^{-2}\| = O(N-K)$ , which completes an  $o(1)$  bound in (B.31).

$\boxed{1}$ -6: Due to the cyclicity, the submultiplicativity, and (d),

$$\begin{aligned} &\text{tr}[\Sigma_y^{-1}\tilde{P}_\perp\tilde{P}_\perp'\Sigma_u\tilde{P}\tilde{P}'PP'\tilde{P}\tilde{P}'\Sigma_u\tilde{P}_\perp\tilde{P}_\perp'\Sigma_y^{-1}] \leq \text{tr}[\tilde{P}_\perp\tilde{P}_\perp'\Sigma_u\tilde{P}\tilde{P}'PP'\tilde{P}\tilde{P}'\Sigma_u\tilde{P}_\perp\tilde{P}_\perp']\text{tr}[\Sigma_y^{-2}] \\ &= \text{tr}[\tilde{P}\tilde{P}'\Sigma_u\tilde{P}_\perp\tilde{P}_\perp'\Sigma_u\tilde{P}\tilde{P}' | \text{span}(P)]O(N) \leq \|\tilde{P}\tilde{P}'\Sigma_u\tilde{P}_\perp\tilde{P}_\perp'\|_F^2 O(N) = O(N^{-2})O(N) = o(1). \end{aligned}$$

Therefore,  $\boxed{1} := \text{tr}[\Sigma_y^{-1} \Sigma_u P P' \Sigma_u \Sigma_y^{-1}] = o(1)$  and

$$d(\text{span}(P), \text{span}(P_1)) = \text{tr}(\Sigma_u \Sigma_y^{-1} P_1 P_1' \Sigma_y^{-1} \Sigma_u) + o(1). \quad (2.11)$$

□

### SECTION 2.4.1

#### STANDARD PROCEDURES OF FACTOR LOADING ESTIMATION

Let

$$Y = BF + U \quad (2.17)$$

under Assumptions 1-2, 6-10 in Sections 2.2.1.1 and 2.4.1. The discussion is for any given, fixed regime, omitting the regime index  $j$ . Standard<sup>17</sup> procedures of estimating factor loading are as follows: First,  $B$  can be estimated by  $\hat{B} = \sqrt{N} \hat{P}_N$ , where  $\hat{P}_N$  is the column augmentation of  $K$  – dominant orthonormal eigenvectors of the sample covariance matrix  $(1/T)YY'$ . Second, it can be estimated by  $\tilde{B} = (1/\sqrt{T})Y \hat{P}_T$ , for  $\hat{P}_T$  the column augmentation of  $K$  – dominant eigenvectors of  $(1/N)Y'Y$ .

The columns of  $\tilde{B}$  span the same space as the  $K$  – dominant eigenvectors of  $(1/T)YY'$ : There exists diagonal matrix  $\Sigma_N^K$  of the  $K$  – largest eigenvalues of  $(1/N)Y'Y$  such that the rank  $K$  linear combination  $\tilde{B}((N/T)\Sigma_N^K)^{-1/2}$  of the columns of  $\tilde{B}$  gives

$$\begin{aligned} & ((N/T)\Sigma_N^K)^{-1/2} \tilde{B}' (1/T)YY' \tilde{B} ((N/T)\Sigma_N^K)^{-1/2} \\ &= (N/T)(\Sigma_N^K)^{-1/2} \hat{P}_T' (1/N)(Y'Y) (1/N)(Y'Y) \hat{P}_T (\Sigma_N^K)^{-1/2} = (N/T)\Sigma_N^K = \Sigma_T^K \end{aligned}$$

which is the diagonal matrix of  $K$  – largest eigenvalues of  $(1/T)YY'$ . Hence, the resulting (factor) spaces spanned by  $\hat{B}$  (or  $\hat{P}_N$ ) and  $\tilde{B}$  are identical.

**THE  $K_j$  – PRINCIPAL SUBSPACE CONSISTENCY** The leading  $K_j$  – principal subspace  $\text{span}(\hat{P}_j)$  of  $\hat{\Sigma}_{y,j}^{\text{sam}}$  or  $\hat{\Sigma}_{\chi,j} = \hat{\Sigma}_{y,j}^{K_j}$ , the spectral decomposition of  $\hat{\Sigma}_{y,j}^{\text{sam}}$  up to  $K_j$ , deviates from  $\text{span}(P_j)$  by  $o_p(1)$ , by [Y. Yu et al., 2015](#):

Measured by the projector metric  $d(\text{span}(\hat{P}_j), \text{span}(P_j)) \equiv \|\mathcal{P}_j^\perp \hat{P}_j\|_F^2$ , where

$$\|\mathcal{P}_j^\perp \hat{P}_j\|_F \lesssim \|\hat{\Sigma}_{\chi,j} - \Sigma_{\chi,j}\| / \lambda_{\chi,j}^{K_j} \leq (\|\hat{\Sigma}_{\chi,j} - \Sigma_{y,j}^{K_j}\| + \|\Sigma_{u,j}\|) / \lambda_{\chi,j}^{K_j} = o_p(1), \quad (\text{B.32})$$

for  $\Sigma_{y,j}^{K_j}$  the spectral decomposition of  $\Sigma_{y,j}$  up to  $K_j$ . The numerator comes by the triangle inequality  $\|\hat{\Sigma}_{\chi,j} - \Sigma_{\chi,j}\| \leq \|\hat{\Sigma}_{\chi,j} - \Sigma_{y,j}^{K_j}\| + \|\Sigma_{y,j}^{K_j} - \Sigma_{\chi,j}\|$ . The latter is bounded by  $\|\Sigma_{u,j}\|$ , the source of the population level deviation. The denominator  $|\hat{\lambda}_{\chi,j}^{K_j+1} - \lambda_{\chi,j}^{K_j}| = \lambda_{\chi,j}^{K_j}$  as  $\hat{\Sigma}_{\chi,j}$

<sup>17</sup>Following in many classical studies such as [Bai and Ng, 2002](#), [Stock and M. W. Watson, 2002b](#).

has the same rank as  $\Sigma_{\chi,j}$ . As  $\|\hat{\Sigma}_{\chi,j} - \Sigma_{y,j}^{K_j}\| \lesssim \|\hat{\Sigma}_{y,j}^{\text{sam}} - \Sigma_{y,j}\| = o_p(N)$  (due to Lemma 4 of Fan et al., 2013) and  $\lambda_{\chi,j}^{K_j} = O(N)$ ,  $d(\text{span}(\hat{P}_j), \text{span}(P_j)) = o_p(1)$ .

**Proposition 2.** Under the Assumptions 1-2 in Section 2.2.1.1 and 6-11 in Section 2.4.1, the event

$$\Upsilon \equiv \{\|\hat{\mathcal{I}}_g\| > \|\hat{\mathcal{I}}_i\| \mid g \in \mathcal{G}, i \in \mathcal{G}^c\} \quad (2.24)$$

holds asymptotically almost surely.

*Proof.* We first prove the following claim for any matrix norm  $\|\cdot\|$ :

**CLAIM:**  $\|\hat{\mathcal{I}} - \mathcal{I}\| = o_p(1)$  for  $\mathcal{I} \equiv \|\Sigma_y^{-1} P_1 P_1' \Sigma_y^{-1} \Sigma_u\|$  and  $\hat{\mathcal{I}}_i = \|\hat{\Sigma}_y^{-1} \hat{P}_1 \hat{P}_1' \hat{\Sigma}_y^{-1} \hat{\Sigma}_u\|$  following the estimation procedure in Section 2.4.1 for  $\omega_{T,j} = o(1)$ .

*Proof of the Claim:* Observe that, by simply adding and subtracting terms,

$$\begin{aligned} \hat{\mathcal{I}} - \mathcal{I} &= (\hat{\Sigma}_y^{-1} - \Sigma_y^{-1})(\hat{P}_1 \hat{P}_1' - P_1 P_1') \hat{\Sigma}_y^{-1} (\hat{\Sigma}_u - \Sigma_u) + (\hat{\Sigma}_y^{-1} - \Sigma_y^{-1})(\hat{P}_1 \hat{P}_1' - P_1 P_1') \hat{\Sigma}_y^{-1} \Sigma_u \\ &\quad + (\hat{\Sigma}_y^{-1} - \Sigma_y^{-1}) P_1 P_1' \hat{\Sigma}_y^{-1} (\hat{\Sigma}_u - \Sigma_u) + (\hat{\Sigma}_y^{-1} - \Sigma_y^{-1}) P_1 P_1' \hat{\Sigma}_y^{-1} \Sigma_u \\ &\quad + \Sigma_y^{-1} (\hat{P}_1 \hat{P}_1' - P_1 P_1') \hat{\Sigma}_y^{-1} (\hat{\Sigma}_u - \Sigma_u) + \Sigma_y^{-1} (\hat{P}_1 \hat{P}_1' - P_1 P_1') \hat{\Sigma}_y^{-1} \Sigma_u \\ &\quad + \Sigma_y^{-1} P_1 P_1' \hat{\Sigma}_y^{-1} (\hat{\Sigma}_u - \Sigma_u) + \Sigma_y^{-1} P_1 P_1' (\hat{\Sigma}_y^{-1} - \Sigma_y^{-1}) \Sigma_u. \end{aligned}$$

By the triangle inequality,

$$\begin{aligned} \|\hat{\mathcal{I}} - \mathcal{I}\| &\leq \|\hat{\Sigma}_y^{-1} - \Sigma_y^{-1}\| \|\hat{P}_1 \hat{P}_1' - P_1 P_1'\| \|\Sigma_y^{-1}\| \|\hat{\Sigma}_u - \Sigma_u\| \\ &\quad + \|\hat{\Sigma}_y^{-1} - \Sigma_y^{-1}\| \|\hat{P}_1 \hat{P}_1' - P_1 P_1'\| o_p(1) \|\hat{\Sigma}_u - \Sigma_u\| \\ &\quad + \|\hat{\Sigma}_y^{-1} - \Sigma_y^{-1}\| \|\hat{P}_1 \hat{P}_1' - P_1 P_1'\| \|\Sigma_y^{-1}\| \|\Sigma_u\| + \|\hat{\Sigma}_y^{-1} - \Sigma_y^{-1}\| \|\hat{P}_1 \hat{P}_1' - P_1 P_1'\| o_p(1) \|\Sigma_u\| \\ &\quad + \|\hat{\Sigma}_y^{-1} - \Sigma_y^{-1}\| \|P_1 P_1'\| \|\Sigma_y^{-1}\| \|\hat{\Sigma}_u - \Sigma_u\| + \|\hat{\Sigma}_y^{-1} - \Sigma_y^{-1}\| \|P_1 P_1'\| o_p(1) \|\hat{\Sigma}_u - \Sigma_u\| \\ &\quad + \|\hat{\Sigma}_y^{-1} - \Sigma_y^{-1}\| \|P_1 P_1'\| \|\Sigma_y^{-1}\| \|\Sigma_u\| + \|\hat{\Sigma}_y^{-1} - \Sigma_y^{-1}\| \|P_1 P_1'\| o_p(1) \|\Sigma_u\| \\ &\quad + \|\Sigma_y^{-1}\|^2 \|\hat{P}_1 \hat{P}_1' - P_1 P_1'\| \|\hat{\Sigma}_u - \Sigma_u\| + \|\Sigma_y^{-1}\| \|\hat{P}_1 \hat{P}_1' - P_1 P_1'\| o_p(1) \|\hat{\Sigma}_u - \Sigma_u\| \\ &\quad + \|\Sigma_y^{-1}\|^2 \|\hat{P}_1 \hat{P}_1' - P_1 P_1'\| \|\Sigma_u\| + \|\Sigma_y^{-1}\| \|\hat{P}_1 \hat{P}_1' - P_1 P_1'\| o_p(1) \|\Sigma_u\| \\ &\quad + \|\Sigma_y^{-1}\|^2 \|P_1 P_1'\| \|\hat{\Sigma}_u - \Sigma_u\| + \|\Sigma_y^{-1}\| \|P_1 P_1'\| o_p(1) \|\hat{\Sigma}_u - \Sigma_u\| \\ &\quad + \|\Sigma_y^{-1}\| \|P_1 P_1'\| \|\hat{\Sigma}_y^{-1} - \Sigma_y^{-1}\| \|\Sigma_u\| (\equiv X). \end{aligned} \quad (\text{B.33})$$

The random variable  $X (= X_{N,T})$  corresponding to the whole expression on the right side of the inequality in (B.33) is  $o_p(1)$  as each term is a multiplication of  $o_p(1)$  and  $O(1)$  under the benchmark assumptions and the estimation procedure in Section 2.4.1: First,  $\|\hat{\Sigma}_y^{-1} - \Sigma_y^{-1}\| = \|\hat{\Sigma}_u - \Sigma_u\| = o_p(1)$ , as stochastically bounded as  $O_p(c_{u,0} \omega_{T,0}^{1-q_0})$  for  $c_{u,0} \omega_{T,0}^{1-q_0} = o(1)$ . Second,  $\|\hat{P}_1 \hat{P}_1' - P_1 P_1'\| \leq \|\hat{P}_1 \hat{P}_1' - \tilde{P}_1 \tilde{P}_1'\| + \|\tilde{P}_1 \tilde{P}_1' - P_1 P_1'\|$  where  $\tilde{P}_1 \tilde{P}_1'$  the  $K_1$  principal subspace of  $\Sigma_{y,1}$ . By the sin  $\theta$  theorem of Davis and Kahan, 1970,  $\|\hat{P}_1 \hat{P}_1' - \tilde{P}_1 \tilde{P}_1'\| = o_p(1)$  as  $\|\hat{\Sigma}_{\chi,1} - \Sigma_{y,1}^{K_1}\| = o_p(N)$ ,  $\lambda_{\chi,1}^{K_1} = O(N)$  and  $\hat{\Sigma}_{\chi,1}$  is rank  $K_1$ . By the same theorem,

$\|\tilde{P}_1\tilde{P}_1' - P_1P_1'\| = o(1)$  as  $\|\Sigma_{u,1}\|$  is bounded by Assumption 2. It makes  $\|\hat{P}_1\hat{P}_1' - P_1P_1'\| = O_p(1/N + \sqrt{\ln(N)/T_1})$  again  $o_p(1)$  under the assumptions.  $\|\Sigma_y^{-1}\|$  and  $\|\Sigma_u\|$  are assumed to be  $O(1)$  in the benchmark model, and the operator norm of a projector  $\|P_1P_1'\| = 1$ . Hence,  $X = O_p\left(\left(c_{u,0}\omega_{T,0}^{1-q_0}\right) \vee \left(1/N + \sqrt{\ln(N)/T_1}\right)\right) = o_p(1)$ . As  $\Pr(X_{N,T} < \delta) \leq \Pr(\|\hat{\mathcal{L}} - \mathcal{I}\| < \delta)$  for any  $\delta > 0$ ,  $\|\hat{\mathcal{L}} - \mathcal{I}\| = o_p(1)$ .  $\square$

The remaining part of the proof of the main statement can proceed the same as the proof of Corollary 1 in [Brownlees and Mesters, 2021](#). First, for any  $i \in \mathcal{N}$ , we know that  $\|\|\hat{\mathcal{L}}_i\| - \|\mathcal{I}_i\|\| \leq \|\hat{\mathcal{L}} - \mathcal{I}\| = o_p(1)$ . Second, the probability of the complement of the event  $\Upsilon$  is

$$\Pr(\Upsilon^c) \lesssim N \max_{g \in \mathcal{G}, i \in \mathcal{G}^c} \max_{\ell=g, i} \Pr\left(\|\|\hat{\mathcal{L}}_\ell\| - \|\mathcal{I}_\ell\|\| > \delta_{gi}\right),$$

where  $\delta_{gi} \equiv (\|\mathcal{I}_g\| - \|\mathcal{I}_i\|)/2 > 0$  for any  $g \in \mathcal{G}$  and  $i \in \mathcal{G}^c$  (page 8 of the Web-Appendix of [Brownlees and Mesters, 2021](#)). As  $\|\|\hat{\mathcal{L}}_i\| - \|\mathcal{I}_i\|\| = o_p(1)$ , for any  $\epsilon = o(N^\gamma)$  for  $\gamma < -1$ ,

$$\Pr\left(\|\|\hat{\mathcal{L}}_\ell\| - \|\mathcal{I}_\ell\|\| > \delta_{gi}\right) < \epsilon$$

for sufficiently large  $N, T$ . Hence  $\Pr(\Upsilon^c) = o(1)$ , that is,  $\Pr(\Upsilon) \rightarrow 1$  as  $N \rightarrow \infty$ .  $\square$

## B.2 A NETWORK-BASED INTERPRETATION OF LATENT FACTOR MODELS

Let us consider a system of  $N$  individual series  $\mathbf{y}_t = [y_{1t}, \dots, y_{Nt}]'$ . During a time window  $\mathcal{I}_0$ , the cross-sectional items are interconnected by a constant relationship  $\Omega$  and experience minor idiosyncratic fluctuations  $u_{it}$ . The interconnections can arise due to mutual investments (including buyer-seller relationships) or borrower-lender relationships or implying an indirect manifestation of holding similar investment portfolios. Assume, for simplicity, that the interconnected performances are balanced with one common source of exposure,  $r$ . It can be a final good demand or a common return from a safe investment. That is, for  $t \in \mathcal{I}_0$ ,

$$y_{it} - u_{it} = r_t + \sum_j \Omega_{ii'}(y_{i't} - u_{i't}), \quad \text{or equivalently,}$$

$$\mathbf{y}_t = (I_N - \Omega)^{-1} \mathbf{1} r_t + \mathbf{u}_t = \mathbf{b} r_t + \mathbf{u}_t. \quad (2.6)$$

Note that, in this example of a single common exposure,

$$\mathbf{b} \equiv (I_N - \Omega)^{-1} \mathbf{1},$$

which equals the Bonacich centrality of the cross-sectional items in the constant network  $\Omega$ . When the common source of exposure and the interconnected structure  $\Omega$  are not observable, one can describe (2.6) by a one-dimensional latent factor model,

$$\mathbf{y}_t = \tilde{B} f_t + \mathbf{u}_t$$

where the factor loading  $\tilde{B}$  amounts to the centrality vector  $\mathbf{b}$ , up to unknown scalings. The idiosyncratic errors  $\{\mathbf{u}_{it}\}$  can capture any individual unit-specific disturbances. For example, for a panel of firms, such disturbances can be caused by a sudden reputation or leadership change in a single or group of companies, which can be seen as a change in the value of organizational capital. One can think of the Enron scandal during the dot-com bubble in 2000 and the ownership change of Twitter(X) in 2022, all able to cause fluctuations in sales or stock returns of certain units. Besides, as a given system of  $N$  cross-section units rarely includes all relevant economic agents in relation, any disruption of a relationship of  $i$  to an entity outside of the system in consideration will be captured as an idiosyncratic error. For the granular units, idiosyncratic disturbances can trigger a viable adjustment of the internal relationships represented by  $\Omega$ . For example, a bank or a firm can perceive idiosyncratic volatilities of their own (or around) as a subjective risk factor of mutual investment. If they make an assessment that the expected disturbances are above a certain level, they can try to adjust their investment portfolio to absorb or mitigate the potential risk.<sup>18</sup> As granular units adjust relationships around,  $\Omega$  is altered, and naturally, all the coefficients of the centrality vector  $\mathbf{b}$  change, not trivially, such as a mere change of the scaling. It will be perceived as a change of the one-dimensional factor space to another, say  $\mathcal{P}_1$ . The one-dimensional factor model based on (2.6) has just provided insight into an observable characteristic of the granular units while staying agnostic without specifying the exact mechanism for how the idiosyncratic disturbances can bridge in the factor space adjustment.

The next regime centrality, say  $\mathbf{b}_1$ , or its counterpart  $\tilde{B}_1$  or  $\mathcal{P}_1$  under unobservability, does not necessarily have a direct functional dependence on the idiosyncratic second moments that may trigger the adjustment. The actual adjustment of linkages, hence the coefficients of  $\mathbf{b}_1$  or  $\mathcal{P}_1$  can depend on parameters indicating the capability of the adjustment – such as market or bargaining power, or information superiority of some units, or system-wide asymmetry of those – rather than the idiosyncratic second moments indicating the demand of an adjustment.

In the most simplified example below, where we assume the common exposure variance is a large constant compared to hypothetically homogeneous idiosyncratic variances, the suggested influence measure detects an individual  $i$  to have a system-wide importance if it adjusts its centrality the most.

---

<sup>18</sup>In a financial network, it could be assumed to keep the leverage level the same as the perceived value at risk. e.g., [Mazzarisi et al., 2019](#).

EXAMPLE 1. Let  $\mathbf{y}_t = \mathbf{b}r_t + \mathbf{u}_t$ , where  $\text{cov}(\mathbf{u}_t) = I_N$  during  $I_0$ . Assume that  $\text{var}(r_t) = \sigma_r^2 \gg 1$  is constant regardless of the regime. It gives  $\Sigma_{\mathbf{y}} = \sigma_r^2 \mathbf{b}\mathbf{b}' + I$  and  $\Sigma_{\mathbf{y}}^{-1} = I_N - \sigma_r^2 \mathbf{b}\mathbf{b}' / (1 + \sigma_r^2 \mathbf{b}'\mathbf{b})$ . Then the  $i$ -th column norm  $\mathcal{L}_i = \|\Sigma_{\mathbf{y}}^{-1} \mathbf{b}_1 \mathbf{b}_1' \Sigma_{\mathbf{y}}^{-1} \sigma_u^i\|$  is the largest if

$$\left[ b_{i,1} - \frac{\sigma_r^2 \mathbf{b}_1' \mathbf{b}}{1 + \sigma_r^2 \mathbf{b}'\mathbf{b}} b_i \right]^2$$

is the largest. As  $\mathbf{b}_1' \mathbf{b}$  is a scalar common to all  $i$ , it implies that the one that changes its centrality the most is the systemic individual. It aligns with our view that a centrality change in any direction is a manifestation of network structure change, which is a result of strategic decisions. In some sense, an adjustment could indicate one's relative vulnerability. However, in any case, it will be better considered as a potential risk component of a given system.<sup>19</sup>

Now, let us consider general cases with multiple ( $K$ ) sources of common exposure:

$$y_{it} - u_{it} = \sum_k \alpha_{ik} r_{k,t} + \sum_j \Omega_{ij} (y_{jt} - u_{jt}), \quad \text{or,}$$

$$\mathbf{y}_t = (I_N - \Omega)^{-1} A \mathbf{r}_t + \mathbf{u}_t = [(I_N - \Omega)^{-1} \boldsymbol{\alpha}^1 | \dots | (I_N - \Omega)^{-1} \boldsymbol{\alpha}^K] \mathbf{r}_t + \mathbf{u}_t = B \mathbf{r}_t + \mathbf{u}_t, \quad (\text{B.34})$$

where a nonnegative matrix of marginal benefits  $A_{NK} = [\alpha_{ik}]$ , whose  $k$ -th column is  $\boldsymbol{\alpha}^k$ . As  $\Omega, A$  and  $\mathbf{r}_t$  are latent, and the  $\{r_k\}$  are strong, it will be described by the  $K$ -dimensional factor model  $\mathbf{y}_t = P \mathbf{f}_t + \mathbf{u}_t$ . Each column of  $B$  consists of a weighted Bonacich centrality  $\mathbf{b}^k \equiv (I_N - \Omega)^{-1} \boldsymbol{\alpha}^k$  (Ballester et al., 2006). It can be seen as an equilibrium action of exposure to  $r_k$  of a simple game (Ballester et al., 2006, Galeotti et al., 2020)

$$\max U_i^k(b_{ik}) = \max \left[ b_{ik} \alpha_{ik} - (1/2) b_{ik}^2 + b_{ik} \sum_j \Omega_{ij} b_{jk} \right] \quad \text{for all } k$$

where the payoff from action is correlated to the others' action through  $\Omega$ , and marginal benefits are given as  $\alpha_{ik}$ .

For the point on our criteria of the number of granular units, if one tries to adjust their action, it will affect all others' equilibrium action as for each  $r_k$ , the actions depend on others' action. Hence, we take the number of common sources whose equilibrium is adjusted as a conservative measure of the number of systemic individuals. Note that the true number of the common source can be larger than the number of latent factors or the dimension of the factor space, as only a subset of  $\{r_k\}$  gives strong enough signals. If there is a significant adjustment in the

<sup>19</sup>The exact extension of this interpretation can be made only in restrictive scenarios in general cases with multiple sources of exposures – we will discuss soon; for example, where the  $N$  agents are partitioned into  $K$  different groups  $\{G_k\}$  by different common exposures, ( $\alpha_{ik} = \mathbf{1}_{i \in G_k}$ ) and the group does not change across regimes. In this particular case, the systemic individuals are the ones with the largest centrality change in each group. In general cases, we will have an interpretation in terms of weighted centrality or equilibrium actions of a game of exposures. We will soon discuss this.

equilibrium for a week  $\{r_k\}$  can be seen as an advert of a new factor.

In the following simplified example, the influence measure gives individuals with the largest changes in action as the granular units, with an additional consideration of how the exposures for different sources are overall correlated.

EXAMPLE 2. Let  $\mathbf{y}_t = B\mathbf{r}_t + \mathbf{u}_t$ , where  $\text{cov}(\mathbf{u}_t) = I_N$  during  $I_0$ . Let  $\text{cov}(\mathbf{r}_t) = \sigma_r^2 I_K$  overall time, for  $\sigma_r^2 \gg 1$ . Then  $\Sigma_{\mathbf{y}} = \sigma_r^2 B B' + I_N$  and  $\Sigma_{\mathbf{y}}^{-1} = I_N - \sigma_r^2 B (I_K + \sigma_r^2 B' B)^{-1} B'$ . The  $i$ -th column norm  $\mathcal{I}_i = \|\Sigma_{\mathbf{y}}^{-1} B_1 B_1' \Sigma_{\mathbf{y}}^{-1} \sigma_u^i\|$  is the largest if

$$\sum_k \left[ b_{i,1}^k - \sigma_r^2 \mathbf{b}_1^{k'} B (I_K + \sigma_r^2 B' B)^{-1} \mathbf{b}_i \right]^2$$

is the largest. Further, let  $B' B = I_K$  to simplify interpretation. The measure of the change of individual's action for  $k$ -th source of exposure has an extra consideration on how regime1 action of all  $\mathbf{b}_1^k$  is correlated to regime 0 actions  $\mathbf{b}_0^\kappa$  for all  $\kappa$ , captured by  $\mathbf{b}_1^{k'} B$ . That is, a player  $i$ 's regime 1 action for each  $k$ -th exposure  $b_{i,1}^k$  is compared to its own action for all  $\kappa$  in the regime 0 ( $\mathbf{b}_i$ ) weighted by the overall similarity of actions across regimes. The change in one's action will be depreciated if actions across regimes overall correlate in the same direction as the individual change. If the chosen action of  $i$  is co-moving with most of all others, the resulting magnitude of change will get a penalty.

In general cases, the measure and interpretation of individuals' importance are based on their actions. It is the combination of an underlying network and marginal benefits on direct exposures to  $\{r_k\}$ . Those factors are jointly determining the correlation structure among cross-sectional items. Our criterion of detection parallels to identify individuals changing the most of their actions, net of the overall comovement of actions.

We close this discussion by presenting the following example, where the change of actions can be visualized as a change in the underlying network.

EXAMPLE 2.A Let  $N = 100$  and  $K = 3$ . Assume  $\mathbf{u}_t \sim \mathcal{N}(\mathbf{0}, 2I_N)$ , and  $\mathbf{f}_t \sim \mathcal{N}(\mathbf{0}, 25I_K)$  for all  $t$ . We consider, for simplicity, a case where  $N$  agents can be partitioned into  $K$  groups regarding the direct exposure to different source  $r^k$ . For instance, let the  $N$  by  $K$  matrix  $A$  of the direct exposure coefficients be given as <sup>20</sup>

$$A = \begin{bmatrix} \mathbf{0} & \mathbf{0} & \mathbf{1}_{20} \\ \mathbf{1}_{30} & \mathbf{0} & \mathbf{0} \\ \mathbf{0} & \mathbf{1}_{50} & \mathbf{0} \end{bmatrix}, \quad (\text{B.35})$$

<sup>20</sup>Or it can be  $A\mathcal{O}_K$  for any orthogonal transformation  $\mathcal{O}_K$

where  $\mathbf{1}_m$  denotes a length  $m$  column vector of ones. It is additionally assumed to be fixed across regimes. Then the units of individuals (nodes) 3, 22, and 55 are the most important in the following change of underlying network structure, from left to right of Figure B.1:

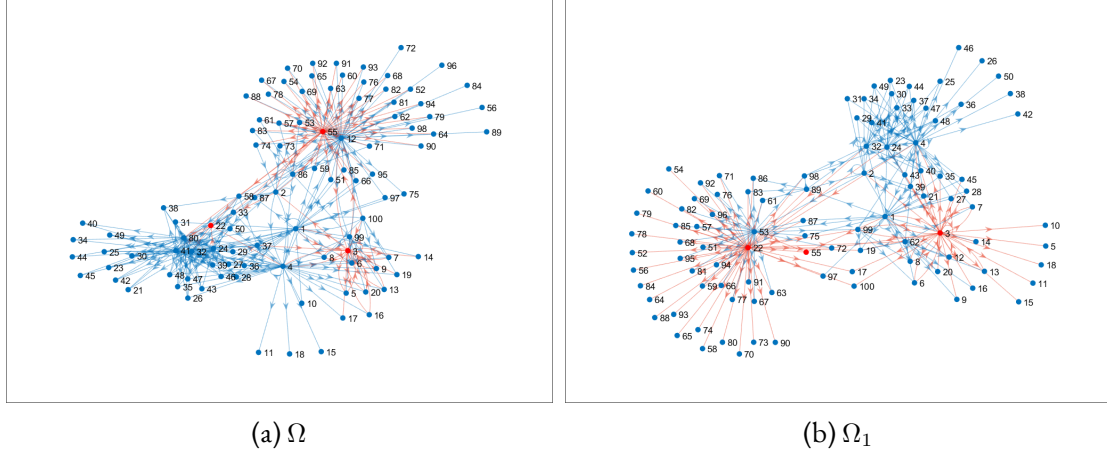


Figure B.1

In this example, by fixing  $A$  in the form (B.35), the change in action  $\mathbf{b}_i$  coincides with changes of importance in propagating the effect of its direct exposure (to some  $r^k$ ) to all. The graphical description of degree centrality can broadly capture the latter due to the setup of  $A$ . The importance of node 22 is revealed by substantially gaining centrality. That of node 55 is the opposite, by substantially losing centrality. Node 3 is counted as important as its centrality spreads to a collection of nodes that were not connected previously.

### B.3 A NOTE ON THE FIRST ORDER EFFECT

It was the partial derivative of the expression

$$d(\text{span}(P_0), \text{span}(P_1)) \simeq \text{tr} \left[ \Sigma_u \Sigma_y^{-1} \mathcal{P}_1 \Sigma_y^{-1} \Sigma_u \right] \quad (2.11')$$

that enabled the measure (2.13) in Section 2.3.2. Mechanically, what we analyze is the first-order effect on the distance, which depends both on the initial state  $\mathcal{P}_0$  and the new state  $\mathcal{P}_1$ . When we considered the first-order effect of  $\Sigma_u$  on this expression,  $\mathcal{P}_1$  was fixed as given as it does not have a direct effect (the first order effect) from a perturbation of  $\Sigma_u$ . A perturbation of  $\Sigma_u$  effectively implies a perturbation on the initial state of the system,  $\mathcal{P}_0$ . It is a hypothetical perturbation on the decomposition structure of the regime-0 system covariance into the common and idiosyncratic covariance, fixing the summation. The granular units have the largest contributions through the state perturbation.

In general cases, the analysis based on the partial effect (2.12) can still provide a measure of systemic influence by assuming the direction (sign) of the potential direct effect on the regime-1 factor space is the same as that of the initial state perturbation due to the perturbation on the

granular units. Let us discuss this in detail for the cases where  $\mathcal{P}_1$  has a direct dependence on  $\Sigma_u$ . Due to the cyclic invariance of the trace operator, the partial derivative gives the first-order effect of  $\sigma_u^i$  as

$$\dot{\mathcal{I}}_i \equiv \left\| \frac{1}{2} [\partial_{\Sigma_u} d(\text{span}(P_0), \text{span}(P_1))]^i \right\| = \left\| \Sigma_y^{-1} \mathcal{P}_1 \Sigma_y^{-1} \sigma_u^i + \Delta^i \right\|, \quad (\text{B.36})$$

where

$$\Delta^i \equiv \sum_{\ell, m}^N \begin{bmatrix} \frac{\partial[\mathcal{P}_1]_{\ell m}}{\partial \sigma_u^{i1}} \\ \vdots \\ \frac{\partial[\mathcal{P}_1]_{\ell m}}{\partial \sigma_u^{iN}} \end{bmatrix} [\Sigma_y^{-1} \Sigma_u^2 \Sigma_y^{-1}]_{m\ell}. \quad (\text{B.37})$$

The  $\Delta$  in (B.36) is infeasible to identify without a specific model of  $\mathcal{P}_1$  with respect to  $\Sigma_u$ . We assume that the second term  $\Delta$  is aligned with the first term in (B.36) for the granular units and misaligned for the others. That is, the direction of the potential direct effect on the regime-1 factor space is the same as that of the initial state perturbation due to  $\sigma_u^g$ .

ASSUMPTION D. Denote  $\mathcal{I}_i \equiv \left\| \Sigma_y^{-1} \mathcal{P}_1 \Sigma_y^{-1} \sigma_u^i \right\|$  for any  $i \in \mathcal{N}$ . Let us assume the following:

- a)  $\text{sgn}[\Sigma_y^{-1} \mathcal{P}_1 \Sigma_y^{-1} \sigma_u^g]_m = \text{sgn}(\Delta_m^g)$  for all  $m \in \mathcal{N}$  for  $g \in \mathcal{G}$ .
- b)  $\text{sgn}[\Sigma_y^{-1} \mathcal{P}_1 \Sigma_y^{-1} \sigma_u^i]_m = -\text{sgn}(\Delta_m^i)$  for all  $m \in \mathcal{N}$  for  $i \notin \mathcal{G}$ .
- c)  $\mathcal{I}_g > \mathcal{I}_m$  for all  $g \in \mathcal{G}$  and  $m \notin \mathcal{G}$ .

Then  $\dot{\mathcal{I}}_g \geq \mathcal{I}_g > \mathcal{I}_i \geq \dot{\mathcal{I}}_i$  for any  $g \in \mathcal{G}$  and  $i \notin \mathcal{G}$ , and we detect the granular units by ranking  $\{\mathcal{I}_i\}_{i \in \mathcal{N}}$  instead of  $\{\dot{\mathcal{I}}_i\}_{i \in \mathcal{N}}$ .

## B.4 A GEOMETRICAL INTERPRETATION ON THE DETECTION CRITERIA

The proposed scheme of detection based on the partial effect of  $\sigma_u^i$  in (2.13) can be explained from a more geometrical point of view aligned with the discussion in Section 2.3.3 and Appendix A.1.2.1. One can be interested in possible geometrical modeling supporting the detection scheme, in addition to the interpretations already presented in Section 2.2.2, Section 2.3, and Appendix B.2.

Let us start by reviewing the geometrical features of the factor space change and the benchmark criteria 2.3.3.1. As discussed mainly in Section 2.3.3 and Appendix A.1.2.1, the factor space dynamics can be seen as a rotation in  $N$ -dimensional space, which is determined by two types of information: directions of change of the basis vectors  $V_{N \times H}$ , and angles  $\Theta = \text{diag}(\theta_1, \dots, \theta_H)$  capturing how far the basis vectors rotate to the chosen directions. For any  $h = 1, \dots, H$ ,  $\theta_h \in [0, \pi/2]$  to describe identifiable rotations.

As the factor space is a multi-dimensional object, its change is also multi-dimensional by nature, which requires several different types of information to represent it: the shape (which can be captured by directional information  $V$ ), the dimension ( $H$ ), and the magnitude ( $\Theta$ ). The distance measure itself (2.10) gives a gross aggregation *after* taking the trace. It captures only one type of information about the change – the overall magnitude – erasing any directional and dimensional information. We can see this point with the help of the discussion in Appendix A.1.2.1 as

$$d(\text{span}(P_0), \text{span}(P_1)) \equiv \text{tr}[P_0^\perp P_0^{\perp'} P_1 P_1' P_0^\perp P_0^{\perp'}] = \text{tr}(V \sin^2 \Theta V') = \sum_{h=1}^H \sin^2 \theta_h \quad (2.10')$$

where  $\sin \Theta = \text{diag}(\sin \theta_1, \dots, \sin \theta_H)$  is the realized principal angles  $\theta_h$  between two subspaces represented by  $P_0 P_0'$  and  $P_1 P_1'$ .

This is one of the reasons why we propose a detection scheme by modeling the argument *inside* the trace operator defining the distance measure (2.10). By doing so, our detection criteria 2.3.3.1 utilize all three types of information representing the change of the factor space. It is important to capture the full characteristics of the factor space change in our proceedings. Especially, the directional information can provide a valuable factor to explain individual shares in the magnitude of the factor space change.

To have a closer look at this point, first recall the discussion on the directional information of the factor space change in Section 2.3.3. As in the paragraph above Assumption 5, what matters to capture the change of the factor space is the component of  $P_1 P_1'$  perpendicular to  $P_0 P_0'$ , whose directional information amounts to  $V$ . The  $V$  is, approximately in large  $N$ , a choice of a size  $H$  subcollection of the eigenvectors of  $\Sigma_y^{-1}$  corresponding to  $N - K$  largest eigenvalues – in other words, the smallest  $N - K$  eigenvalues of  $\Sigma_y$ .<sup>21</sup>

Let  $V = \tilde{P}_{N \times H}$  by column-augmenting a chosen set of eigenvectors  $\{\tilde{\mathbf{p}}_h\}_{h=1, \dots, H}$  of  $\Sigma_y^{-1}$ , and denote  $\tilde{\Lambda}_y^{-1}$  the diagonal matrix of the eigenvalues of  $\Sigma_y^{-1}$  corresponding to the chosen eigenvectors. Combined with the discussion in Appendix A.1.2.1, the proposed influence measure (2.13) can be written as

$$\mathcal{I}_i = \left\| \Sigma_y^{-1} P_1 P_1' \Sigma_y^{-1} \boldsymbol{\sigma}_u^i \right\| = \left\| \Sigma_y^{-1} V D V' \Sigma_y^{-1} V' \boldsymbol{\sigma}_u^i \right\| = \left\| V \tilde{\Lambda}_y^{-1} D \tilde{\Lambda}_y^{-1} V' \boldsymbol{\sigma}_u^i \right\| \quad (= \|V \tilde{D} V' \boldsymbol{\sigma}_u^i\|) \quad (2.13')$$

where  $D \equiv \sin^2 \tilde{\Theta}$ , for  $\tilde{\Theta}$  denoting the distance perturbed due to the first-order effect of  $\Sigma_u$ . That is, the directional information plays a crucial role in explaining how the magnitude of the factor space change  $\sin^2 \tilde{\Theta}$  is decomposed into the individual shares;  $\mathcal{I}_i$  measures the length of a weighted (by  $\tilde{D} \equiv \tilde{\Lambda}_y^{-1} D \tilde{\Lambda}_y^{-1}$ ) projection of  $\boldsymbol{\sigma}_u^i$  on the directions  $V$  represents. We can clearly see that the membership detection employs two types of information: the directional and the magnitude, based on the measure  $\{\mathcal{I}_i\}$ . The dimensional information determines the

<sup>21</sup>More precisely, the chosen  $V V'$  is a subspace of the  $N - K$  principal subspace of  $\Sigma_y^{-1}$ .

number of granular units. Hence, all three types of information are utilized for granular unit detection in criteria 2.3.3.1.

# 3 GENERAL INSTABILITIES IN NETWORKED SYSTEMS AND EARLY WARNINGS

## 3.1 INTRODUCTION

A system of interest is often intertwined. The interconnected structure captures a defining characteristic of a system of  $N$  agents or nodes in many different fields, including economics, finance, and engineering. Various types of network models provide essential descriptions of these linked structures within.

The configuration of interconnectedness can result from layers of different types of interactions. The true characteristics of the most relevant network structure may not be readily known. From this perspective, studies have been conducted to extract network structures from data assumed to be defined on an unknown or unobservable network. The cross-correlation structure of network-supported data can be exploited to estimate the underlying latent network.

As the network structure captures the essence of a given system, instabilities in this structure can indicate important structural changes. Early detection of such instabilities is crucial for preparedness and resilience against potential crises, anomalies, or attacks. However, methodologically, capturing instabilities in latent structure is a non-trivial task. In the previous chapters, we discussed how a popular method, latent factor models and PCA, can provide a minimalist framework for this task, considering discrete and deterministic structural changes. In this chapter, we further discuss the conceptual link between latent factor models and network models, considering more general instabilities in the underlying interconnected structure. More languages and tools to incorporate general instabilities will be explored, with the aim of designing an early warning framework for large structural instabilities in latent networks.

The contribution of this chapter is to bridge diverse research domains. We design a new, intuitive early warning framework that incorporates a broad range of instabilities, grounded in the resulting integrated insights. First, we provide a conceptual link between two important modeling schemes: network models and latent factor models, addressing a broad class of instabilities. Second, our discussion also brings together classical approaches in factor analysis

and distributional approaches to multi-dimensional geometric objects. This joint perspective offers an intuitive interpretation of factor structure analysis and a popular sequential early detection scheme based on cumulative sum methods.

This chapter consists of the following sections. In Section 3.2, we recall and summarize the conceptual link between network models and factor models introduced in Chapter 2. Section 3.3 extends this interaction between network models and latent factor models to a general class of instabilities in the networked structure. In Section 3.4, we bring together various approaches facilitating analysis of structural changes and design a new early warning framework for large structural instabilities. Section 3.5 concludes.

## 3.2 UNOBSERVABLE NETWORKS AND LATENT FACTOR MODELS

In this section, we recall the duality between unobservable network models and latent factor models introduced in Chapter 2. The resulting model with a dual representation as a network or a factor model will be called a *network-factor* model. This modeling can provide a means to define and analyze structural breaks in a networked system, leveraging well-established language and tools from factor models.

### 3.2.1 STATIC LATENT NETWORK-FACTOR MODEL

Consider a system of  $N$  individual series  $\mathbf{y}_t = [y_{1t}, \dots, y_{Nt}]'$ . During a time window  $I_0$ , the cross-sectional units – the nodes of a network, representing different agents or different variables – are interconnected by a constant relationship  $\Omega$  and experience minor idiosyncratic fluctuations  $u_{it}$ . Interconnections can arise for various reasons. They can be due to mutual investments (including buyer-seller relationships) or borrower-lender relationships, or may imply an indirect manifestation of holding similar investment portfolios, or a shared ownership structure. The true characteristics of the relationships can be unknown or unobservable.

Assume, for the moment and for simplicity, that the interconnected performances are balanced with one common source of exposure,  $r$ . It can be a final good demand or a common return from a safe investment, whose genuine characteristic can again be unknown or unobservable. The marginal benefit from the exposure is simply assumed to be 1 for the simplest exposition. For given  $\Omega$  and  $r$ , the networked system can be written as follows, for  $t \in I_0$ ,

$$y_{it} - u_{it} = r_t + \sum_{i'} \Omega_{ii'}(y_{i't} - u_{i't}), \quad \text{or equivalently,}$$

$$\mathbf{y}_t = (I_N - \Omega)^{-1} \mathbf{1} r_t + \mathbf{u}_t = \mathbf{b} r_t + \mathbf{u}_t. \quad (3.1)$$

Note that, in this example of a single common exposure with homogeneous unit marginal benefits,

$$\mathbf{b} \equiv (I_N - \Omega)^{-1} \mathbf{1},$$

which equals the Bonacich centrality of the cross-sectional items in the constant network  $\Omega$ . When the common source of exposure and the interconnected structure  $\Omega$  are not observable, one can describe (3.1) by a one-dimensional latent factor model,

$$\mathbf{y}_t = \tilde{B} f_t + \mathbf{u}_t$$

where the factor loading  $\tilde{B}$  amounts to the centrality vector  $\mathbf{b}$ , up to an unknown scaling. For general cases with multiple ( $K$ ) sources of common exposure, we can represent the system as

$$y_{it} - u_{it} = \sum_k \alpha_{ik} r_{k,t} + \sum_j \Omega_{ij} (y_{jt} - u_{jt}), \quad \text{or,}$$

$$\mathbf{y}_t = (I_N - \Omega)^{-1} A \mathbf{r}_t + \mathbf{u}_t = [(I_N - \Omega)^{-1} \boldsymbol{\alpha}^1 | \dots | (I_N - \Omega)^{-1} \boldsymbol{\alpha}^K] \mathbf{r}_t + \mathbf{u}_t = B \mathbf{r}_t + \mathbf{u}_t, \quad (3.2)$$

where  $A_{NK} = [\alpha_{ik}]$  is a non-negative matrix of marginal benefits whose  $k$ -th column is  $\boldsymbol{\alpha}^k$ . Each column of  $B$  consists of a weighted Bonacich centrality  $\mathbf{b}^k \equiv (I_N - \Omega)^{-1} \boldsymbol{\alpha}^k$  (Ballester et al., 2006). It can be seen as an equilibrium action of exposure to  $r_k$  of a simple game (Ballester et al., 2006, Galeotti et al., 2020)

$$\max U_i^k(b_{ik}) = \max [b_{ik} \alpha_{ik} - (1/2) b_{ik}^2 + b_{ik} \sum_j \Omega_{ij} b_{jk}] \quad \text{for all } k = 1, \dots, K \quad (3.3)$$

where the payoff from action is correlated to the others' action through  $\Omega$ , and marginal benefits are given as  $\alpha_{ik}$ .

As  $\Omega, A$  and  $\mathbf{r}_t$  are latent, and the  $\{r_k\}$  are strong, it can be described by the  $K$ -dimensional factor model

$$\mathbf{y}_t = \tilde{B} \mathbf{f}_t + \mathbf{u}_t. \quad (3.4)$$

### 3.2.2 CHANGING NETWORKS AND STRUCTURAL BREAKS IN LATENT FACTOR MODEL

The underlying network and the resulting networked actions can change for various reasons. For example, idiosyncratic disturbances experienced by important economic agents can trigger a viable adjustment of the internal relationships represented by  $\Omega$ . As a more detailed example, a bank or firm can perceive the idiosyncratic volatilities of its own (or its adjacent entities) as a subjective risk factor in mutual investment. If it assesses that the expected disturbances exceed a certain level, it can attempt to adjust its investment portfolio to absorb or mitigate

the potential risk.<sup>1</sup>

As important nodes adjust neighboring relationships substantially,  $\Omega$  is altered. Naturally, all the centrality vectors ( $\mathbf{b}^k$ , in model (3.2)) can change, which can be interpreted as major changes in equilibrium actions, as presented in (3.3). We take such a substantial change in centrality as a structural change in a networked system. Through the conceptual linkage introduced in the previous section, (3.1) to (3.3), such a change will be captured by large breaks in factor loading. Moreover, even if the characteristics of the underlying network is unknown or unobservable, such a structural change can still be captured by instabilities in *factor space*, in the language of the latent factor model. It is the column space of the factor loading, which can capture instabilities in factor loading while being free from inherent identification issues of latent factor models. We refer to the previous chapters for a full explanation.

The previous chapters mainly consider discrete changes in factor space, which can serve as a benchmark. We have also briefly discussed that the discrete change model in Chapter 1 can be extended to allow broader scenarios of small perturbations within one regime. However, the coverage of a discrete change type model is still restrictive in interpreting instabilities in networked systems. In the next section, we extend the duality between network and factor models, to account for more general types of instabilities.

### 3.3 LATENT NETWORK-FACTOR MODEL WITH INSTABILITIES

Recall the simple 1-dimensional model with a general marginal benefit vector  $\alpha$ ,

$$\mathbf{y}_t = (I_N - \Omega)^{-1} \alpha r_t + \mathbf{u}_t = \mathbf{b} r_t + \mathbf{u}_t. \quad (3.5)$$

The (weighted) Bonacich centrality  $b_i = [(I_N - \Omega)^{-1} \alpha]_i$  of unit  $i$  is determined by the networked marginal benefits through the Leontieff inverse as follows:

$$[(I_N - \Omega)^{-1} \alpha]_i = \sum_{j \in \mathcal{N}} \sum_{\ell} \pi_{i \leftarrow j, \ell} \alpha_j.$$

Here,  $\pi_{i \leftarrow j, \ell}$  represents the sum of all paths of length  $\ell$  from unit  $j$  to unit  $i$ , such that

$$\pi_{i \leftarrow j, \ell} \equiv \sum_{(j_1, \dots, j_{\ell-1})} \Omega_{ij_1} \Omega_{j_1 j_2} \cdots \Omega_{j_{\ell-1} j}, \quad (3.6)$$

---

<sup>1</sup>In a financial network, it could be assumed to keep the leverage level the same as the perceived value at risk, e.g., [Mazzarisi et al., 2019](#).

where the summation runs over all collections of nodes that constitute a path of length  $\ell$  from  $j$  to  $i$ . This implies that the propagation of the source of common exposure ( $r_t$ ) in (3.5) follows

$$y_{it} = \sum_{j \in \mathcal{N}} \sum_{\ell} \pi_{i \leftarrow j, \ell} \alpha_j r_t + \epsilon_{it}.$$

In the above expression, the propagation through any path of length  $\ell$  is instantaneous, and the underlying network structure is fixed during the transmission. This can be seen as a consequence of having an equilibrium given a fixed network. However, it can be a restrictive scenario to expect to be realized, especially in high-frequency observations. In this section, we first introduce an extended network-factor model that incorporates general changes in interconnectedness and review existing approaches that address structural changes in a networked system.

### 3.3.1 FACTOR MODEL REPRESENTATION OF CHANGING NETWORKS

Let  $y_{it}$  be a realized performance of an economic activity at time  $t$  for unit  $i$  considered previously. A (net) return of the economic activity (e.g., investment) is intertwined with all others' returns in a lagged manner:

$$y_{it} - \epsilon_{it} = \sum_k \alpha_{ik} x_{kt} + \sum_j L \Omega_{ij,t} L(y_{jt} - \epsilon_{jt}), \quad (3.7)$$

where  $L \Omega_{ij,t} \equiv \Omega_{ij}[t, t-1]$ , broadening the concept of a lag operator, indicates a relation of  $i$  and  $j$  during the window  $t-1$  and  $t$ . Here,  $\mathbf{x}_t = [x_{kt}]_{k=1, \dots, K}$  represents common sources of exposure.  $A = [\alpha_{ik}]_{i \in \mathcal{N}, k=1, \dots, K}$  captures individuals' marginal benefits to the common exposure. The expression (3.7) can be written in a matrix form as

$$\mathbf{y}_t = (I_N - L \Omega_t L)^{-1} A \mathbf{x}_t + \boldsymbol{\epsilon}_t = B_t(L) \mathbf{x}_t + \boldsymbol{\epsilon}_t. \quad (3.8)$$

Parallel to the Leontief inverse,  $(I_N - L \Omega_t L)^{-1}$  captures the (infinite) summation of all time-affected paths from  $j$  to  $i$  of any length. That is,

$$y_{it} = \sum_{j \in \mathcal{N}} \sum_{\ell} \pi_{t, i \leftarrow j, \ell} L^{\ell}(\mathbf{a}_j \mathbf{x}_t) + \epsilon_{it}$$

where  $\mathcal{N}$  is the set of individuals and  $\mathbf{a}_j$  is the  $j$ -th row of  $A$ . Here  $\pi_{t, i \leftarrow j, \ell}$  denotes the sum of all paths of length  $\ell$  from  $j$  to  $i$  lasting until time  $t$  from time  $t-\ell$ ,

$$\pi_{t, i \leftarrow j, \ell} \equiv \sum_{(j_1, \dots, j_{\ell-1})} (\Omega_{ij_1} \Omega_{j_1 j_2} \cdots \Omega_{j_{\ell-1} j})[t, t-\ell],$$

where the summation runs over all collections of nodes that constitute the existing paths of length  $\ell$  from  $j$  to  $i$ . The time-specific references within the parentheses are omitted for

simplicity. That is, the path components are allowed to be time-specific;  $\Omega_{j_{h-1}j_h} = \Omega_{j_{h-1}j_h}[t - (h - 1), t - h]$ ,  $\Omega_{ij_1} = \Omega_{ij_1}[t, t - 1]$  and  $\Omega_{j_{\ell-1}j} = \Omega_{j_{\ell-1}j}[t - (\ell - 1), t - \ell]$ .

If only those  $\{\mathbf{a}_g \mathbf{x}_t\}$  of a certain set of individual units  $g \in \mathcal{G}$ , for  $|\mathcal{G}| < \infty$  are important to the transmission,

$$y_{it} = \sum_{g \in \mathcal{G}} \sum_{\ell} \pi_{t,i \leftarrow g, \ell} L^{\ell}(\mathbf{a}_g \mathbf{x}_t) + \epsilon_{it} \quad \text{for all } i \in \mathcal{N} \quad (3.9)$$

assuming that  $\sum_{\ell=1}^{\infty} \pi_{t,i \leftarrow g, \ell} L^{\ell}$  exists for every pair  $(i, g) \in \mathcal{N} \times \mathcal{G}$ . We simply consider cases where there is no path lasting more than a few lags. More precisely, it is only up to the maximum lag  $M$  that matters, regardless of  $t$ . Assume further that  $\{\mathbf{a}_j\}$  are constant, and denote,

$$\pi_{t,i \leftarrow j, \ell}^a \equiv \sum_{(j_1, \dots, j_{\ell-1})} (\Omega_{ij_1} \Omega_{j_1 j_2} \cdots \Omega_{j_{\ell-1} j}) \mathbf{a}_j.$$

The transmission will be effectively represented as

$$\mathbf{y}_t = \Pi_t(L) \mathbf{x}_t + \boldsymbol{\epsilon}_t, \quad (3.10)$$

where  $\Pi_t(L)$  is an  $N \times K$  matrix of lag polynomials generated by  $\pi_{t,i \leftarrow j, \ell}^a$ . It corresponds to the description of dynamic factor models of observable or latent versions depending on the observability of  $\mathbf{x}_t$ . The latent version can have a reduced representation by assuming all lags of  $\mathbf{x}_t$  are strong factors as follows:

$$\mathbf{y}_t = \Pi_t \mathbf{f}_t + \boldsymbol{\epsilon}_t (= \chi_t + \boldsymbol{\epsilon}_t), \quad (3.11)$$

where  $\Pi_t$  is  $N \times KM$  factor loading matrix consisting of the coefficients  $\pi_{t,i \leftarrow j, \ell}^a$  of matrix polynomial in (3.10). It captures the pathways of transmitting  $KM$  number of factors  $\mathbf{f}_t \equiv [L^{\ell}(\mathbf{x}_t)]_{\ell=1, \dots, M}$ . This aspect of reduced representations is discussed in the dynamic factor models literature, such as [Forni et al., 2009](#). A factor model can similarly represent the cases with time-varying marginal benefits by taking  $[\mathbf{a}_g \mathbf{x}_t]_{g \in \mathcal{G}}$  or their lags as the factors.<sup>2</sup>

We take the reduced representation (3.11) as the benchmark in further discussion. The transmission rule  $\Pi_t$  is changing as the paths or the path component edges  $\Omega_{ij}$  can adjust throughout time.

Once a networked system is mapped into a factor model, such as in (3.4) or (3.11), well-established methods in the factor model literature can be used to analyze its structural instabilities. In the next subsection, we briefly discuss existing approaches to analyzing factor structure instabilities. The focus is on the instabilities in the factor loading  $\Pi_t$  or its column space (the

---

<sup>2</sup>See Appendix C.1.

*factor space*) that captures changes in the transmission rule due to perturbations of a latent network structure.

### 3.3.2 INSTABILITIES IN FACTOR STRUCTURE: DISCRETE VS.

#### CONTINUOUS

As discussed in the previous chapters, the latent factor model is essentially a modeling of the system covariance matrix. The decomposition of the common component ( $\chi_t$ ) and the idiosyncratic component ( $\epsilon_t$ ),

$$\mathbf{y}_t = \chi_t + \epsilon_t,$$

is guaranteed by conditioning on the system covariance:

$$\Sigma_y = \Sigma_\chi + \Sigma_u. \quad (3.12)$$

We call the properties of the system covariance that guarantee such additive decomposition as *factor structure*. Instabilities in a factor structure and instabilities in a factor model are interchangeable expressions.

There have been numerous studies on structural instabilities in factor models. Large breaks in factor structure, especially in the factor loading, have been analyzed and interpreted in relation to structural changes or crises in economic or financial systems. Instabilities in latent factor structures correspond to changes in cross-correlation structures, as discussed in the previous chapters. Cross-correlations have been used to identify latent interconnectedness by containing rich information about the underlying linkages among variables or channels of spillovers among the cross-sectional units. Instabilities in the correlation structure have been widely studied using various methods, including factor models, which naturally imply changes in the underlying network.

In those streams of research on structural instabilities, structural changes are primarily considered to occur either at discrete points in time or gradually in a continuous manner. The majority of approaches take the former stance, differing in their considerations of deterministic or random locations of breakpoints. The previous two chapters considered discrete, deterministic change points. Although it is most popular to assume a static factor model within one regime, when the method focuses on factor space changes — changes in the column space of the factor loading matrix — it can accommodate perturbations of the factor loading matrix itself. It can also allow for certain types of non-stationarity in factor signals and idiosyncratic components within a single regime. This is mainly because small perturbations do not affect the factor structure decomposition or factor space. We discuss in detail in the next section.

Among the methods for analyzing discrete, probabilistic changes, Markov-switching-type models are one of the most popular approaches. In the most popular forms of modeling, the

number of different regimes is assumed to be small and fixed. In this literature, regimes often represent recurring macroeconomic regimes defined by aggregate economic activities or monetary policy, or financial regimes, such as bull or bear markets, depending on the applications. The modeling can be extended to cover an infinite number of regimes as well.

The approaches for continuous changes often operate within a major framework of local stationarity. For example, one can assume that the potential network adjustments occur slowly and gradually in the model discussed in the previous subsection. Then it leads the model to be locally stationary. Following [Dahlhaus, 2012](#), we express the (3.10) in terms of a local time variable  $u \equiv t/T$  for  $T$  as the size of the whole time domain:

$$\mathbf{y}_u = \Pi_u(L)\mathbf{x}_u + \boldsymbol{\epsilon}_u, \quad (3.10)$$

where  $L$  should be interpreted as the infinitesimal time translation operator at the local time point  $u$  as  $T \rightarrow \infty$ .

The discrete or continuous types of changes can be two extremes, but pragmatic models of instabilities. Discrete changes can be restrictive scenarios. However, this class of scenarios provides the simplest description of structural breaks, leading to straightforward analysis and interpretation of "breakpoints" in time. Continuous types of changes can be more illustrative of a system's dynamics. However, the concept of breaks or large changes becomes less straightforward, alongside the methods of analysis.

Our aim is to design models and methods that incorporate general instabilities in the factor structure to provide early warnings of structural changes in a system. For the most straightforward construction and interpretation of such methods, we focus on deterministic or random breaks at discrete time points. In the next section, we explore new directions and perspectives in relation to existing methods of early detection and factor structure analysis.

## 3.4 EARLY WARNINGS OF STRUCTURAL CHANGES IN A NETWORKED SYSTEM

When broader types of changes are allowed in the factor structure—particularly in the factor space representing the underlying variation of a latent network—it becomes necessary to distinguish between "small" perturbations and "large" or structural instabilities.

To be precise, we will classify variations in the factor structure into three categories. The first category consists of *perturbations*, the most restrictive type of change. These are always considered "small" variations, as they preserve the factor space. The second category is *small instabilities*, involving minor changes of the factor space. The final category is *large instabilities* that incur considerable changes of factor space. This last type of variation indicates structural changes in a networked system and can be a precursor to a potential crisis. Developing a

method to provide early warning of such changes can be of practical importance.

In the next subsection, we begin by characterizing the first category – small perturbations. In subsequent sections, we propose a method for providing early warnings of structural changes, closely related to existing methods of analysis in latent factor models.

### 3.4.1 SMALL PERTURBATIONS IN FACTOR STRUCTURE

In Section 3.3.1, we represent perturbations of a latent network structure by instabilities in the factor loading matrix  $\Pi_t$  through a latent factor model. By the nature of this latent model, instabilities in the factor loading matrix are not distinguished from those in the factor signal covariance when the number of factors is fixed. The column space of the factor loading ( $\mathcal{P}_t \equiv \text{span}(\Pi_t)$ , the *factor space*) is an object introduced to capture instabilities in the factor loading matrix that are robust to potential instabilities in latent factors. That is, any change in the factor loading that is robust to changes in the latent factor signal covariance will be captured by a change of the factor space. We refer to the previous chapters for a detailed discussion.

A large change in the factor space indicates a considerable change in the transmission rule, or a structural change in a networked system. On the contrary, any variations in the factor structure that do not affect the factor space can be considered *small perturbations*.

We assume an interval  $I_0$  in which a mean-zero process  $\mathbf{y}_t$  presents the following small perturbations in the factor structure.

For  $t \in I_0$ ,  $\mathbf{y}_t$  and  $\Sigma_{\mathbf{y},t} = E_t[\mathbf{y}_t \mathbf{y}_t']$  satisfy the following properties:

**Assumption 1.** For any  $t \in I_0$ ,  $\mathbf{y}_t = \chi_t + \epsilon_t$  for mean-zero processes  $\chi_t$  and  $\epsilon_t$ .

**Assumption 2.** For any  $t \in I_0$ ,  $\Sigma_{\mathbf{y},t} = \Sigma_{\chi,t} + \Sigma_{\epsilon,t}$ , where  $\Sigma_{\chi,t} = P_t \Lambda_{\chi,t} P_t'$  satisfies the following:

- a.  $\Lambda_{\chi,t} = \text{diag}(\lambda_{\chi,t}^k)_{k=1,\dots,K}$ , for  $K \ll N$  non-zero eigenvalues  $\lambda_{\chi,t}^k$  satisfying

$$\inf_{t \in I_0} \lambda_{\chi,t}^k \asymp O(N).$$

- b.  $P_t = P_0 \mathcal{O}_t$  for some orthonormal  $\mathcal{O}_t$  and  $P_0' P_0 = I_K$ .

**Assumption 3.** There exists a constant  $q \in [0, 1]$  such that

$$c_\epsilon \equiv \sup_{t \in I_0} \max_{i=1,\dots,N} \sum_{i'=1,\dots,N} |\text{cov}(\epsilon_{it}, \epsilon_{i't})|^q = O(1).$$

Assumption 1 states that  $\mathbf{y}_t$  can be decomposed into two parts,  $\chi_t$  and  $\epsilon_t$ . We consider the processes  $\chi_t$  and  $\epsilon_t$  uncorrelated, presenting the additive decomposition at the system covariance level as in Assumption 2. Certain types of non-stationarity are allowed at the covariance level.

The covariance of  $\chi_t$  can vary as long as its eigenspaces  $\mathcal{P}_0 = P_0 P_0' = P_t P_t'$  remain fixed and the eigenvalues are large relative to the cross-sectional dimension  $N$ , as stated in Assumptions 2a and 2b.

Recall that, although the classical specification of a loading-factor model, such as  $\chi_t = \Pi_t \mathbf{f}_t$ , provides motivational interpretations, latent factor models can be fully stated at the level of second moments. It does not require further specification of the low-dimensional component, especially when the purpose of modeling does not aim to identify the factor loading matrix and factor signals separately. If such a specification –  $\chi_t = \Pi_t \mathbf{f}_t$  – is made, the fixed eigenspace  $\mathcal{P}_0$  is identical to the column space of the factor loading matrix  $\text{span}(\Pi_t)$ , as discussed in the previous chapters. That is, Assumption 2 implies that the factor loading ( $\Pi_t$ ) can vary, but in a way that does not alter its column space. The covariance of  $\epsilon_t$  can also vary, as long as it is sparse, as in Assumption 3. Hence, at the population level, regardless of the characterized perturbations, the low-dimensional component  $\chi_t$  or  $\Sigma_{\chi,t}$  captures the dense structure of the covariance of  $\mathbf{y}_t$ , distinguished from the remaining small and sparse component  $\epsilon_t$  or  $\Sigma_{\epsilon,t}$ .

We assume that  $\mathbf{y}_t$  follows the non-stationary process described by Assumptions 1 to 3 in a certain period  $I_0$ . After this time period, the factor space may present a more general form of instabilities. These can still be small instabilities, deviating slightly from  $\mathcal{P}_0$ , or they can be large deviations from  $\mathcal{P}_0$ , indicating a structural change. In the following subsections, we discuss language and tools for describing and analyzing these general factor space instabilities.

#### 3.4.2 OPTIMAL FACTOR SPACE AND RESIDUAL PROBABILITY

One way to describe more general types of instabilities of factor spaces is through a distribution. There is a class of distributions named *von Mises-Fisher* or *Matrix Bingham* or *Langevin* (Chikuse, 2003), which describes distributions of subspaces or projectors. We introduce one example within this class of distributions: subspaces  $\mathcal{P}$  of dimension  $K$  can be distributed with probability proportional to  $\exp[-\text{tr}(\mathcal{P}^\perp \Sigma_\chi)]$ , for some rank  $K$  symmetric matrix  $\Sigma_\chi = P_K \Lambda P_K'$ . The mode  $\mathcal{P}_K^m$  of the distribution corresponds to the projector  $P_K P_K'$ , which represents the column space of the top  $K$  – eigenvectors of  $\Sigma_\chi$  corresponding to the non-zero eigenvalues.

Although the literature on those subspace distributions is not frequently discussed in the literature on factor models, this probabilistic idea can interact with a very popular method in factor model estimation introduced in Bai and Ng, 2002. Recall that the object  $\text{tr}(\mathcal{P}^\perp Y Y')$  for  $Y Y' = \sum_{t \in I} \mathbf{y}_t \mathbf{y}_t'$  is the major component of the information criteria to determine the optimal factor space in  $I$  in this line of methods. The optimal factor space  $\hat{\mathcal{P}}_K$  of dimension  $K$ , of the process  $\mathbf{y}_t$  during  $I$  solves  $\min_{\mathcal{P}_K} \text{tr}(\mathcal{P}^\perp Y Y') / (NT)$  under a penalization.

The underlying idea of this classical method is as follows. Assume a single static factor model over a time period  $I$ . Recall that the top  $K$ -eigenspace, corresponding to the largest  $K$  eigen-

values of the sample covariance, consistently approximates the top  $K$ -eigenspace of the cross-covariance  $\Sigma_y$ , for large  $N, T$ , under standard regularization conditions. This  $K$ -eigenspace of  $\Sigma_y$  approximates the factor space, i.e., the top  $K$ -eigenspace of  $\Sigma_x$  at the population level in the large  $N$  limit. Hence, searching for  $K$  such that the top  $K$ -eigenspace  $\mathcal{P}_K$  minimizes the error, or the projection residual  $\text{tr}(\mathcal{P}^\perp Y Y')$ , solves the optimal factor space of  $\mathbf{y}_t$ .

In terms of the subspace distribution, the procedure to solve  $\min_{\mathcal{P}_K} [\text{tr}(\mathcal{P}^\perp Y Y') / (NT)]$  corresponds to finding the mode of a subspace distribution, maximizing the probability  $\exp[-\text{tr}(\mathcal{P}^\perp Y Y') / (NT)]$ . In other words, the estimated factor space  $\mathcal{P}_K$  in the classical approach is the mode estimator  $\hat{\mathcal{P}}$  of a subspace distribution given the sample  $Y_{NT}$ .

In a distributional approach, the expression  $\exp[\text{tr}(\mathcal{P}^\perp \Sigma)]$  can be interpreted as a residual probability of  $\mathcal{P}$  given the directional characteristic of  $\Sigma$ . In this interpretation, the mode  $\mathcal{P}_K$  is minimizing the residual probability by maximizing  $\exp[-\text{tr}(\mathcal{P}^\perp \Sigma)]$ .

The probability of having a substantial change after  $I_0$  can be measured in relation to this concept of residual probability. Recall that  $\mathbf{y}_t$  is assumed to experience small perturbations in its factor structure as described in Section 3.4.1 in a certain period  $I_0$ . After this time period, there can be more general instabilities in the factor space. We denote any time window after this historical period  $I_0$  as  $I$ .

In relation to the classical method of [Bai and Ng, 2002](#) discussed above, it is not surprising that the following expression can measure the difference of a factor structure after a certain period  $I_0$ :

$$(1/NT)\text{tr}(\mathcal{P}_0^\perp Y Y'), \quad (3.13)$$

where  $\mathcal{P}_0$  captures the factor space in  $I_0$  and  $Y Y' = \sum_{t \in I} \mathbf{y}_t \mathbf{y}_t'$ . The underlying idea of finding the optimal factor space can be extended and reinterpreted in terms of the residual probability. If there are only small instabilities in the factor structure of  $I$  compared to that of  $I_0$ , the residual probability will be small. As  $\mathcal{P}_0$  will be closely aligned with the dominant directions  $\mathcal{P}_1$  – corresponding to the largest eigenvalues, whose number is likely the same as the dimension of  $\mathcal{P}_0$  – of  $Y Y'$  (normalization factors do not affect the directional properties), only a small *residuals* are left after netting out the projected component  $\mathcal{P}_0 Y Y'$ . A large value of the  $\text{tr}(\mathcal{P}_0^\perp Y Y')$  indicates a likelihood of substantial structural changes.

In practice, we consider the object  $\text{tr}(\hat{\mathcal{P}}_0^\perp Y Y')$  where  $\hat{\mathcal{P}}_0$  is an approximation of the factor space of  $I_0$ , combined with the sample  $Y$  from  $I$ , collected after  $I_0$ .

In the next subsection, we design a cumulative sum (CUSUM) type early warning framework for large instabilities. The construction will have a natural interpretation in terms of the probability of change we introduced.

### 3.4.3 PROBABILITY OF STRUCTURAL CHANGES AND EARLY WARNINGS

The Cumulative Sum (CUSUM) method is one of the most popular ways of detecting emerging changes and providing early warnings. In particular, once the historical observations in  $I_0$  are given, subsequent observations  $\mathbf{y}_t$  after  $I_0$  can be examined sequentially, or *online*, to provide a warning of a change point as quickly as possible. The *online* methods are designed to examine each point of the available data sequentially at the moment it becomes available. This branch of methods deviates from *offline* methods, which aim to identify changes retrospectively (Xie et al., 2021) by examining the entire available past time window.

Consider a process

$$\mathbf{y}_t = P_t \mathbf{f}_t + \boldsymbol{\epsilon}_t = \chi_t + \boldsymbol{\epsilon}_t, \quad \text{for } t \in I \quad (3.14)$$

where  $\mathcal{P}_t \equiv \text{span}(P_t)$  is realized following certain dynamics or distribution. We allow a broad class of factor space fluctuations, whose realization is independent of those of  $\mathbf{f}_t$  or  $\boldsymbol{\epsilon}_t$ . For example, it can jump to  $\mathcal{P}_1$  and stay fixed, presenting a discrete type of change discussed in previous chapters. Or, it can be randomly realized following a von Mises-Fisher type of distribution, for example, where the probability of realizing particular directions  $\mathcal{P}_t$  can be proportional to  $\exp[-\text{tr}(\mathcal{P}_t^\perp \Sigma_\chi)]$  for some matrix parameter  $\Sigma_\chi$ .

In the most classical CUSUM method, the distributions of the process ( $\mathbf{y}_t$ ) before and after are assumed to be known. The detection procedure relies on the cumulative sum of log-likelihood ratios:  $S_T = \sum_{t=1}^T \ell(\mathbf{y}_t)$ , providing the optimal stopping point  $\underline{T}$  such that

$$\underline{T} \equiv \inf \left\{ T \geq 1 \mid \sum_{t=1}^T \ell(t) > \Psi \right\}$$

for some pre-set threshold level  $\Psi > 0$ . As the requirement of the known distribution is highly restrictive, numerous variations have been developed to be distribution-free. Assume that the procedure aims to provide a warning for state 1. An intuitive and important qualification of the CUSUM score  $\ell_t = \ell(\mathbf{y}_t)$  is that it is expected to be positive when  $\mathbf{y}_t$  is in state 1, and negative otherwise.

We suggest the following quantity to be the base of the CUSUM score,

$$L_t \equiv \text{tr}(\hat{\mathcal{P}}_0^\perp \mathbf{y}_t \mathbf{y}_t') / N, \quad (3.15)$$

which is closely related to the classical measure introduced in the above-discussed Bai and Ng, 2002. This measure has been employed across various fields; for example, in Jiao et al., 2018, a study on the early detection of subspace change points with applications in human motion change detection.

The historical period  $I_0$  can be heuristically determined by reasonable information or can be estimated from available historical data by offline detection methods, such as our study in

Chapter 1.

We aim to assign a score  $\ell_t$  derived from  $L_t$ , to be positive in expectation if  $\mathbf{y}_t$  is in a state of "large" instabilities and negative in expectation otherwise. In this presentation, the state of "large" instabilities will be defined heuristically based on the properties of the most restrictive state, small perturbations. Assume that the upcoming observations have the following finite moments:

**Assumption 4.**  $m_0 \equiv E \sup_{t \in \mathcal{I}} (\mathbf{f}_t' \mathbf{f}_t) / N = O(1)$  and  $m_1 \equiv E \sup_{t \in \mathcal{I}} (\boldsymbol{\epsilon}_t' \boldsymbol{\epsilon}_t) / N = O(1)$ .

Then we can observe the following:

**Proposition 1.** Under Assumption 4,

$$E[L_t] \leq c \max \left\{ E[\text{tr}(\hat{\mathcal{P}}_0^\perp P_t P_t')], \left( E[\text{tr}(\hat{\mathcal{P}}_0^\perp P_t P_t')] \right)^{1/2} \right\} + m_1, \quad (3.16)$$

for  $c = m_0 + 2\sqrt{m_0 m_1}$ .

Let us first examine the most restrictive case:  $\mathbf{y}_t$  experiences only a small perturbation in its factor structure compared to that of  $\mathcal{I}_0$ , and  $\text{span}(P_t) = \mathcal{P}_0$ . In this case,  $E[L_t]$  in (3.16) is dominated by the estimation errors of  $\hat{\mathcal{P}}_0$  during the pre-period  $\mathcal{I}_0$ . We denote

$$\psi_0 \equiv c^0 \max \left\{ E[\text{tr}(\hat{\mathcal{P}}_0^\perp \mathcal{P}_0)], \left( E[\text{tr}(\hat{\mathcal{P}}_0^\perp \mathcal{P}_0)] \right)^{1/2} \right\} + m_1^0,$$

where  $c^0$  and  $m_1^0$  indicate the corresponding values for the state of small perturbations. These terms  $c^0$  and  $m_1^0$  become feasible to estimate by the information from  $\mathcal{I}_0$ . Denote the  $\mathcal{I}_0$  estimation error as  $g_0 = E[\text{tr}(\hat{\mathcal{P}}_0^\perp \mathcal{P}_0)]$ .<sup>3</sup> That is, by setting

$$\ell_t \equiv L_t - \hat{c}g_0 - \hat{m}_1,$$

we will have  $E[\ell_t] < 0$  for the state of small perturbations.

Intuitively,  $E[L_t]$  increases as  $\mathbf{y}_t$  is in a state where the  $\mathcal{P}_t = P_t P_t'$  deviates far from  $\mathcal{P}_0$ . A simple approach is to define a "large" deviation such that  $E[L_t]$  becomes larger than  $\psi_0$ . In this way, by construction,  $E[\ell_t] > 0$  for the states of large instabilities. Now, we summarize the design of this procedure.

---

<sup>3</sup>An upper bound can be found as the penalty terms of  $g_0$  of [Bai and Ng, 2002](#), under the extended regularity conditions in Chapter 1.

EARLY WARNING FRAMEWORK FOR LARGE INSTABILITIES Let  $\mathbf{I}_0$  be a given historical time window. For each  $t \geq 1$  of a sequential observation, set a score

$$\ell_t = L_t - \psi_0.$$

A warning for a structural instability is provided at the time

$$\underline{T} \equiv \inf \left\{ T \geq 1 \mid \sum_{t=1}^T \ell(t) > \Psi \right\} \quad (3.17)$$

for some threshold  $\Psi$ .

The average of the resulting cumulative sum  $(1/T) \sum_{t=1}^T \ell(t)$  is  $(1/T) \sum_{t=1}^T \text{tr}(\hat{\mathcal{P}}_0^\perp \mathbf{y}_t \mathbf{y}_t') / N = \text{tr}(\hat{\mathcal{P}}_0^\perp \mathbf{Y} \mathbf{Y}') / (NT)$ , the residual probability up to a penalty term. Hence, following the discussion in Section 3.4.2, the cumulative sum criterion (3.17) aims to provide a warning as soon as the probability of a structural change given the sample exceeds a certain threshold.

### 3.5 CONCLUDING REMARKS

Network and factor models are two important techniques for analyzing interconnected systems. An interconnected system can naturally have a dual representation through our network-factor model. This modeling can assist in analyzing instabilities in latent network structures using various tools of factor analysis. Diverse approaches can be integrated to facilitate the analysis of broad types of instabilities in latent structures. We design a new early warning framework for structural changes that accommodates a broad range of instabilities in the underlying network. The framework can be of practical importance for various systems represented by network-supported data, where the underlying structure is unknown or unobservable.

# APPENDIX TO CHAPTER 3

## C.1 FURTHER DISCUSSIONS ON NETWORK–FACTOR MODEL

In Section 3.3.1, assume that only those  $\{\mathbf{a}_g \mathbf{x}_t\}$  of a certain set of individual units  $g \in \mathcal{G}$ , for  $|\mathcal{G}| < \infty$  are important to the transmission,

$$y_{it} = \sum_{g \in \mathcal{G}} \sum_{\ell} \pi_{t,i \leftarrow g, \ell} L^{\ell}(\mathbf{a}_g \mathbf{x}_t) + \epsilon_{it} \quad \text{for all } i \in \mathcal{N}. \quad (3.9)$$

The cases when the marginal benefits are time-varying, can be similarly represented as a factor model. Taking  $\tilde{\mathbf{f}}_{\mathcal{G},t} \equiv [\mathbf{a}_g \mathbf{x}_t]_{g \in \mathcal{G}}$  of size  $|\mathcal{G}| \times 1$ , (3.9) is written as

$$\mathbf{y}_t = \tilde{\Pi}_{t, \mathcal{N} \leftarrow \mathcal{G}}(L) \tilde{\mathbf{f}}_{\mathcal{G},t} + \boldsymbol{\epsilon}_t, \quad (3.10)$$

where  $\tilde{\Pi}_{t, \mathcal{N} \leftarrow \mathcal{G}}(L)$  is a  $N \times |\mathcal{G}|$  matrix of lag polynomials. Assume that all lags of  $\tilde{\mathbf{f}}_{\mathcal{G},t} = [\mathbf{a}_g \mathbf{x}_t]_{g \in \mathcal{G}}$  are strong factors, it also allows the following reduced expression:

$$\mathbf{y}_t = \Pi_{t, \mathcal{N} \leftarrow \mathcal{G}} \mathbf{f}_{\mathcal{G},t} + \boldsymbol{\epsilon}_t, \quad (3.11)$$

where  $\Pi_{t, \mathcal{N} \leftarrow \mathcal{G}}$  is  $N \times |\mathcal{G}|M$  factor loading matrix consisting of the coefficients  $\pi_{t,i \leftarrow g, \ell}$  with  $|\mathcal{G}|M$  number of factors  $\mathbf{f}_{\mathcal{G},t} \equiv [L^{\ell}(\mathbf{a}_g \mathbf{x}_t)]_{g \in \mathcal{G}, \ell=1, \dots, M}$ .

## C.2 PROOF

**Proposition 1.** Under Assumption 4,

$$\mathbb{E}[L_t] \leq c \max \left\{ \mathbb{E}[\text{tr}(\hat{\mathcal{P}}_0^{\perp} P_t P_t')], \left( \mathbb{E}[\text{tr}(\hat{\mathcal{P}}_0^{\perp} P_t P_t')] \right)^{1/2} \right\} + m_1, \quad (3.16)$$

for  $c = m_0 + 2\sqrt{m_0 m_1}$ .

*Proof.* Observe that

$$\text{tr}(\hat{\mathcal{P}}_0^{\perp} \mathbf{y}_t \mathbf{y}_t') = \text{tr}(\hat{\mathcal{P}}_0^{\perp} (P_t \mathbf{f}_t + \boldsymbol{\epsilon}_t)(P_t \mathbf{f}_t + \boldsymbol{\epsilon}_t)') = \text{tr}(P_t' \hat{\mathcal{P}}_0^{\perp} P_t \mathbf{f}_t \mathbf{f}_t') + 2\text{tr}(P_t' \hat{\mathcal{P}}_0^{\perp} \boldsymbol{\epsilon}_t \mathbf{f}_t') + \text{tr}(\hat{\mathcal{P}}_0^{\perp} \boldsymbol{\epsilon}_t \boldsymbol{\epsilon}_t').$$

The trace operator is sub-multiplicative following the (matrix) Cauchy-Schwarz inequality, which gives

$$\begin{aligned} \text{tr}(\hat{\mathcal{P}}_0^\perp \mathbf{y}_t \mathbf{y}_t') &\leq \sqrt{\text{tr}((\mathbf{f}_t' \mathbf{f}_t)^2)} \sqrt{\text{tr}(P_t' \hat{\mathcal{P}}_0^\perp P_t P_t' \hat{\mathcal{P}}_0^\perp P_t)} + 2 \sqrt{\text{tr}(\hat{\mathcal{P}}_0^\perp P_t P_t')} \sqrt{\text{tr}(\mathbf{f}_t \boldsymbol{\epsilon}_t' \boldsymbol{\epsilon}_t \mathbf{f}_t')} \\ &\quad + \text{tr}(\hat{\mathcal{P}}_0^\perp \boldsymbol{\epsilon}_t \boldsymbol{\epsilon}_t') \leq (\mathbf{f}_t' \mathbf{f}_t) \text{tr}(\hat{\mathcal{P}}_0^\perp P_t P_t') + 2 \sqrt{(\boldsymbol{\epsilon}_t' \boldsymbol{\epsilon}_t)(\mathbf{f}_t' \mathbf{f}_t)} \sqrt{\text{tr}(\hat{\mathcal{P}}_0^\perp P_t P_t')} + \boldsymbol{\epsilon}_t' \boldsymbol{\epsilon}_t, \end{aligned}$$

as  $\text{tr}(A^2) \leq (\text{tr}(A))^2$  for a positive semi-definite matrix  $A$ , with basic properties (e.g., cyclic invariance) of the trace operator. Further inequalities are implied

$$\begin{aligned} L_t \equiv \text{tr}(\hat{\mathcal{P}}_0^\perp \mathbf{y}_t \mathbf{y}_t')/N &\leq \left( \sup_{t \in \mathcal{I}_1} (\mathbf{f}_t' \mathbf{f}_t)/N \right) \text{tr}(\hat{\mathcal{P}}_0^\perp P_t P_t') \\ &\quad + 2 \sqrt{\left( \sup_{t \in \mathcal{I}_1} (\mathbf{f}_t' \mathbf{f}_t)/N \right) \left( \sup_{t \in \mathcal{I}_1} (\boldsymbol{\epsilon}_t' \boldsymbol{\epsilon}_t)/N \right)} \sqrt{\text{tr}(\hat{\mathcal{P}}_0^\perp P_t P_t')} + \sup_{t \in \mathcal{I}_1} (\boldsymbol{\epsilon}_t' \boldsymbol{\epsilon}_t)/N, \end{aligned}$$

under Assumption 4. Then it leads to (3.16), due to the concavity of the square root function for Jensen's inequality.  $\square$



# BIBLIOGRAPHY

- Acemoglu, D., V.M. Carvalho, A. Ozdaglar, and A. Tahbaz-Salehi (2012). *The Network Origins of Aggregate Fluctuations*. Technical report 5, pp. 1977–2016. eprint: <https://onlinelibrary.wiley.com/doi/pdf/10.3982/ECTA9623>.
- Acemoglu, D. and A. Tahbaz-Salehi (2020). *Firms, Failures, and Fluctuations: The Macroeconomics of Supply Chain Disruptions*. Working Paper 27565. National Bureau of Economic Research.
- Acharya, V. V., I. Hasan, and A. Saunders (2006). “Should banks be diversified? Evidence from individual bank loan portfolios”. *Journal of Business* 79:3, pp. 1355–1412.
- Albanesi, S., G. DeGiorgi, and J. Nosal (2022). “Credit growth and the financial crisis: A new narrative”. *Journal of Monetary Economics* 132, pp. 118–139.
- Amiti, M., S. J. Redding, and D. E. Weinstein (2019). “The Impact of the 2018 Tariffs on Prices and Welfare”. *Journal of Economic Perspectives* 33:4, pp. 187–210.
- (2020). “Who’s Paying for the US Tariffs?” *AEA Papers and Proceedings* 110, pp. 541–546.
- Bai, J. and S. Ng (2002). “Determining the Number of Factors in Approximate Factor Models”. *Econometrica* 70:1, pp. 191–221. eprint: <https://onlinelibrary.wiley.com/doi/pdf/10.1111/1468-0262.00273>.
- Ballester, C., A. Calvó-Armengol, and Y. Zenou (2006). “Who’s Who in Networks. Wanted: The Key Player”. *Econometrica* 74:5, pp. 1403–1417.
- Baltagi, B. H., C. Kao, and F. Wang (2021). “Estimating and testing high dimensional factor models with multiple structural changes”. *Journal of Econometrics* 220:2. Annals Issue: Celebrating 40 Years of Panel Data Analysis: Past, Present and Future, pp. 349–365.
- Banerjee, A., M. Marcellino, and I. Masten (2008). “Chapter 4 Forecasting Macroeconomic Variables Using Diffusion Indexes in Short Samples with Structural Change”. *Frontiers of Economics and Globalization* 3.
- Baqae, D. R. (2018). “Cascading Failures in Production Networks”. *Econometrica* 86:5, pp. 1819–1838. eprint: <https://onlinelibrary.wiley.com/doi/pdf/10.3982/ECTA15280>.
- Barigozzi, M. and C. Brownlees (2019). “NETS: Network estimation for time series”. *Journal of Applied Econometrics* 34:3, pp. 347–364. eprint: <https://onlinelibrary.wiley.com/doi/pdf/10.1002/jae.2676>.

- Barigozzi, M., H. Cho, and P. Fryzlewicz (2018). “Simultaneous multiple change-point and factor analysis for high-dimensional time series”. *Journal of Econometrics* 206:1, pp. 187–225.
- Barigozzi, M. and M. Hallin (2017). “A network analysis of the volatility of high dimensional financial series”. *Journal of the Royal Statistical Society: Series C (Applied Statistics)* 66:3, pp. 581–605. eprint: <https://rss.onlinelibrary.wiley.com/doi/pdf/10.1111/rssc.12177>.
- Basu, S. and S. S. Rao (2021). *Graphical models for nonstationary time series*.
- Basu, S., A. Shojaie, and G. Michailidis (2015). “Network Granger Causality with Inherent Grouping Structure”. *J. Mach. Learn. Res.* 16:1, pp. 417–453.
- Bernanke, B. S., J. Boivin, and P. Elias (2005). “Measuring the Effects of Monetary Policy: A Factor-Augmented Vector Autoregressive (FAVAR) Approach”. *The Quarterly Journal of Economics* 120:1, pp. 387–422. eprint: <https://academic.oup.com/qje/article-pdf/120/1/387/5442603/120-1-387.pdf>.
- Bianchi, D., M. Billio, R. Casarin, and M. Guidolin (2019). “Modeling systemic risk with Markov Switching Graphical SUR models”. *Journal of Econometrics* 210:1. Annals Issue in Honor of John Geweke “Complexity and Big Data in Economics and Finance: Recent Developments from a Bayesian Perspective”, pp. 58–74.
- Billio, M., M. Getmansky, A. W. Lo, and L. Pelizzon (2012). “Econometric measures of connectedness and systemic risk in the finance and insurance sectors”. *Journal of Financial Economics* 104:3. Market Institutions, Financial Market Risks and Financial Crisis, pp. 535–559.
- Brownlees, C., G. S. Guðmundsson, and G. Lugosi (2022). “Community Detection in Partial Correlation Network Models”. *Journal of Business & Economic Statistics* 40:1, pp. 216–226. eprint: <https://doi.org/10.1080/07350015.2020.1798241>.
- Brownlees, C. and G. Mesters (2021). “Detecting granular time series in large panels”. *Journal of Econometrics* 220:2. Annals Issue: Celebrating 40 Years of Panel Data Analysis: Past, Present and Future, pp. 544–561.
- Chamberlain, G. and M. Rothschild (1983). “Arbitrage, Factor Structure, and Mean-Variance Analysis on Large Asset Markets”. *Econometrica* 51:5, pp. 1281–1304.
- Chen, L. (2015). “Estimating the common break date in large factor models”. *Economics Letters* 131, pp. 70–74.
- Chen, L., J. J. Dolado, and J. Gonzalo (2014). “Detecting big structural breaks in large factor models”. *Journal of Econometrics* 180:1, pp. 30–48.
- Cheng, X., Z. Liao, and F. Schorfheide (2016). “Shrinkage Estimation of High-Dimensional Factor Models with Structural Instabilities”. *The Review of Economic Studies* 83:4, pp. 1511–1543. eprint: <https://academic.oup.com/restud/article-pdf/83/4/1511/17416907/rdw005.pdf>.

- Chikuse, Y. (2003). *Statistics on Special Manifolds. Lecture Notes in Statistics*. Vol. 174. ISBN: 978-0-387-00160-9.
- Dahlhaus, R. (2000). “Graphical interaction models for multivariate time series<sup>1</sup>”. *Metrika* 51:2, pp. 157–172.
- (2012). “Locally stationary processes”. In: *Handbook of statistics*. Vol. 30. Elsevier, pp. 351–413.
- Davis, C. and W. M. Kahan (1970). “The Rotation of Eigenvectors by a Perturbation. III”. *SIAM Journal on Numerical Analysis* 7:1, pp. 1–46.
- Demirgüç-Kunt, A. and H. Huizinga (2010). “Bank activity and funding strategies: The impact on risk and returns”. *Journal of Financial Economics* 98:3, pp. 626–650.
- DeYoung, R. and G. Torna (2013). “Nontraditional banking activities and bank failures during the financial crisis”. *Journal of Financial Intermediation* 22:3, pp. 397–421.
- Diebold, F. X. and K. Yilmaz (2014). “On the network topology of variance decompositions: Measuring the connectedness of financial firms”. *Journal of Econometrics* 182:1. Causality, Prediction, and Specification Analysis: Recent Advances and Future Directions, pp. 119–134.
- Dinopoulos, E., G. Heins, and B. Unel (2024). “Tariff wars, unemployment, and top incomes”. *Journal of Monetary Economics* 148, p. 103616.
- Düker, M.-C. and V. Pipiras (2024). *Testing for common structures in high-dimensional factor models*. arXiv: 2403.19818 [stat.ME].
- Edelman, A., T. Arias, and S. T. Smith (1998). “The Geometry of Algorithms with Orthogonality Constraints”. *SIAM J. Matrix Anal. Appl.* 20, pp. 303–353.
- Eichler, M. (2012). “Graphical modelling of multivariate time series”. *Probability Theory and Related Fields* 153:1, pp. 233–268.
- Fajgelbaum, P. D., P. K. Goldberg, P. J. Kennedy, and A. K. Khandelwal (2020). “The Return to Protectionism”. *Quarterly Journal of Economics* 135:1, pp. 1–55.
- Fan, J., Y. Liao, and M. Mincheva (2013). “Large covariance estimation by thresholding principal orthogonal complements”. *Journal of the Royal Statistical Society. Series B (Statistical Methodology)* 75:4, pp. 603–680.
- Forni, M., D. Giannone, M. Lippi, and L. Reichlin (2009). “Opening the Black Box: Structural Factor Models with Large Cross Sections”. *Econometric Theory* 25:5, pp. 1319–1347.
- Freund, C., R. Piermartini, and N. Rocha (2021). “Tariffs and Politics: Evidence from Trump’s Trade Wars”. *Economic Journal* 131:636, pp. 1253–1277.
- Gabaix, X. (2011). “The Granular Origins of Aggregate Fluctuations”. *Econometrica* 79:3, pp. 733–772. eprint: <https://onlinelibrary.wiley.com/doi/pdf/10.3982/ECTA8769>.
- Gabaix, X. and R. S. J. Koijen (2021). *In Search of the Origins of Financial Fluctuations: The Inelastic Markets Hypothesis*. Working Paper 28967. National Bureau of Economic Research.

- Galeotti, A., B. Golub, and S. Goyal (2020). “Targeting Interventions in Networks”. *Econometrica* 88:6, pp. 2445–2471. eprint: <https://onlinelibrary.wiley.com/doi/pdf/10.3982/ECTA16173>.
- Gaubert, C. and O. Itskhoki (2021). “Granular Comparative Advantage”. *Journal of Political Economy* 129:3, pp. 871–939.
- Guðmundsson, G. S. and C. Brownlees (2021). “Detecting groups in large vector autoregressions”. *Journal of Econometrics* 225:1. Themed Issue: Vector Autoregressions, pp. 2–26.
- Guillén, M. F. (2015). “The Global Economic & Financial Crisis: A Timeline”. *Lauder Institute*.
- Han, X. and A. Inoue (2015). “TESTS FOR PARAMETER INSTABILITY IN DYNAMIC FACTOR MODELS”. *Econometric Theory* 31:5, pp. 1117–1152.
- Heipertz, J., A. Ouazad, and R. Rancière (2019). *The Transmission of Shocks in Endogenous Financial Networks: A Structural Approach*. Working Paper 26049. National Bureau of Economic Research.
- Horn, R. A. and C. R. Johnson (2013). *Matrix Analysis*. 2nd. Cambridge University Press, Cambridge; New York. ISBN: 9780521839402.
- JEC (2008). “Subprime Mortgage Market Crisis Timeline”. *Joint Economic Committee*.
- Jiao, Y., Y. Chen, and Y. Gu (2018). “Subspace Change-Point Detection: A New Model and Solution”. *IEEE Journal of Selected Topics in Signal Processing* 12:6, pp. 1224–1239.
- Koo, B., B. Wong, and Z.-Y. Zhong (2024). *Disentangling Structural Breaks in Factor Models for Macroeconomic Data*. arXiv: 2303.00178 [stat.ME].
- Laeven, L. and R. Levine (2009). “Bank governance, regulation and risk taking”. *Journal of Financial Economics* 93:2, pp. 259–275.
- Ma, S. and L. Su (2018). “Estimation of large dimensional factor models with an unknown number of breaks”. *Journal of Econometrics* 207:1, pp. 1–29.
- Massacci, D. (2021). “Testing for Regime Changes in Portfolios with a Large Number of Assets: A Robust Approach to Factor Heteroskedasticity\*”. *Journal of Financial Econometrics* 21:2, pp. 316–367. eprint: <https://academic.oup.com/jfec/article-pdf/21/2/316/49676570/nbaa046.pdf>.
- Mayer, C., K. Pence, and S. M. Sherlund (2009). “The Rise in Mortgage Defaults”. *Journal of Economic Perspectives* 23:1, pp. 27–50.
- Mazzarisi, P., F. Lillo, and S. Marmi (2019). “When panic makes you blind: A chaotic route to systemic risk”. *Journal of Economic Dynamics and Control* 100, pp. 176–199.
- McCracken, M. W. and S. Ng (2016). “FRED-MD: A Monthly Database for Macroeconomic Research”. *Journal of Business & Economic Statistics* 34:4, pp. 574–589.
- Merlevède, F., M. Peligrad, and E. Rio (2011). “A Bernstein type inequality and moderate deviations for weakly dependent sequences”. *Probability Theory and Related Fields* 151:3, pp. 435–474.

- Parker, J. and D. Sul (2016). "Identification of Unknown Common Factors: Leaders and Followers". *Journal of Business & Economic Statistics* 34:2, pp. 227–239. eprint: <https://doi.org/10.1080/07350015.2015.1026439>.
- Phillips, P. C. B. and J. Yu (2011). "Dating the timeline of financial bubbles during the sub-prime crisis". *Quantitative Economics* 2:3, pp. 455–491. eprint: <https://onlinelibrary.wiley.com/doi/pdf/10.3982/QE82>.
- Pourahmadi, M. (2013). "High-Dimensional Covariance Estimation". Copyright © 2013 John Wiley & Sons, Inc. All rights reserved Wiley Series in Probability and Statistics.
- Ross, S. A. (1976). "The arbitrage theory of capital asset pricing". *Journal of Economic Theory* 13:3, pp. 341–360.
- Schmid, M. M. and I. Walter (2009). "Do financial conglomerates create or destroy economic value? Evidence for the European financial industry". *Journal of Financial Economics* 94:2, pp. 99–122.
- Sherman, M. (2009). "A Short History of Financial Deregulation in the United States". CEPR.
- Shleifer, A. and R. W. Vishny (2010). "Unstable banking". *Journal of Financial Economics* 97:3, pp. 306–318.
- Stiroh, K. J. and A. Rumble (2006). "The dark side of diversification: The case of US financial holding companies". *Journal of Banking & Finance* 30:8, pp. 2131–2161.
- Stock, J. H. and M. Watson (2009). "Forecasting in dynamic factor models subject to structural instability". *The Methodology and Practice of Econometrics. A Festschrift in Honour of David F. Hendry* 173, p. 205.
- Stock, J. H. and M. W. Watson (2002a). "Macroeconomic Forecasting Using Diffusion Indexes". *Journal of Business & Economic Statistics* 20:2, pp. 147–162. eprint: <https://doi.org/10.1198/073500102317351921>.
- (2002b). "Forecasting Using Principal Components from a Large Number of Predictors". *Journal of the American Statistical Association* 97:460, pp. 1167–1179.
- Tao, T. (2023). *Topics in Random Matrix Theory*. Graduate studies in mathematics. American Mathematical Soc. ISBN: 9780821885079.
- Taschereau-Dumouchel, M. (2019). "Cascades and Fluctuations in an Economy with an Endogenous Production Network". *SSRN Electronic Journal*.
- Wang, W. and J. Fan (2017). "ASYMPTOTICS OF EMPIRICAL EIGENSTRUCTURE FOR HIGH DIMENSIONAL SPIKED COVARIANCE". *The Annals of Statistics* 45:3, pp. 1342–1374.
- Xie, L., S. Zou, Y. Xie, and V. V. Veeravalli (2021). "Sequential (Quickest) Change Detection: Classical Results and New Directions". *IEEE Journal on Selected Areas in Information Theory* 2, pp. 494–514.
- Yamamoto, Y. (2016). "Forecasting With Nonspurious Factors in U.S. Macroeconomic Time Series". *Journal of Business & Economic Statistics* 34:1, pp. 81–106.

## *Bibliography*

Yu, Y., T. Wang, and R. J. Samworth (2015). “A useful variant of the Davis—Kahan theorem for statisticians”. *Biometrika* 102:2, pp. 315–323.

# AUTHOR'S DECLARATION

**Eidesstattliche Versicherung gemäß §8 Absatz 2 Buchstabe a) der Promotionsordnung der Universität Mannheim zur Erlangung des Doktorgrades der Volkswirtschaftslehre (Dr. rer. pol.)**

1. Bei der eingereichten Dissertation mit dem Titel „Essays on the Econometric Analysis of Structural Instabilities and Systemic Risk“ handelt es sich um mein eigenständig erstelltes Werk, das den Regeln guter wissenschaftlicher Praxis entspricht.
2. Ich habe nur die angegebenen Quellen und Hilfsmittel benutzt und mich keiner unzulässigen Hilfe Dritter bedient. Insbesondere habe ich wörtliche und nicht wörtliche Zitate aus anderen Werken als solche kenntlich gemacht.
3. Die Arbeit oder Teile davon habe ich bislang nicht an einer Hochschule des In- oder Auslands als Bestandteil einer Prüfungs- oder Qualifikationsleistung vorgelegt.
4. Die Richtigkeit der vorstehenden Erklärung bestätige ich.
5. Die Bedeutung der eidesstattlichen Versicherung und die strafrechtlichen Folgen einer unrichtigen oder unvollständigen eidesstattlichen Versicherung sind mir bekannt. Ich versichere an Eides statt, dass ich nach bestem Wissen die reine Wahrheit erkläre und nichts verschwiegen habe.

Die eingereichten Dissertationsexemplare sowie der Datenträger gehen in das Eigentum der Universität Mannheim über.

Mannheim, 2025

So Jin Lee

# CURRICULUM VITAE

## EDUCATION

**University of Mannheim**, Mannheim, Germany

Ph.D. in Economics, Department of Economics

**Sogang University**, Seoul, Korea

M.A. in Economics, Graduate School of Sogang University

**Yonsei University**, Seoul, Korea

M.Sc. in Mathematics, Graduate School of Yonsei University

**Yonsei University**, Seoul, Korea

B.Sc. in Astronomy and B.Sc. in Mathematics, College of Science